UNIVERSITAT POLITÈCNICA DE VALÈNCIA

UNIVERSITAT POLITÈCNICA DE VALÈNCIA

Escuela Técnica Superior de Ingeniería Industrial

Modular multilevel converter laboratory prototype commissioning and control in three operative scenarios

Trabajo Fin de Master

Master Universitario en Ingeniería Industrial — Màster Universitari en Enginyeria Industrial

AUTOR: Beneit Barajas, Adrián

Tutores: Antonino Daviu, José Alfonso; Brenna, Morris

CURSO ACADÉMICO: 2023/2024

POLITECNICO
MILANO 1863

SCUOLA DI INGEGNERIA INDUSTRIALE
E DELL'INFORMAZIONE

Modular Multilevel Converter laboratory prototype commissioning and control in three operative scenarios

Tesi di Laurea Magistrale in
Electrical Engineering - Ingegneria Eletrica

Author: **Adrian Beneit Barajas**

Student ID: 10736341
Advisor: Prof. Morris Brenna
Co-advisors: No
Academic Year: 2023-24

Abstract

The introduction of advanced technological components, such as modular multilevel converters (MMC), is crucial to reach a more meshed and interconnected electrical system with the increasing percentage of renewable generation, storage systems and all the required technology to move towards a sustainable energy model. This MSc thesis has carried out a practical study on MMCs. A Simulink model has been developed to simulate a laboratory prototype and develop controllers for the three operating modes investigated: isolated, grid-connected and STATCOM. Moreover, the required energization, synchronization, and connection procedures have also been designed. Then, the tests have been reproduced in the real prototype. The results prove the versatility of the MMC in the mentioned scenarios. The work provides an integral overview of the MMC possibilities in the future electrical system and establishes a robust base for experimentation in coming studies.

Keywords: MMC, HVDC, prototype

Abstract in lingua italiana

L'introduzione di componenti tecnologici avanzati, come i convertitori modulari multivello (MMC), è cruciale per raggiungere un sistema elettrico più interconnesso e a maglia, con una percentuale crescente di generazione rinnovabile, sistemi di accumulo e tutta la tecnologia necessaria per avanzare verso un modello energetico sostenibile. Questa tesi di MSc ha condotto uno studio pratico sugli MMC. È stato sviluppato un modello Simulink per simulare un prototipo di laboratorio e sviluppare controllori per i tre modi operativi investigati: isolato, connesso alla rete e STATCOM. Inoltre, sono stati progettati anche le procedure necessarie per l'energizzazione, la sincronizzazione e la connessione. Successivamente, i test sono stati riprodotti nel prototipo reale. I risultati dimostrano la versatilità dell'MMC negli scenari menzionati. Il lavoro fornisce una panoramica integrale delle possibilità degli MMC nel futuro sistema elettrico e stabilisce una base solida per la sperimentazione negli studi futuri.

Parole chiave: MMC, HVDC, prototipo

Contents

Introduction

Government authorities and general society are becoming more concerned about the challenges of climate change and the reliability and cost of energy supply. In response, the administrations are reconsidering their energetic strategies, focusing on using renewable resources. On the path to a sustainable electrical system, it is crucial to introduce advanced technology, such as modular multilevel converters (MMCs), not only to optimize efficiency but also to ensure the stability and resilience of the grid. MMCs stand out for their ability to enhance the interconnections and meshability of the electrical system and facilitate the integration of different renewable energy sources, energy storage, etc.

The work developed in this thesis is a theoretical and practical study of MMCs, starting with a theoretical overview of this type of converter and following with simulated and experimental analysis with a laboratory prototype. It is framed within a research project called 'Control "Grid Forming" para Operacion Avanzada de Sistemas Electricos con Gran Penetracion de Energia Renovable' at UPV (Universitat Politècnica de València), where the author is hired as a researcher. Then, one of the initial tasks of the project, which is to commission a recently purchased laboratory MMC prototype, has been employed to complement the already started theoretical study for the MSc Thesis.

Three different operation modes have been analysed: isolated mode, grid-connected mode and STATCOM mode, each representing one of the main applications of the MMCs. Furthermore, the process of bringing the converter from a disconnected and de-energised state towards each operation mode is developed and tested. In this way, the work done in this thesis provides a solid base for research and testing for the mentioned project.

The thesis is divided into four main chapters. The first one provides the context of MMCs, explaining how they fit into the electrical system as the best alternative for specific applications where their advantages excel. It starts with an overview of the actual system and other converters, exposing their differences from MMCs to show why these are preferred for high-voltage conversions.

While the first chapter justifies the purpose of the MMCs and the necessity of research, the second chapter provides an overview of these converters' state of the art. The chapter

is centred around the structure of the converter, the operation and the main applications. With this chapter, the theoretical base of the thesis is concluded, so the following two chapters are dedicated to the practical work.

The third chapter of the thesis describes the system under study. First, the MMCs laboratory prototype is described, along with how it is modelled in Simulink to conduct the desired tests. Then, the powering-up issues of the converter are explained, as well as the circuitry that has been designed to manage them. Finally, the three scenarios under study are defined, and their respective control algorithms are specified.

Finally, the fourth chapter focuses on the results obtained for each defined scenario. In all cases, the simulation results are first shown and validated afterwards by the physical testing in the MMC test bench. The results confirm the suitability of the converter and the controllers employed for the indicated applications. Furthermore, the procedures designed to reach the operation modes are proven to drive the converter safely towards the operation, constituting a reliable starting point for further study with the MMC along the project.

The thesis is closed with the conclusion chapter, where the project's outcome is summarized, highlighting the work's applicability. The main contributions are briefly acknowledged, and the future work to be continued after this thesis is commented on.

1 | Modular Multilevel Converters context

1.1. Electrical Power Transmission

Among the diverse forms of energy, electricity stands as an exceptionally versatile resource, capable of efficient transmission over extensive distances and seamless conversion into mechanical energy and vice versa. These characteristics make it suitable for human utilization, powering homes, industries, and technology, as it enables consumption at considerable distances from its generation sources.As our society becomes increasingly dependent on electricity, the efficient and reliable transmission of power becomes crucial to meet the ever-increasing energy demands.

There are two ways in which electricity is transmitted: continuous and alternating current. Historically, the development of electrical power transmission has been primarily based on Alternating Current (AC) systems, which have proven well-suited for different voltage applications, distribution networks, and general power grid infrastructures. Its adoption spread rapidly worldwide due to its numerous advantages, among which stands out the voltage regulation. This feature enables power to be efficiently stepped up to high voltages for long-distance transmission, reducing losses during transportation. Conversely, consumption and generation are done at more suitable lower voltages.

On the other hand, AC power transmission also has some drawbacks the electric system has dealt with over the years. Firstly, the alternating voltage must be perfectly synchronized along the grid to keep it stable, which involves several control actions and limitations. Also, AC loads involve inductive and capacitive phenomena that must be appropriately managed. Even line conductors have intrinsic inductive and capacitive properties affecting AC transmission. Indeed, intermediate taps for reactive power compensation are needed at long-distance AC lines.

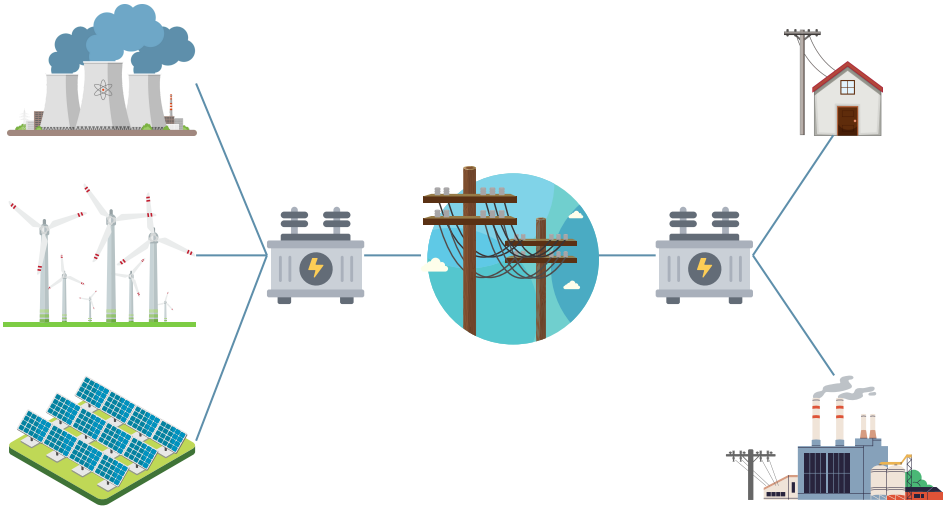

Figure 1.1: Traditional electrical energy transmission system.

Despite the AC disadvantages, DC transmission has been traditionally displaced due to the high cost and complexity of high voltage DC voltage operation compared to AC power transformers. However, advancements in power electronics have made DC systems more and more affordable in the later years. While AC transmission is still the dominant choice for power grids worldwide, some limitations have led to the rise of High-Voltage Direct Current (HVDC) applications such as long-distance transmission, interconnecting asynchronous grids, submarine power transmission, or efficient offshore wind integration.

HVDC is a power transmission technology that employs direct current at high voltage levels, taking advantage of both DC transmission benefits and the small power losses associated with high voltage. In this way, large amounts of power can be transmitted in direct mode.

With the increasing adoption of HVDC in a system where alternating current is unquestionably imposed, research and development efforts have been focused on high-power converters. These converters are crucial components in HVDC systems, responsible for converting AC power to DC and vice versa, allowing bidirectional power flow and efficient integration of the HVDC systems into the central AC system.

This energy conversion is complex and expensive for high voltage and power, so it has not been commonly implemented throughout history. However, the technological advancements are making it more and more affordable.

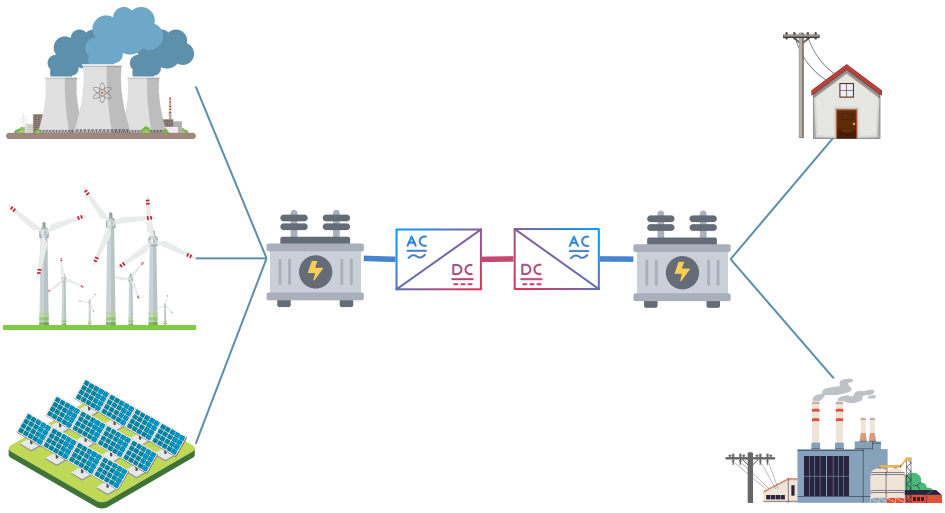

Figure 1.2: Alternative HVDC electrical energy transmission system.

To this effect, Modular Multilevel Converter technology (MMC) has been recently developed to provide a high voltage and high power solution. The MMC modular structure makes it ideal for many advanced power applications that will be gaining importance in the electric system soon. In particular, MMC has been proven as the most suitable partner of the HVDC technology.

1.1.1. AC vs. DC Power transmission

The developments of MMC and HVDC are making the HVDC technology more and more attractive for power transmission systems. Indeed, this technology is the only technically acceptable at a reasonable cost for some scenarios. In order to see the applications in which HVDC transmission arises as the most appropriate solution, it is necessary to explore the technical differences between both transmission technologies, highlighting their strong and weak aspects. However, it should be noted that HVDC is not the only niche where MMC can be employed, and other applications will also be studied in this project.

Advantages of HVDC transmission

1. **Line cost:** The first and one of the most important aspects is the economical one, as it is what determines whether or not the engineering projects are carried out. It has been emphasized how AC/DC converter station costs have traditionally limited the application of high-voltage DC systems. However, the unitary cost of the transmission line itself is lower for DC than for AC for several reasons:

- The number of conductors in DC is 2 (or even just 1), while there are always three conductors in triphase systems. The reduction of conductors involves a significant downsizing in terms of space and required structures, especially in the case of aerial lines. In addition, this becomes a crucial issue in places where obtaining the 'right of path' for electrical lines is a difficult task.
- The skin effect is an important phenomenon affecting AC lines. Due to constant variation of the alternating current, the current tends to concentrate on the periphery of the conductor, so its effective section is reduced. DC conductors carry constant current, so they do not suffer this effect, and all the conductor section is exploited. In other words, DC transmission allows the use of smaller conductors compared to AC transmission with the same current rating, which reduces line cost.
- An essential feature of DC systems is that they do not involve reactive power. Only active power is transmitted through DC lines. Therefore, the conductors can be fully loaded with maximum active current. If the DC line is connected to an AC system with some reactive power requirements, they are provided by the converter station but are invisible to the DC line. Thus, the DC conductors are sized just for the active power requirements, reducing the line section and, consequently, its cost.
- The sizing of conductor isolation requirements depends on the voltage peak. In AC systems, the peak voltage is $\sqrt{2}$ times greater than the Root Mean Square (RMS) value, which relates to the actual power delivered. Conversely, the peak voltage in DC systems coincides with the nominal value. Consequently, a DC line necessitates lower isolation than an AC line with an equivalent power rating and, consequently, a reduced unitary cost.

The unitary line cost is lower for DC transmission, while the converter cost is still higher. Therefore, there is a critical distance where the total cost of an AC line and a DC line are equal, as it is represented in fig. 1.3. DC lines become a more cost-efficient solution for line lengths above this distance, which is around 500 km for onshore lines and 50 km for offshore ones. Enhancements on power converters will enable the reduction of station costs and, therefore, the value of the critical distance.

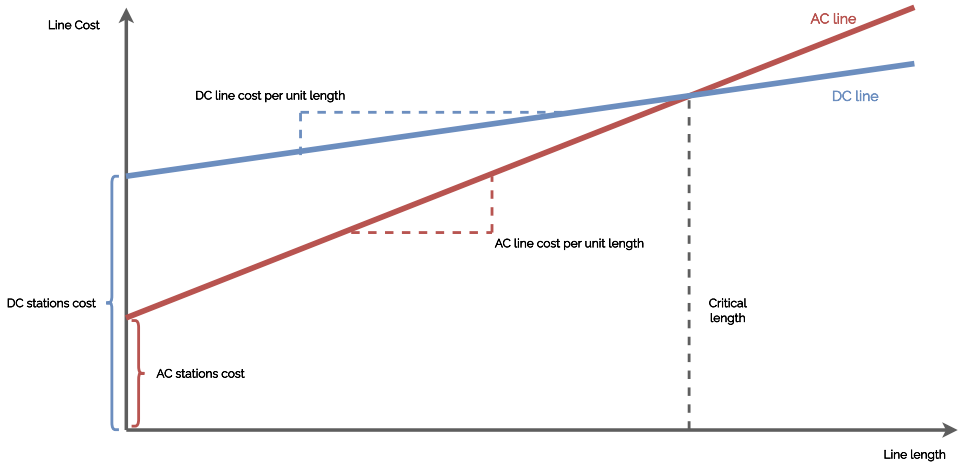

Figure 1.3: Cualitative cost comparison of HVDC line vs. traditional AC line.

2. **Reactive power losses at the lines:** In general, the presence of reactive power, characteristic of AC systems, involves a capability reduction and a cost increase. This issue enhances the previous point: line unitary cost of AC lines is increased so that the HVDC station over cost is more easily compensated for long-distance lines.

   Moreover, not only do the AC loads consume reactive power but also AC lines have capacitive and inductive behavior that have a significant effect when the line is long enough. Then, series and shunt compensation taps are needed to compensate for the reactive power consumed by the lines, making them remarkably more expensive. These reactive power compensation stations are another per unit length cost that makes long AC lines costlier compared to DC lines.

   Electrical lines have parasitic capacitances between conductors and between the conductors and the ground, usually represented as two shunt elements in the classical π-line-model seen in Fig. 1.4. This capacitance (actually, per-unit-length capacitance) takes important values for underground and especially underwater lines. In addition, the high voltages and low currents used for long-distance high power transfer emphasize the capacitive behavior of the lines.

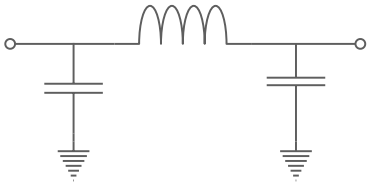

Figure 1.4: π-Model of electrical line.

In general, a permanent reactive component is established through the capacitance in the case of AC transmission. Figure 1.5 shows the current phasors on a line model whose per-unit-length capacitance has been discretized in 3 steps, assuming that the power demanded by the right (receiving) port has unity power factor.

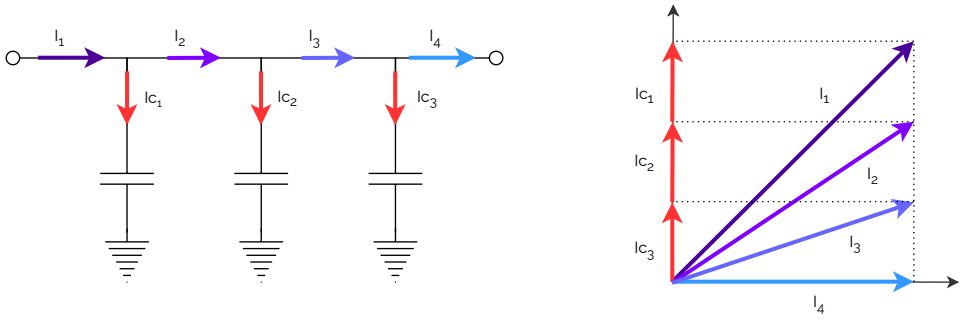

Figure 1.5: Phasor diagram currents flowing through a discretized highly capacitive line.

The line must be sized to withstand the maximum current magnitude, which is significantly higher at the beginning of the line. Therefore, the line would be designed for a much higher current than the one that arrives at the end of the line. In other words, the useful conductor capability is underexploited from the receiver's point of view. Conversely, the capacitance has no steady-state effect on DC transmission. Once the final DC voltage is achieved and the 'capacitor' is charged, it acts as an open circuit, and there is no extra current to flow through it.

This issue becomes critical in places where the line capacitance value gets high values, being the submarine cables the primary instance. For this application, cables would have to be sized up to a conductor section much greater than the section that the useful active power would require, making the critical distance much shorter. In this case, medium-distance submarine lines practically require the use of HVDC. The line capacitance effect impacts all kinds of lines, but the distance at which it becomes decisive is much higher for classical aerial lines.

3. **Grid Synchronization:** The backbone of a well-functioning AC grid lies in its ability to maintain a controlled and consistent frequency across the interconnected network of power generation, transmission, and consumption. Each connected generator contributes to the overall grid frequency, typically maintained at 50 or 60 Hz, depending on the region. Differences in frequency or phase can prevent direct connection of two separate AC grids. By converting AC to DC and back to AC, HVDC systems allow energy to flow seamlessly between grids operating at distinct frequencies, effectively harmonizing their operation.

The importance of grid synchronization is critical for the reliability of power systems. De-synchronization could lead to frequency imbalances, voltage instabilities, and potentially catastrophic blackouts. Stabilization mechanisms are crucial in maintaining grid synchronizationeven under dynamic conditions. Not only does HVDC allow the coupling of unsynchronized systems, but also contributes to stabilizing the grid's frequency when proper grid-forming controls are implemented at the converter stations.

Disadvantages of HVDC transmission

1. **DC/AC conversion complexity:** One of the main obstacles lies in the process of converting significant amounts of power from AC to DC and vice versa, specially when dealing with high voltages. These difficulties traduce to fixed costs related to HVDC stations, which are always higher than the corresponding for an AC station.

   Converting large power quantities while maintaining efficiency and reliability demands advanced high-power electronics capable of seamless switching and minimal energy loss. Such technology come with associated complexities and costs. Despite modern power electronics have significantly enhanced the efficiency of these processes, the challenges of managing significant power and voltage persist, and the economic cost is still high.

2. **HVDC Circuit Breakers:** AC and DC circuit breakers have the same job: interrupting or isolating faulty circuits in case of overloads, short circuits, or other abnormal conditions. However, their operating principles diverge due to the distinctive characteristics of AC and DC systems. AC circuit breakers are designed to extinguish the arc from current interruption during natural zero-crossing points in the AC waveform. In contrast, DC circuit breakers face the challenge of interrupting continuous current flow.

   The absence of zero crossings means the arc generated during interruption persists until deliberately put out. This difficulty demands more robust designs, arc extinguishing methods, and insulation to counteract the sustained arc and maintain safe operation. Ensuring the security of DC grids requires enhancing circuit breaker technology.

1.2. HVDC Converter stations

The distinctions between AC and DC transmission methods have been exposed, revealing the circumstances in which HVDC emerges as the optimal solution. The core challenge (and the associated cost) of HVDC transmission lies in the conversion between AC and DC. This section provides an overview of the technology that drives these converters in order to understand the application of the core converter of the thesis: MMCs.

The core of every HVDC station is the converter that transforms AC into DC and viceversa. Various technologies have been historically used for HVDC systems:

- **Initial systems:** One of the earliest methods designed for HVDC is the Thury system, developed at the end of the 19th century. It was an alternative to AC transmission and power transformers, consisting of series-connected generators to obtain a high voltage, but it had high energy losses and maintenance requirements, leading to its displacement.

  The Mercury-arc valve, developed at the beginning of the 20th century, is the technology that first allowed current rectification for high-power applications. It was predominant in HVDC systems until it became obsolete due to the beginning of high-power solid-state electronics.

- **Line Commutated Converters (LCC):** Since the 70s decade, only solid-state converters have been employed for HVDC applications, and some previous HVDC systems were enhanced with this technology. The first type of solid-state converters for HVDC uses thyristors (silicon-controlled rectifiers) as the main switching devices. This system, shown in the left side of fig.1.6 is currently the most used for HVDC applications.

  They rely on some control signal to switch on and can be turned on at specific points in the AC waveform when the voltage across them naturally goes through zero, which is known as natural commutation. LCCs have limited control over the power flow once the thyristors are triggered. This means that they require an external circuit to extinguish the current. The role of this external commutation circuit is played by the AC power grid to which the converter is connected, that is why these converters are called Line-commutated.

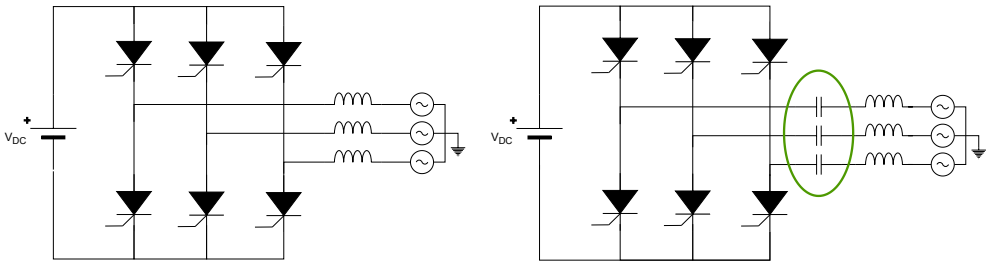

Figure 1.6: LCC (left) and CCC (right) converter structures.

This line-commutated characteristic is shared with the previous mercury-arc systems and made it impossible for these converters to work on passive circuits, they need the presence of traditional AC generators in the circuit to operate as an inverter. It also limits their control over reactive power, which can be critical in maintaining grid stability, especially during contingencies or fault conditions.

In addition, LCCs generate a considerable amount of harmonic distortion at relatively low frequencies in the AC grid due to their abrupt switching action, leading to power quality degradation and increased electromagnetic interference. As a result, LCC stations require the use of bulky filters and reactive power compensators that increase the cost and complexity of the station, limiting their applicability.

- **Capacitor Commutated Converters (CCC):** This system is just an improvement of the LCC that enhances the commutation performance. The upgrading of this system lies in the series connection of some capacitors between the thyristor valves and the AC transformers, as depicted at the right side of fig. 1.6. They reduce the required period of reverse voltage to effectively switch off, a limitation derived from the need for an active AC system to turn off the thyristor valves. Despite the improvements, this system has not become very popular due to the development of VSCs, that overcome the limitations of the line-commutated converters.

- **Voltage Source Converters (VSC):** The voltage source converters consist of other types of semiconductors such as GTO or IGBT that are capable of turning on and off just by employing the control signal. These converters do not need an external active AC system and provide an independent control of active and reactive power, besides some other advantages. For this reason, these systems are expected to totally displace the LCC ones in the near future. This type of converter was employed in motor drives by the last decades of the 20th century, but it was not until almost the change of the century that the development of high-power semiconductors made cost-effective HVDC systems equipped with this technology.

VSCs provide several advantages over LCC ones. The semiconductors used in these converters can be turned off freely; that is why they are also called 'self-commutated' converters. In this way, there is no longer any dependence on the AC synchronous generators, allowing the feeding of passive grids. Neither there is need for power transformers with on-load tap-changers to regulate the AC voltage, which is always required in LCC to keep the thyristors firing angle at their operating range.

LCCs produce a current waveform that is heavily distorted, so filters on the AC side are always required to deal with the low frequency and high magnitude harmonics, which involves high complexity and cost. The filtering task is far more manageable with VSCs even though PWM modulation produces a higher amount of distortion than LCC operation. However, it is displaced to the higher frequency domain, easing the filtering [1]. Additionally, LCC systems require 12-pulse transformers with a dedicated thermal design due to the harmonics involved. VSCs can employ standard power transformers, which are undoubtedly a cheaper solution.

The ability to independently turn on and off makes it possible to generate any voltage wave from the DC voltage source using high switching frequency techniques. Thus, active and reactive power can be controlled independently by modifying the magnitude and phase of the generated voltage. Consequently, the separate shunt capacitors (always used with LCCs) are unnecessary with VSCs.

This ability is essential to provide additional services to the grid and help frequency stabilization. In addition, the possibility of deploying a future multi-terminal HVDC grid and black start capability are some factors that make VSC the best solution. VSCs can be classified depending on the number of voltage levels employed to build the voltage wave intended to be produced:

- **Two-level Converters:** Two-level VSC converter is the simplest and most widely used for HVDC applications. It comprises a simple 6-pulse converter with two semiconductor valves for each phase. It is called 'two-level' because the alternative switching of a pair of complementary switches produces only two possible voltage levels at the output, as seen in the fig. 1.7.

[1] Notably, traditional VSC converters still require bulky AC filters to eliminate harmonic distortion

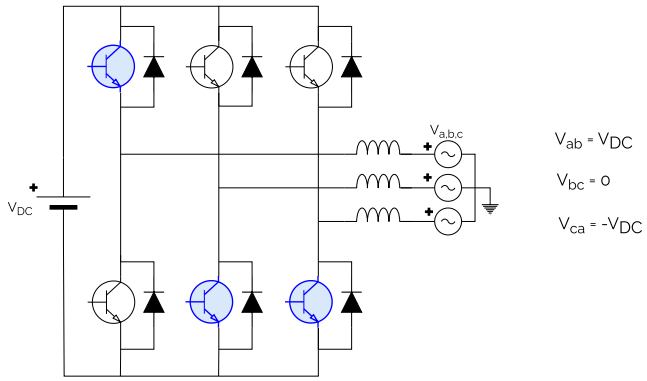

Figure 1.7: 2-level Voltage Source Converter.

By using PWM techniques, this controllable converter can produce an AC output voltage with a high degree of distortion at high frequencies related to the frequency employed for the switching. This switching frequency should be elevated to have lower and easier-to-filter distortion. However, this implies higher switching losses.

In high-voltage applications such as HVDC, each of the six transistor valves is composed of several devices connected in series to withstand the required voltage, and they must switch simultaneously. This switching concurrency is also challenging for this kind of converter, especially with the high switching frequency.

- **Three-level Converters:** Different designs with more voltage levels were developed to mitigate the disadvantages associated with traditional two-level converters, such as voltage stress on semiconductor devices and harmonic distortion. Introducing multiple voltage levels generates waveforms closer to a perfect sinusoidal (lowering the distortion), while the voltage held by each valve is reduced.

  One common three-level configuration is the Neutral point Clamped Converter (NPC), which can produce three different voltage levels. NPC converters use clamping diodes in parallel with the semiconductor switching devices, providing additional voltage levels between the DC bus voltage and the neutral point (usually the midpoint of the DC bus). Another typical three-level arrangement is the 'Flying Capacitor Converter'. FCCs use a series of capacitors connected between non-consecutive semiconductor switches to generate multiple voltage levels. Both structures are shown in fig. 1.8.

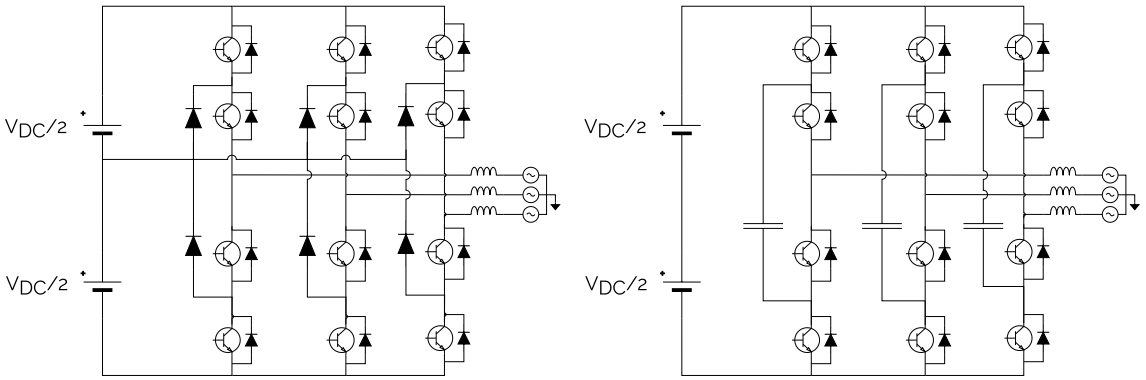

Figure 1.8: 3-level classic structures: NPC, FC.

Both schemes can be upgraded with more voltage levels to synthesize a multilevel output voltage waveform, typically consisting of several discrete voltage levels. However, these converters have not been very diffused for HVDC applications due to the low harmonic improvement compared to the additional complexity that exponentially increases with the number of additional voltage levels.

- **Multilevel Converters:** To reduce output distortion, converters with more voltage levels have been developed. This technology allows using low voltage devices to produce several low voltage steps. When combined, a higher voltage output is obtained, with such a low distortion level that filters could even be avoided.

  The Cascaded H-Bridge is the predecessor of the Modular Multi-Level Converter, the core of this project. Each of the voltage steps of the Cascaded H-Bridge is obtained by a classic H-Bridge containing an isolated voltage source that can be switched on and off from the circuit. The structure of the module and its operation is very similar to that of the MMC that will be explained along this chapter.

  The main issue of this converter is the isolated voltage source, that is challenging to obtain. Usually, each voltage source is given by a three-phase classic rectifier. These rectifiers are connected to a power transformer composed by a primary winding and several secondary ones, one per each source. In this way, each source is electrically isolated from the others. That is why this converter is not bidirectional.

- **Modular Multilevel Converters (MMCs):** It is a multi-level converter family member that was developed by A. Lesnicar and R. Marquardt by the beginning of 21st century [7]. The name of the converter actually describes its basic characteristics: it is composed by a number of identical modules and it is capable of generating several voltage levels.

It is a VSC type converter that, by the series-connection of several low voltage modules, produces high voltages between its terminals. The constant voltage of each module can either be bypassed or kept connected at the main circuit. This is how the total high voltage produced by the array of modules is controlled.

Compared with the cascaded H-Bridge, the MMC does not need several isolated sources, which is technically complex. The voltage sources are substituted by the capacitors, which store and provide the energy required.

However, MMC retains the advantages of modularity and scalability of the cascaded H-Bridge. Indeed, they are far more applicable, allowing to connect hundreds of cells in series. That is why they are especially suitable for very high-voltage applications.

1.2.1. MMC comparative with other converters

Before deepening into the details of MMCs, it is necessary to explore its advantages and disadvantages to prove why this converter is the most suitable for HVDC applications. VSCs stand out as a superior choice compared to LCC within HVDC systems, thanks to the ability of generating the output voltage waveform at will. Their convenience in terms of complexity, operation, and cost positions VSC converters as the favored technology for modern HVDC applications. Among these converters, MMC is a promising technology for high voltage applications due to the several benefits summarized hereafter. Most of these advantages are derived from the unique feature of being composed of many simple identical cells.

- The modular structure makes it very robust, as the failure of a single cell does not affect the whole converter and can be easily substituted by a non-faulted one. In fact, by including some redundant modules, the converter's operation would not be perturbed by the failure of a statistically normal amount of cell failures. Any cell can be permanently bypassed in case of fault if an external bypass contactor is added to each submodule.
- High scalability of the system. Each module implies one of the multiple low voltage steps that, when series connected, build up the characteristic high voltage. This way, the converter can easily reach higher voltages by adding more modules to the system without essential modifications.
- Each module's voltage step does not depend on an isolated voltage source [8], which is problematic, as with other multilevel converters. The voltage of each cell is produced by capacitors that periodically suffer charge and discharge processes.

- The independent connection and disconnection of the proper modules allows for producing a nearly perfect sinusoidal waveform with minimal harmonic distortion, without increasing the switching frequency at the individual submodules. Usually, no filters are required due to low distortion levels, which contrasts with most other converter types that do require filters.
- Each module has relatively low voltage rating when compared with the total line voltage. Thus, module connection or disconnection produces a small voltage step, and the output has low values of voltage slope (dV/dt).
- Classic two-level valves comprise several series connected transistors to withstand higher voltages. For the proper operation of these converters, simultaneous switching of all transistors at each valve is needed, which implies considerable complexity. Conversely, in MMC, the connection of each module is not subject to the rest of the modules, so the switching of the transistors is independent.
- The short-circuit current is critical because DC circuit breakers are problematic and expensive. At MMCs, it is limited through the arm inductance. When a DC fault is produced, power flows from the AC to the DC side through the arm inductors, and they help reduce the rate of rise of fault current, simplifying the breaker operation. In this regard, it should be introduced that a module variation named 'full-bridge' temporarily stops this current at the beginning of the fault, providing better protection.
- In a traditional two-level converter, switching losses at the semiconductors are much higher than the conduction losses; however, in MMC, the opposite is true. The switching is produced at the low-voltage module, resulting in an increased efficiency of the MMC compared to the 2-level converter, going from around 98% to 99,5%. In high-power applications, this improvement could make a difference in operation costs and cooling systems.
- The combined energy storage of each submodule makes the presence of a bulky DC-link capacitor unnecessary, as it is in other converters. The absence of this concentrated capacitor avoids the damage associated with high surge currents in the case of a DC-side short circuit [8].
- Finally, the converter is bidirectional: the same structure and control can be used as a rectifier and inverter. It is just a matter of generating the proper voltage wave.

Every system has some drawbacks that should be considered as well. This converter has some limitations derived from the vast number of modules involved:

- First of all, using a high number of components implies a high cost. Each module requires, apart from the switching devices and the capacitor, its driver, protection, sensors, etc. Therefore, the investment for this type of converter is comparatively high. However, it should be noted that the remarkable reduction in filtering requirements cheapens the station cost. In addition, chain manufacturing of many identical modules is very convenient, and the efficiency is higher (due to the low switching losses), reducing the operative costs.
- The amount of components also reduces the system reliability as module faults are relatively probable. Therefore, it is necessary to add redundancy modules and bypass switches to have a high level of system availability so the operation of the converter is rarely compromised.
- The control algorithm is complex as it involves the independent control of several components. However, the control strategy is repeated for all cells.
- The capacitors are energy storage devices, and their energy (and, therefore, voltage) balance must be ensured for the proper operation of the converter.
- The operation of the converter involves a circulating current, which entails power losses and stress on devices.

2 | MMC theoretical background

2.1. MMC structure

2.1.1. MMC Architecture

MMCs were first proposed in [7] as a new converter topology whose main technical feature is its modular structure, producing an output waveform with several voltage levels. It is composed by a number of identical modules connected in series. The first step is to describe these modules; and then, how these cells are connected.

MMC cells

The submodules (or cells) that compose the converter, can be considered as controlled voltage sources. They consist of a DC energy storage element (capacitor) with a two-terminal connection through switches that allow the insertion of either zero or the full DC voltage into the circuit to which they are connected.

The converter is built by a series connection of a number of these cells and the total voltage in the circuit will depend on the quantity of them that are simultaneously switched on[1]. Each cell usually has a bypass contactor, that allows the permanent bypass of a cell in case of failure, without shutting down the whole converter. Thus, if designed with some degree of redundancy (with more modules than strictly necessary) MMCs are fault-tolerant and provide high availability to the system, as can work without interruptions despite the high number of elements involved.

Different types of submodules have been developed for this converter. The first and most basic one is the Half-Bridge (HB) cell. Its simplicity is also the reason why it is the most popular solution. It consists of two complementary switches that connect and disconnect the cell's capacitor into the circuit, as is observed in fig. 2.1.

[1] In addition, it is possible also to freely control the voltage at each of the modules. However, it is usually better to keep the same voltage for all of them, which ensures equally distributed stress.

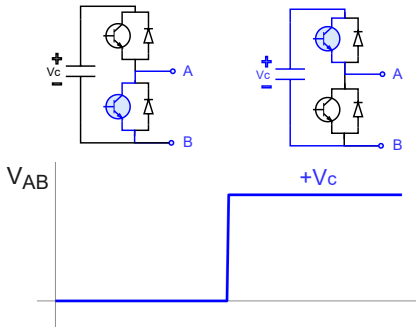

Figure 2.1: Half-Bridge submodule.

The switching elements are generally composed of a bipolar transistor (IGBT) with an anti-parallel diode. These switches only allow a short-circuit connection or the insertion of the capacitor between A and B, but it is not possible to achieve an open circuit at the terminals.

An evolution of the HB cell is the Full-Bridge (FB) cell, which gets its name because it looks like a classic bridge used in traditional inverters. It is composed of two pairs of complementary switches, unlike the HB module with just one pair.

The possible switching combinations of the FB module allow the connection of the inner capacitor with both polarities to the cell ports, as seen in fig. 2.2. This feature adds more possibilities (along with more complexity) to the control strategy of the converter.

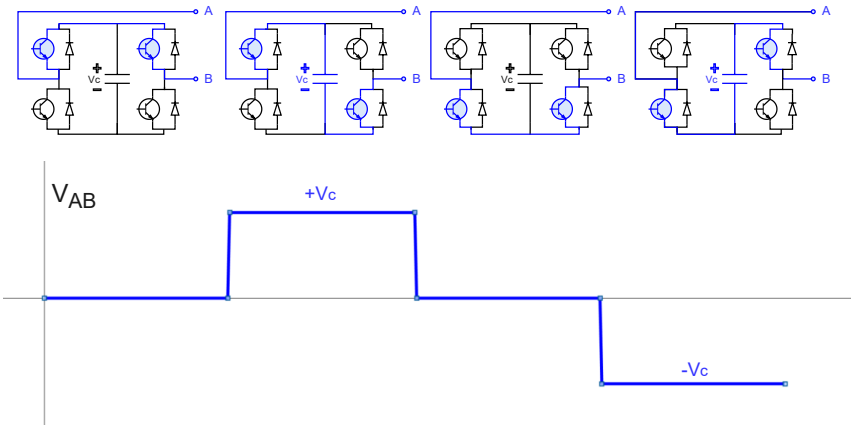

Figure 2.2: Full-Bridge submodule.

The main enhancement lies in the possibility of temporarily blocking short-circuit currents from the AC side to the DC side, as it is possible to disconnect both sides if all IGBTs are simultaneously switched off. Additionally, it offers some features that make it interesting for some applications [13] such as the connection of photovoltaic or wind

turbine generation systems to the grid. It can either increase or decrease the DC voltage (buck and boost function), making the AC and DC voltages independent from each other, making it possible to remove the grid transformer of a wind turbine.

However, it has not been as popular as the HB because the number of switching elements is doubled for the same number of voltage levels. This issue implies an important increment in conduction losses and, especially, in the converter cost.

Other structures have been developed to overcome some of the disadvantages presented by the previous ones. Clamp-Double-Submodule is a compromise solution that implies a modest increase in losses and costs compared to HB modules. In fault conditions, the middle transistor is switched off to clamp the voltage, blocking the short-circuit currents. This solution is interesting for applications in which shorting the DC-fault clearing times is required, such as HVDC multi-terminal networks [8] and the expense of the system remains a critical factor. However, the complexity of the system increases.

MMC topologies

MMC converters are constructed by the series connection of several modules. Each string of modules is usually called in bibliography “arm” or “cluster”. The arrangement of these strings determines a different structure with its own features and applications.

There are two basic structures of the converter, one has three strings (one per phase) and the other has six (two per phase). The 3-string structures always require by FB modules, contrary to the structures that have six strings, that can be either built by FB or HB cells. All of the structures include at least a reactor in series with each submodule string, essentially required for current controlling and limiting purposes.

Three-terminal circuits, the simplest MMC configurations, resemble three-phase load shunts linked to the grid. They lack connection to a single DC source, rendering them impractical for power transmission or motor drives unless multiple isolated DC sources like batteries or solar panels are connected to the submodules [2]. Their applications are essentially energy storage and reactive power balance.

These circuits can be arranged in star or triangle configurations, each comprising three strings of series-connected FB submodules, linked to the AC system through arm reactors. FB submodules are crucial for enabling reverse polarity connection. The Single-Star-Bridge-Cell (SSBC) and Single-Delta-Bridge-Cell (SDBC) are the two basic configurations, seen in fig. 2.3. SSBC employs a star configuration with a floating neutral point, while SDBC utilizes a delta configuration without a neutral point.

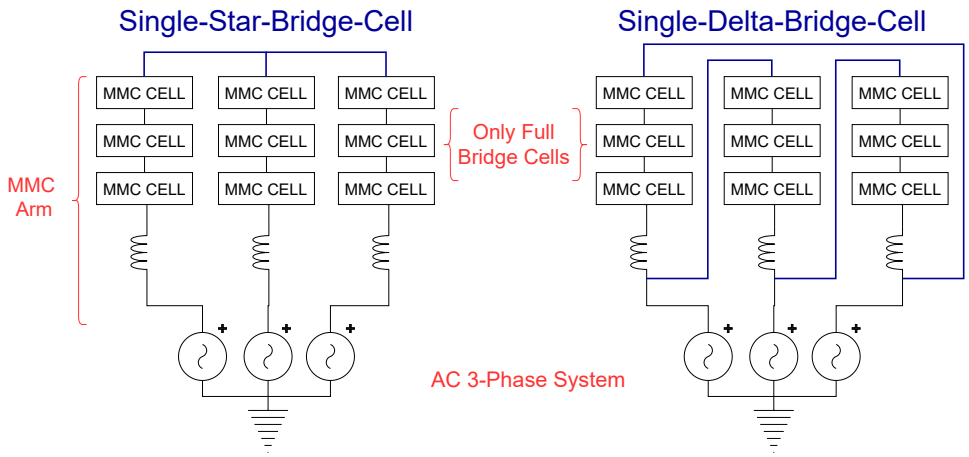

Figure 2.3: Single-Star / Single-Delta Bridge Cells.

The star/delta connection presents cost and application variances. Having identical blocking voltage and converter power ratings, SSBC requires fewer cells than SDBC, making it cheaper. SSBC's neutral point allows for the introduction of a zero-sequence voltage, beneficial for tasks like SOC balancing in batteries or voltage balancing in STATCOM applications [1]. However, SDBC is necessary for controlling negative-sequence reactive power, a capability SSBC lacks [2].

Five-terminal circuits are composed by the connection of two Single-Star circuits to the same AC network. The two neutral points of the star-connected circuits provide the two extra terminals to which it is possible to connect a single DC source. This feature provides the capability to transfer power between two systems in applications such as motor drives or HVDC [1].

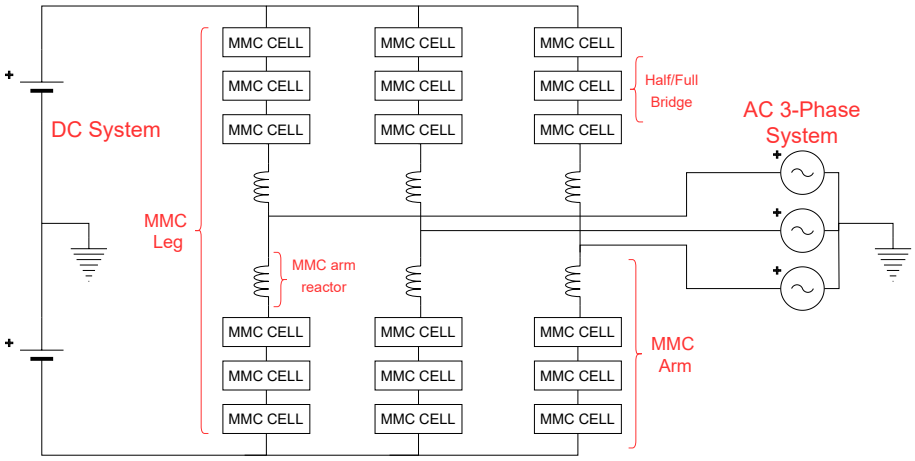

Figure 2.4: Five-terminal MMC structure.

As shown in fig. 2.4, there is one vertical leg for each of the three AC phases, all of them connected to the same DC source. These legs are composed of an upper and lower arm, formed by an identical number of series connected submodules.

The arms of each leg are connected by a reactor to the corresponding AC phase[2]. The arm inductance is important to control the power transmitted between the converter and the AC system. A crucial function is to limit the short circuit current raise in case of fault. In addition, it limits the harmonic circulating current.

2.1.2. MMC Operation

Each arm is composed of several modules connected in series. By the connection or disconnection of these submodules, a wide range of discrete voltages can be obtained. With a high enough number of cells, this set of discrete values can be seen as nearly continuous from a high-voltage point of view. In addition, it is possible to use PWM at each voltage step, so virtually any voltage value can be obtained.

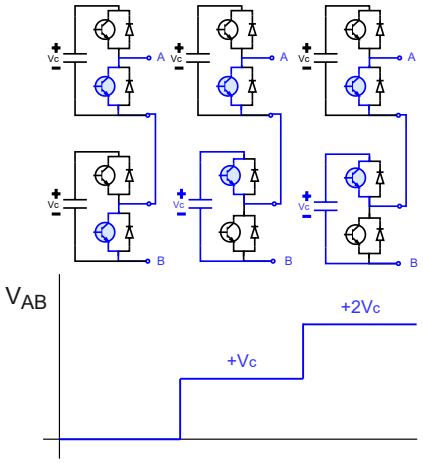

Figure 2.5: Half-Bridge arm operation.

Fig. 2.5 shows graphically how an arm composed of 2 HB cells can generate 3 different voltage values. In general, HB modules can generate voltages from 0 up to $n_{cells} \cdot V_c$, being V_c the voltage step. FB submodules are capable of connecting the capacitor in both polarities. Then, an arm composed of 2 FB cells can generate 5 different voltage values, ranging from $-n_{cells} \cdot V_c$ up to $+n_{cells} \cdot V_c$, as shown in fig. 2.5.

[2]The system can be slightly modified by using a center-tapped inductor for each phase. In this way, the size and weight is lower, which is of great importance for many motor drive applications [1].

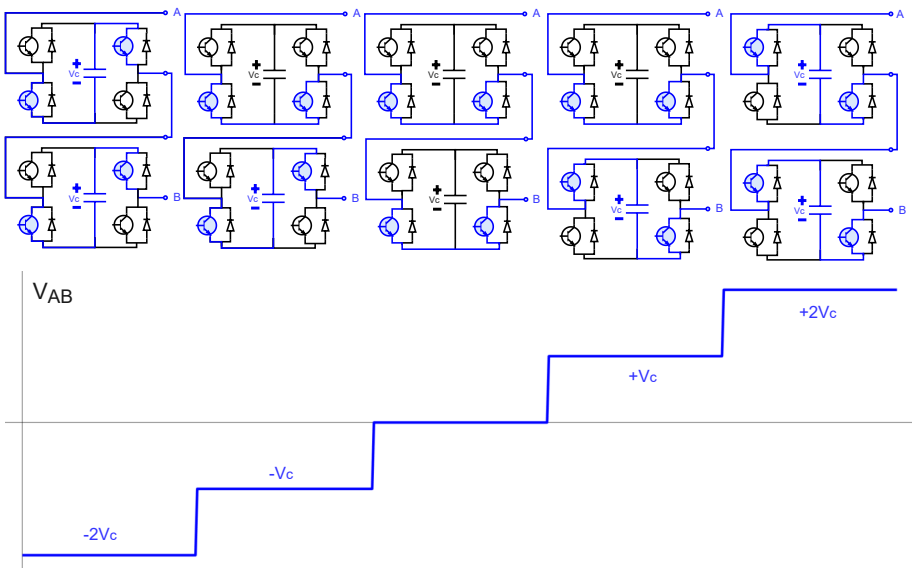

Figure 2.6: Full-Bridge arm operation.

An arm composed of HB cells always has a positive DC offset value. On the contrary, this DC offset with FB modules can either be positive, negative or zero, providing more flexibility in operation.

In general, with the proper gate signal the arms can produce any voltage value within the allowed range. This is why each arm can be considered an independent fully controllable voltage source. With a sufficient number of modules, the harmonic behaviour can become so good that no filter is needed.

The converter arms are controlled to produce the voltage wave required to transmit the desired power. Considering each phase independently and with the mid-point of the DC link grounded as in fig. 2.7, it is possible to determine the voltage that should be applied to the MMC arms.

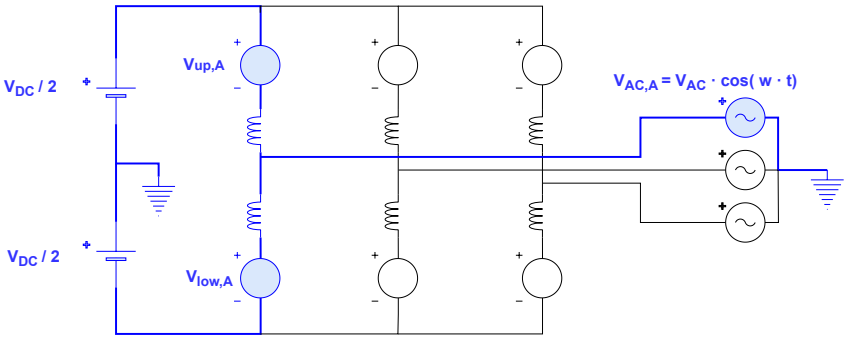

Figure 2.7: Monophasic simplified analysis of MMC operation.

For this simplified analysis, the arms are modelled as ideal voltage sources and the voltage drop at the arm inductors is neglected[3]. Then, for the rectification/inversion, the controllable sources of the arms must provide the exact voltage difference between the expected/desired voltages at the DC and AC sides as in eqs. (2.1), (2.2). Both upper and lower arm voltage sources are the sum of a DC value and a sine wave (with different signs), so the result is a sinewave with a DC offset.

$$V_{arm,UP,i} = \frac{V_{DC}}{2} - V_{AC} \cdot cos(\omega t + \phi_i) \tag{2.1}$$

$$V_{arm,LOW,i} = \frac{V_{DC}}{2} + V_{AC} \cdot cos(\omega t + \phi_i) \tag{2.2}$$

The modulation index can be defined as the ratio between the line-to-ground AC amplitude and half the value of the DC link. In normal operation, the maximum value is 1, meaning that the maximum AC voltage amplitude that can be produced by this converter is exactly half the DC voltage, as shown in fig. 2.8.

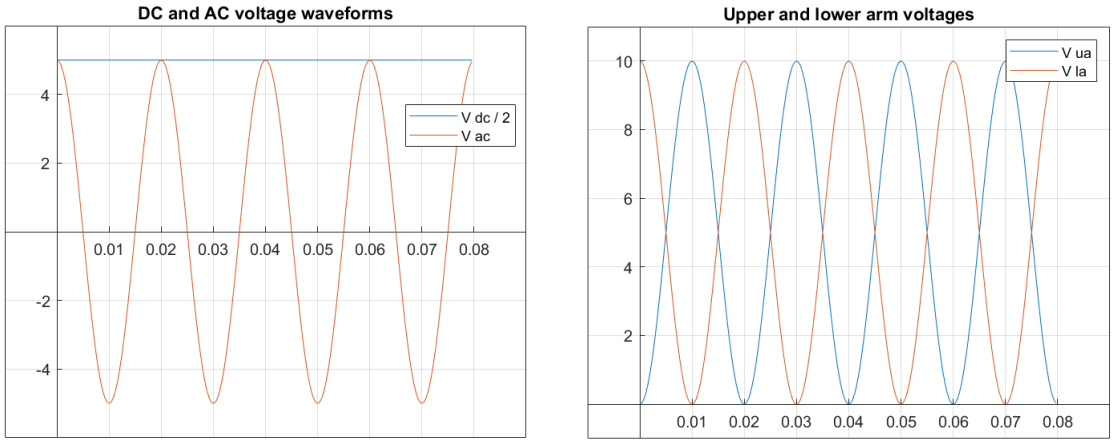

(a) (b)

Figure 2.8: MMC voltages in normal operation.

This condition ensures that the arm voltages are always positive so HB modules can produce it. However, this 'normal operation conditon' may not be always fulfilled, for example in case of some kind of perturbation that decreased the DC voltage (a DC short-circuit in the worst case).

[3]Indeed, if no impedance is considered and the voltages produced at the arms were the indicated below, no power would be flowing through the system. Actually the phase and amplitude difference of the voltages would produce the current to flow through the circuit.

In this case, the required upper and lower arm voltages will take positive and negative values as shown in fig. 2.9. HB modules can only generate unidirectional voltage, so an arm composed by HB modules would not be able to produce such wave.

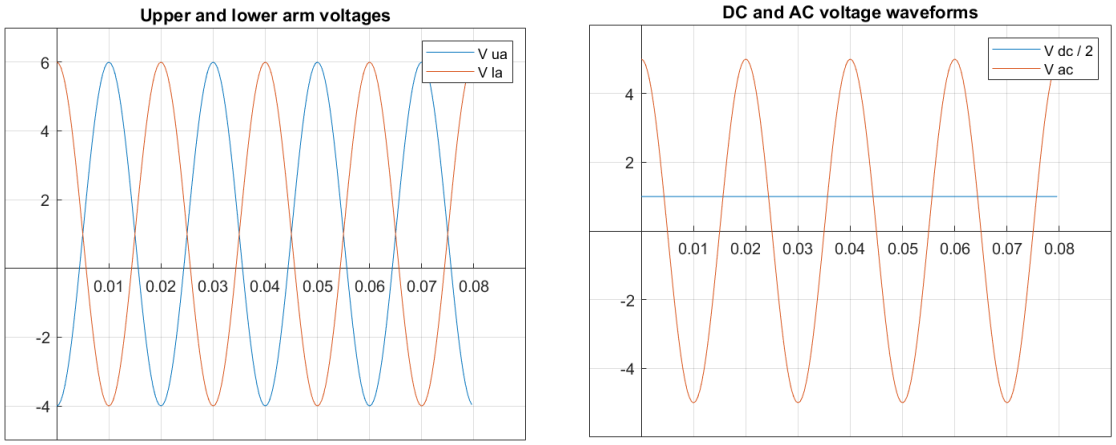

(a) (b)

Figure 2.9: MMC voltages with reduced DC voltage (over-modulation).

In this situation, with FB modules, the energy stored at the modules' capacitors can be used to produce a voltage opposed to the difference between AC and DC side. This maintains the operation of the converter, at least for some time. Eventually, the energy stored at the capacitors will get too low to continue operating. But, the protection devices would have time enough to act without the presence of high short-circuit currents.

FB converters protect the converter from DC faults by preventing high short-circuit currents to arise at the first instants of the fault, which leaves some time for the AC circuit breakers to interrupt the fault current before reaching dangerous values.

On the other hand, a further understanding of the converter requires analysing the current that flows through the converter arms. It comprises different frequency components:

- From an inverter point of view, the current flowing into the AC system is the 'load current', which transfers power to the AC side at the fundamental frequency. The symmetry of the converter means that each arm carries half of the corresponding phase's load current, as shown in fig. 2.10a. This current can be assumed to be almost a perfect sinewave.
- A DC component is required to transfer active power from the DC side to the converter arms and maintain the power balance. MMC arms are formed by cells whose energy source is a capacitor, which are charged or discharged when current

flows through them. The net energy growth at each of the arms should be zero for a complete cycle during regular converter operation. If the energy stored at the arm varied, the capacitor voltages would diverge from the operation point, compromising the capability of generating the required voltage (or even the system's security).

The DC circulating current drawn from the DC side is equally divided and flows through each converter leg's upper and lower arm, as shown in fig. 2.10b.

- Finally, some harmonics can be found at the current arms, with the second-order harmonic being the dominant one. When looking at the arm energy evolution, it can be seen that some energy exchanges occur at the fundamental frequency and some at twice the fundamental frequency. The power fluctuation at the fundamental frequency is equal but opposite at the two arms of each phase, which indicates that this energy does not go out of each leg; it flows between the upper and lower arms of each phase. The second harmonic means an energy exchange between the phases at the second-order harmonic frequency. Therefore, as shown in fig. 2.10c, a corresponding harmonic current will flow between the converter legs, while the DC side and AC side systems will not perceive it.

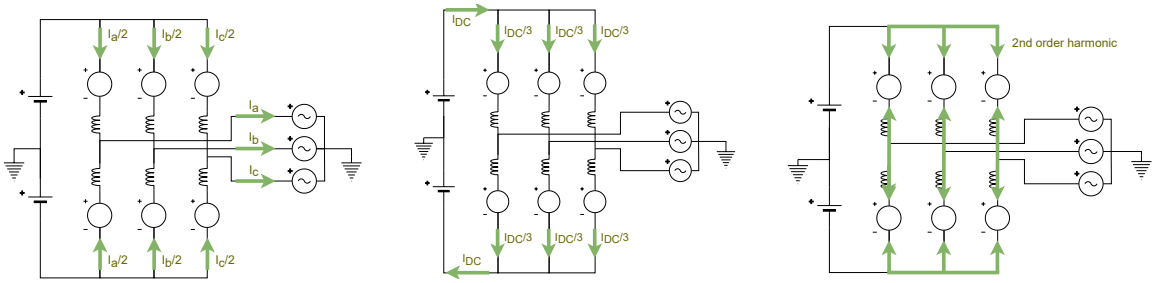

(a) (b) (c)

Figure 2.10: MMC voltages with reduced DC voltage (over-modulation.

Finally, it is necessary to introduce an important concept regarding the selection of connected and disconnected cells: the individual capacitor voltage balance. An ideal capacitor can be modelled through $I_c = C \cdot \frac{dV_c}{dt}$. When positive current flows in the direction of the positive pole, capacitor voltage increases, and vice versa. The connected capacitors at each instant will suffer a voltage variation. These variations must be compensated to maintain all the capacitor voltages within certain limits; otherwise, the converter output would be distorted. This has to be taken into account at the modulation algorithm.

Several modulation techniques have been proposed in literature [12]. Generally, the different modulation types are classified by the switching frequency between fundamental

frequency and Pulse-Width-Modulation (PWM) techniques. Lower switching frequency involves lower switching losses but also lower output quality The modulation techniques applied to an MMC have to consider not only the voltage wave produced but also the voltage balance between the submodules' capacitors.

Some techniques, such as PS-PWM, inherently apply the same duty cycle to all the submodules, making the load ideally shared and the losses identical in all cells. However, the capacitors' voltage balance still needs to be ensured, requiring an additional controller. The major part require a sorting algorithm that selects the capacitors with lower voltage when the direction of the corresponding arm current is in "charging" mode and vice versa. On the other hand, it is also possible to control each submodule with an individual reference signal, so there is no need to implement a sorting algorithm.

2.2. MMC applications

Chapter 1 already introduced the main application of MMCs: HVDC transmission in order to provide the necessary context to the thesis and place the value to research in MMCs. Understanding why HVDC (and therefore MMCs) are important for the development of a more sustainable electrical system is essential to clarify the purpose of what is done along the project. However, not only HVDC is not the unique application of MMCs, but also it is not the only application regarding DC transmission. This section provides an overview of the different uses of MMCs found in the bibliography.

2.2.1. DC energy transmission

HVDC lines

As found in the vast bibliography about MMC, one of the main applications of this converter is HVDC power transmission systems, as it overcomes its challeneges, as exposed in section 1.2.1. The MMC application to HVDC is studied in [3], addressing design, semiconductor rating, and efficiency.

MT-HVDC networks

Multi-terminal (MT) HVDC configuration is an arrangement where more than two converter stations are implied. They are usually connected in parallel, especially for larger-capacity stations. All stations in a parallel share a common DC link that can be arranged radially or meshed.

Extended HVDC networks are possible solutions to integrate solar and wind power generation into the electric system [9]. However, this promising technology still has some technical difficulties, especially the ones related to DC fault clearing.

DC failures are especially critical in MT-HVDC, as it is undesirable to compromise the operation of the unfaulty part of the DC network. The most employed method is to limit the currents using the arm inductances and acting on the AC switches, but time required to trip the AC switches requires disconnecting every station at the grid. Fast-acting DC switches are complex to manufacture and they would make no significant difference in clearing times. Electronic switches are an alternative, but their cost would constitute nearly 50% of a complete converter station [9].

However, it is possible to electronically act at the MMC converter itself, limiting the DC-fault currents fast. FB cells double the number of semiconductors but can cut the fault currents by applying the proper polarity to the modules. The MMC stands as the best alternative for this scenario, not only for its effectiveness, but also for employing the converter infrastructure itself, reducing the cost.

MVDC

The advantages of HVDC transmission are leading to the investigation of complementary technologies that will work together to meet the demands of the electric system. One of the most remarkable is the Medium Voltage DC (MVDC) grid, and the benefits of MMCs can be transferred to this grid's requirements.

One of the most significant applications of MVDC grids working along with HVDC transmission is the collection of energy from scattered energy sources, which are also far away from the consumption point, as in offshore wind power plants (WPPs). The MVDC grid also benefits from submarine DC transmission, and the distributed operation is easier to control than in AC transmission [6], enhancing its adequacy for this application.

In general, the fast increase of distributed renewable energy sources can be integrated by MVDC grids that interface the HVDC transmission lines. In addition, demand for DC loads is also expected to increase, for which medium voltage DC transmission lines will be essential to [15]. DC/DC converters are crucial in handling the power flowing through the DC grid [14]. MMCs have several characteristics, such as modularity, redundancy, efficiency and good harmonic performance, that make them a perfect choice for this application.

However, to work as a DC/DC converter, its structure and control must be slightly modi-

fied. [6] studies a configuration where an AC stage with a classic AC transformer changes the voltage levels between two DC grids. A monophase MMC converter can interface these medium and high-voltage DC and AC systems. The relationship between the number of connected and switching modules provides the elevation ratio. [5] developed unique modulation methods for this application, which proved very efficient.

2.2.2. Renewable energy integration

One of the inherent challenges of renewable energy lies in the geographical dispersion of these resources. They are often found far from major population centres where energy consumption is highest. When the distance is long enough, HVDC transmission often emerges as the most economical and, at times, the only viable option. The most evident case is the transportation of the energy generated by offshore WPPs to the coast. Submarine cables, which connect these installations to the mainland, almost invariably require MMC-based HVDC systems to facilitate the efficient integration of offshore wind energy.

However, HVDC connection of offshore WPPs and remote renewable sources is not the only scenario where MMCs can be applied. They can incorporate solar power through their modular structure, accommodating a set of solar panels to each submodule.

In this way, each set of panels can be equipped with a dedicated DC/DC converter with its own MPPT algorithm (contrary to the traditional multi-string structure), optimizing the efficiency.MMC's modularity provides flexibility, allowing seamless power plant expansion. Redundancy is another notable asset; if one submodule faces an issue or malfunction, the rest of the system continues to operate.

The result is an efficient, scalable and robust system that adapts to varying sunlight conditions and contributes to grid stability by delivering a high-quality voltage waveform. However, it's important to note that this advanced configuration involves a higher upfront investment than conventional PV systems.

2.2.3. Energy storage

Non-controllable renewable sources such as wind and solar power are notorious for their intermittency, generating electricity when the elements align but not necessarily when consumers demand it. This misalignment underscores the need for energy storage solutions to integrate renewable energy into the grid. Furthermore, energy storage enables ancillary grid services, such as frequency regulation and voltage support, which are pivotal in maintaining the grid's equilibrium.

The traditional centralized structure of electrical batteries faces certain limitations, particularly in terms of cost-efficiency, which have slowed its widespread adoption. MMCs emerge as a promising technology to overcome these challenges using their modular structure to integrate low-voltage batteries at each submodule (as with the PV panels). This approach takes advantage of the flexibility, enhanced availability, reliability, and superior harmonic quality of MMCs, along with a simplified structure without transformers and bulky filters.

Moreover, the high voltage achieved allows the storage of substantial amounts of energy with a low current rating. Such an advantage significantly prolongs the batteries' useful life while minimizing energy losses during storage.

2.2.4. FACTS

Some recent developments in power systems are going toward enabling the existing electric infrastructure to use its total transmission capacity and providing operational flexibility. FACTS (Flexible AC Transmission Systems) technology optimises the flow of electricity through the grid by dynamically controlling AC critical parameters, such as voltage, phase angle, and impedance. MMCs, with their modular structure and precise control capabilities, offer an ideal platform for FACTS technology. This converter allows for high-voltage applications with the flexibility provided by the modular structure.

STATCOM

STATCOM (Static Synchronous Compensator) is a FACT device whose objectives are providing reactive power support and voltage regulation to the AC grid. The STATCOM can actively inject or absorb reactive power into/from the grid, which produces local variations in the AC voltage amplitude at the connection point. This operation allows the MMC to support the stability and quality of the AC grid and maintain the desired voltage levels, compensating for voltage disturbances. Additionally, reactive power support can improve the use of actual lines for active power, increasing the effective transport capacity. This capability can be employed in grid voltage regulation, particularly in high-voltage applications where MMC technology is extensively utilized. This application has been practically implemented in section 3.3.3.

UPFC

Unified Power Flow Controller (UPFC) is another example of FACT that is gaining popularity as it allows control of the reactive power flow and the active one through defined

lines. It is an advancement from the previous STATCOM combined with another FACT concept: Static Synchronous Series Compensator (SSSC). Additionally, it allows fast-acting regulation, improving the transient stability of the system (active power control) and voltage regulation (reactive power control).

UPFC has been traditionally built using three-level VSC. MMC is an exciting alternative [4], as it allows avoiding the zigzag transformers required with 3L-VSC, which imply a higher cost and additional energy losses, as well as a reduction in the converter lifespan. In addition, MMC provide the modular structure currently demanded for power systems' reliability and scalability, along with the superior harmonic performance.

2.2.5. Other applications

The number of applications where MMCs can be employed is large, as it is the best solution for high-voltage and power converters where the benefits derived from the modular structure are decisive. The main applications have been detailed, although many others, such as high-voltage motor drives or active filters, can be named. Therefore, the importance of research and testing with MMCs can be validated, justifying the work done in this thesis.

3 | System description

Up to this point of the thesis, the purpose of MMCs has been defined, along with its general structure and operation. As introduced, the objectives of this work are to start up a laboratory prototype of the converter and run it in three classic operative scenarios in which it can be employed. In this way, the work serves as the base for further research with the prototype.

This chapter describes the prototype, from its structure to its components. Then, it addresses the simulation model developed to represent it accurately in Simulink and study the system's response before testing it in the real bench. The energization issues and the circuitry implemented to deal with them are exposed.

A series of test scenarios were defined to conduct the experiments, each designed to evaluate specific aspects of the proposed control systems. The parameters and operating conditions were selected to ensure the validity and reproducibility of the results. These scenarios are described at the final part of the chapter, detailing the control mechanisms developed, which leads to the results exposed in chapter 4.

3.1. Simulation model and experimental set up

3.1.1. Imperix MMC test bench

The empirical results of the thesis were obtained using the MMC test bench provided by Imperix. The converter system, seen in fig. 3.1, offers a reliable and versatile platform for conducting experiments in power electronics.

It comprises 24 individual converter modules, which are interconnected to form a multilevel converter topology. The control system manages the system and communicates through the ADC channels and PWM optical outputs. The converter includes the arm inductors through which it can be connected to the desired grid or load on the AC bus.

Figure 3.1: Imperix MMC test bench at UPV laboratory.

The following is a description of the main elements of the experimental setup:

1. Converter submodules: The heart of the MMC test bench consists of multiple converter modules constituting the multilevel topology. The MMC prototype consists of four submodules at each arm, resulting in 24 for the entire system. Fig. 3.2 shows the interconnected submodules of one phase.

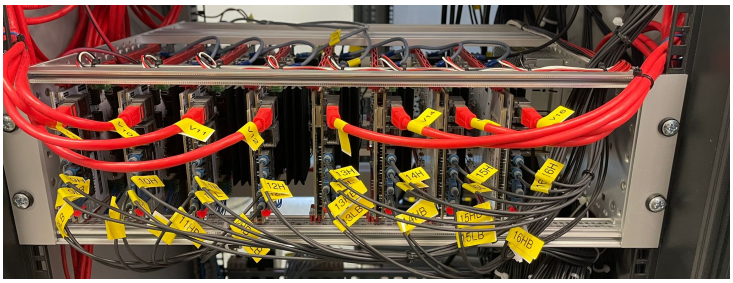

Figure 3.2: Phase B submodules rack.

The submodules offer robust power conversion capabilities for high-power applications, with switching frequencies up to 50 kHz. The rated voltage for each submodule

is 400V, and the current is 10A, although it can withstand up to 50A. Depending on the connection of their terminals, the modules can be arranged in Full-Bridge or Half-Bridge configuration, which is more straightforward for this project. The switches are composed of IGBTs and antiparallel diodes, that connect or bypass the 1.35 mF capacitors.

They include embedded protection and safety features to safeguard the system, including overcurrent protection, overvoltage protection, and temperature protection. The voltage and current measurement, and the respective communication interfaces allow for seamless integration with the control system.

2. Control system: The Imperix Bbox (fig. 3.3) is an advanced and versatile hardware platform designed for power electronics R&D. It incorporates high-performance DSPs, FPGAs and other integrated circuits to handle complex calculations and execute control algorithms efficiently, enabling real-time control. The Bbox provides various communication interfaces such as Ethernet, through which it is connected to the computer to transfer the code and retrieve the sensed data.

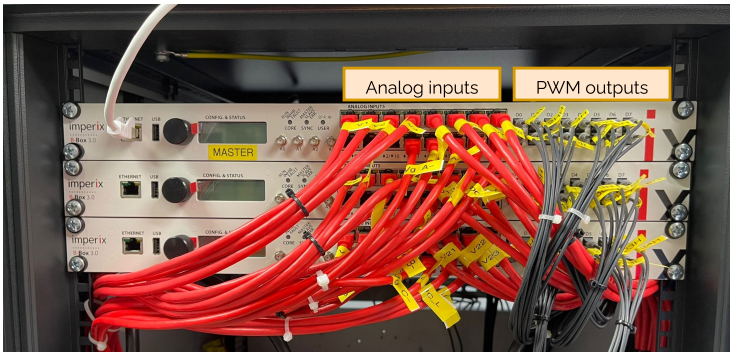

Figure 3.3: Imperix BBox.

The multichannel ADCs and optical PWM outputs allow for the simultaneous acquisition and generation of multiple signals. The ADC channels can be configured with safety thresholds that turn off the PWM outputs automatically. Analog low-pass filters can be configured at each channel at various cut-off frequencies.

3. Power sources and load circuits: The experimental setup includes the test bench connection to the necessary power sources and load circuits. External power sources are required to provide the necessary input power for the MMC test bench. The configuration of these sources is exposed in 3.2. On the other hand, load circuits represent the electrical loads or systems being powered by the converter. For the experiments conducted, the load circuit employed has been either a resistive circuit

(fig. 3.4b) or the AC grid itself connected through an autotransformer (fig. 3.4a). The arm inductors of 2.3 mH serve as interface at the AC bus to connect these circuits.

(a) Grid-connected autotransformer.

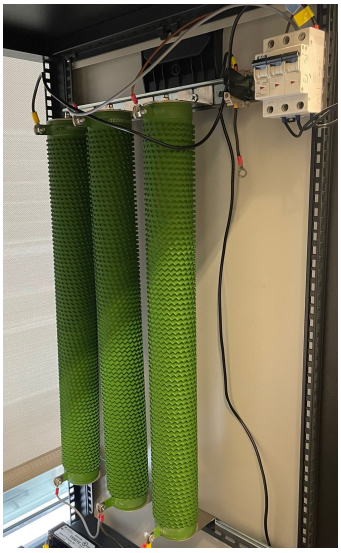

(b) Resistive loads.

Figure 3.4: Power sources and loads for test bench.

4. Measurement devices: Various sensors (fig. 3.5) are integrated into the setup at different points within the system to capture and monitor real-time measurements through the data acquisition system.

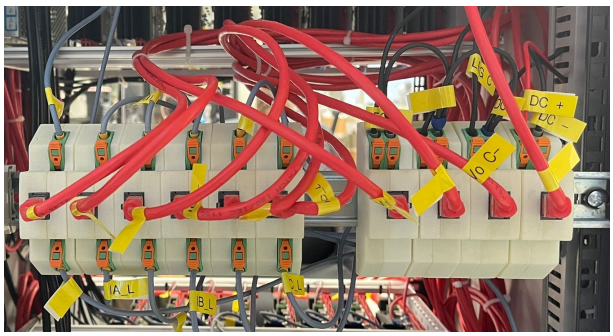

Figure 3.5: Measurement devices.

The voltage across each submodule capacitor is measured, which allows for voltage balancing. Additionally, the currents flowing through the MMC arms are constantly monitored, making it possible to determine both the circulating and output currents. Finally, the system is designed to sense the AC and DC bus voltages.

3.1.2. Simulation model

The first step to test the proposed control schemes is to accurately implement them in a simulation program that replicates the behavior of the physical MMC test bench. The model must include all relevant components and their interactions, ensuring a one-to-one correspondence with the physical system. In this way, the simulation's control strategies can be validated with a precise representation of the experimental system, before implementing them on the hardware platform.

A Simulink model has been employed to capture the essential elements of the physical MMC test bench. This model includes an embedded PLECS module containing the converter modules, power sources, and load circuits. The model should be calibrated to match the physical system's parameters, ensuring their characteristics and interactions are faithfully reproduced in the simulation.

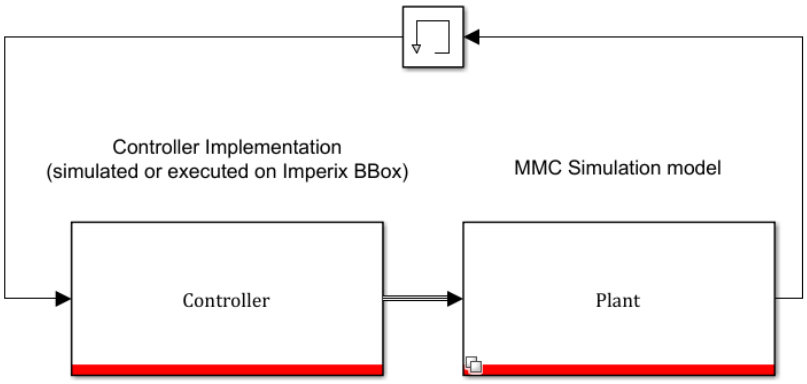

Figure 3.6: Imperix execution modes

The plant and the control part of the Simulink model are divided into two different subsystems related to the two distinct modes of execution that the Imperix Blockset offers (fig. 3.6). These modes are selected at the Imperix 'configuration' block, as shown in fig. 3.7:

1. **Simulation Mode:** allows for the execution entirely within the Simulink environment. The full Simulink model (encompassing the control and plant subsystems) is run in this mode, which enables a virtual representation of the complete system, including the behaviour of the control algorithms and the dynamics of the physical components. The simulation mode is used for analyzing and refining the control scheme without physical hardware and avoids the risk of damaging the test bench.

2. **Imperix BBox Mode:** involves the transfer of the control scheme code to the Imperix BBox, explicitly targeting the section between the ADC inputs and the PWM outputs. All the content of the Simulink model inside the plant subsystem is automatically omitted when transferring the code. This Hardware-In-The-Loop system enables real-time testing and evaluation to validate the control schemes in a real-world setting.

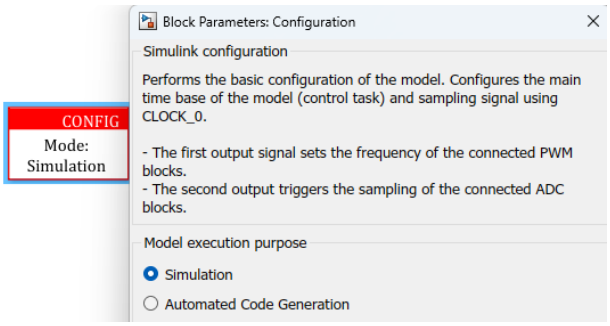

Figure 3.7: Imperix execution configuration

One of the most critical parts is signal interfacing. The inputs and outputs of the control system must match the corresponding inputs and outputs of the real-life Imperix BBox. The input-output consistency requires the utilization of the Imperix Simulink Blockset, which is specifically designed to interface with the BBox and enable seamless integration between the control system implemented in Simulink and the physical device.

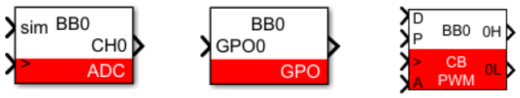

Figure 3.8: Imperix ADC, GPO and PWM blocks

Fig. 3.8 shows the main blocks employed for input-output interfacing: Analog to Digital Converter for sensing the measured magnitudes, General Purpose Outputs to send the user commands to the contactors and PWM for the optical signals that rule the switching of the submodules. The blocks must be adequately configured to match the intended channel and its real characteristics, such as sensibility, scale, etc. The appendix A offer detailed documentation regarding the configuration parameters , enhancing transparency and reproducibility.

3.2. Powering the system up

Capacitors are essential components in the MMC as they store electrical energy corresponding to the voltage of each step. It is crucial to be cautious during the charging and discharging phases to prevent the occurrence of high currents that could potentially damage the MMC electronics.

Various current limiting techniques can be employed to protect the MMC submodules during the charging and discharging phases. These techniques may include resistors, inductors, or advanced control strategies. Implementing such procedures allows the current flow to be regulated, ensuring that it remains within safe operating limits, thus safeguarding the MMC submodules from potential damage. This section provides an overview of the connection procedures for the MMC test bench.

3.2.1. External connection

DC-side connection

Either a diode rectifier connected to the AC mains or a dedicated DC source can establish the DC grid. Both methods provide the necessary DC voltage for operation, but the rectifier only allows active power flow in one direction. In this case, all the experiments have been conducted using a rectifier.

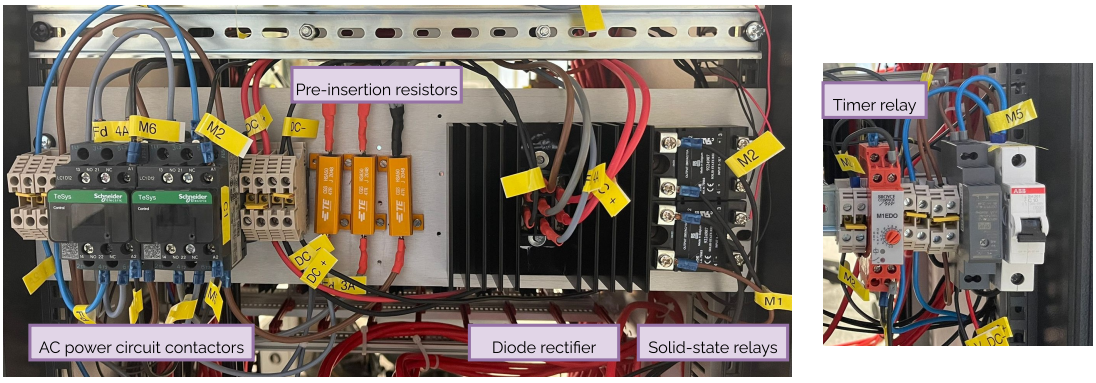

Figure 3.9: DC bus connection system.

A connection setup has been implemented to ensure the system's safety and prevent dangerous currents. Fig 3.9 shows this setup, that employs pre-insertion resistors during the initial stages of the rectifier connection to the AC grid, as shown in fig. 3.11. The pre-insertion resistors restrict current flow during these stages, allowing for a gradual charge of the converter's capacitors.

The connection of the resistors is ruled by a monophasic maneuver circuit. The maneuver circuit is activated manually during the experiment through a user-controlled signal from the Electrical GPO (General Purpose Output) of the Imperix BBox. This user-controlled signal triggers a solid-state relay, the intermediary between the Imperix BBox and the AC-monophasic maneuver circuit.

The maneuver circuit consists of a timer relay that regulates the operation of two three-phase contactors. The timer relay, controlled by the solid-state relay, sets the duration for which the pre-insertion resistors are connected. The appendix B has a detailed electrical scheme of the system.

After the time period fixed at the timer relay, the maneuver circuit bypasses the pre-insertion resistors, allowing for the unimpeded current flow through the rectifier and the subsequent establishment of the DC grid at its total capacity.

In addition to the described connection setup, an autotransformer has been introduced to enhance safety during the experiments. It enables a gradual and controlled increment of the AC voltage at the rectifier input, enhancing the safety. In addition, it allows the user to employ lower voltages to conduct the initial experiments without risk to the equipment. Once the control works safely at low voltages, the autotransformer ratio can be set to 100% and rely on the pre-insertion resistors.

AC-side connection

The AC bus of the MMC can be connected to either a passive load or the 3-phase AC grid, depending on the conducted experiment. A contactor linked to a three-phase passive load employed but this configuration is so straightforward that it does not need a dedicated explanation. Conversely, a dedicated circuit is required to integrate the MMC into the AC power network.

Similar to the DC bus connection, a connection setup has been implemented to ensure a controlled and safe connection to the AC grid, thanks to the respective AC maneuver circuit. The pre-insertion resistors restrict current flow allowing for a gradual establishment of the connection and preventing excessive current surges.

Unlike the DC bus, the AC maneuver circuit is managed by two user-controlled signals provided by the Bbox GPOs. This user-controlled signal triggers solid-state relays, which, in turn, activate the contactors responsible for establishing or bypassing the connection of the pre-insertion resistors. In this case, no timer relay is used because the resistors must be bypassed once the synchronization condition is met (sections 3.3.2, 3.3.3).

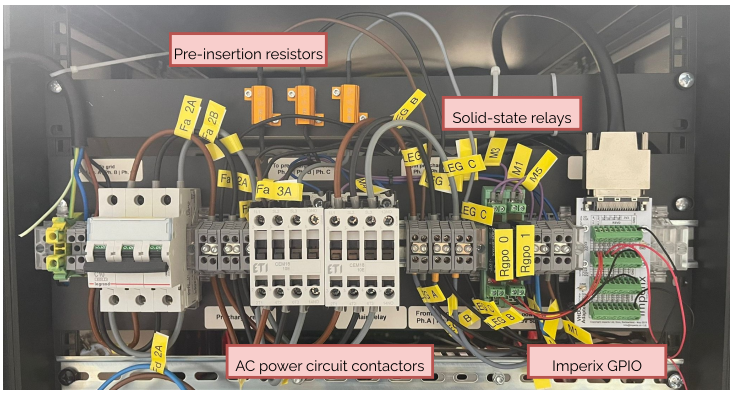

Figure 3.10: AC bus connection system.

In addition, experiments have been conducted utilizing an autotransformer to further enhance safety during the connection of the MMC to the AC grid. Besides the additional layer of protection, the autotransformer at the AC side provides another required function: grid voltage reduction. In normal operation, the DC voltage is directly related to the maximum AC voltage amplitude at the AC bus. The maximum AC amplitude that the converter can produce in HB configuration is $V_{AC,max} = \frac{V_{DC}}{2}$. Since the rectification of the grid voltage produces a value of $V_{DC} = V_{grid,RMS}\sqrt{2}\sqrt{3}$, the maximum AC amplitude is $V_{AC,max} = V_{grid,RMS}\sqrt{\frac{6}{4}}$, which is less than the actual grid amplitude: $V_{grid,peak} = V_{grid,RMS}\sqrt{2}$.

It is impossible to directly connect the rectifier of the DC side and the AC output to the same grid, as there would be a voltage incompatibility. Therefore, the AC autotransformer must adequate the AC grid to the DC voltage provided. Figure 3.11 shows the connection circuits described. The appendix B has a detailed electrical scheme of the system, including the maneuver and control circuits that handle the connection processes.

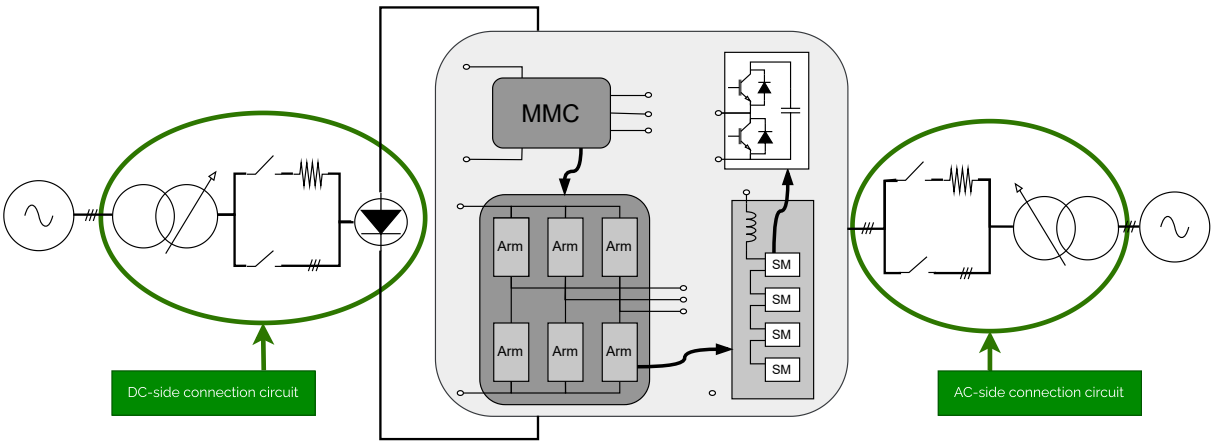

Figure 3.11: Electrical power circuit.

3.2.2. Capacitors charging process

Irrespective of the use of autotransformers and pre-insertion resistors, the charging process of the MMC involves the flow of current through the anti-parallel diodes of the switches. The capacitors will naturally charge until they reach a final voltage value based on the applied voltage and the characteristics of the circuit. However, this final value will be inferior to the desired operating voltage of the MMC system.

A second stage is required, where the capacitors are actively charged through switching. A control algorithm and the activation of PWM outputs are necessary at a certain point of the charging process to attain the desired operating voltage. The involved controls and techniques will be explained in further detail in subsequent sections. The strategy to increase the capacitor voltage of the MMC to the desired operating value differs depending on whether the MMC is energized from the DC side or the AC side.

- Energization from the DC Side: Once the capacitors have charged through the antiparallel diodes until they naturally reach the equilibrium voltage, the PWM outputs are enabled and an open-loop voltage reference is provided to the submodule controllers. If the energization relies upon the pre-insertion resistors, the control is enabled once the resistors have been bypassed due to the timer relay[1]. The voltage generation at the MMC output automatically takes the capacitors' voltage to the operational value. To prevent voltage and current overvalues, a low voltage reference value must be initially applied, as it is explained later on.
- Energization from the AC Side: In this case, the controllers in section 4.3 are activated after getting to the capacitors equilibrium voltage. The DC voltage control regulates the voltage at the DC bus, which is proportional to the individual capacitors' voltages, and adjusts it to the desired operating value.

3.3. Definition of cases of study

This section provides an overview of the specific cases that have been tested. These cases encompass different operating conditions, system configurations, and control strategies. By running these scenarios, the behaviour of the MMC system can be observed under various scenarios, allowing for a detailed analysis of its performance, efficiency, and control dynamics. The scenarios are first simulated using the Simulink model and validated within the physical MMC test bench.

[1]If energizing manually with the autotrafo, the control can be enabled from the beginning. This strategy ensures that the voltage across the capacitors gradually increases without sudden current surges.

1. The first case explores the operation of the MMC when powered from the DC side and connected to a passive three-phase load on the AC bus. This configuration aims to investigate the MMC's performance working in an isolated grid and evaluate its capability to deliver power to the grid loads when no other power source exists.

2. In the second case, the MMC is also powered from the DC side but is interconnected with an AC grid in a grid-following mode of operation. This case delves into the MMC's behavior when integrated into an AC grid.The study evaluates the converter's performance in maintaining stable grid operation while effectively delivering power to the grid.

3. Lastly, the third case focuses on the MMC being powered from the AC side while disconnected from the DC side. The MMC is employed as a Static STATCOM which was introduced in section 2.2.4. In this configuration, the MMC can provide reactive power support, voltage regulation, and compensation for power quality issues, such as voltage sags and harmonics. This case can also be extrapolated to a converter in charge of keeping the DC voltage in HVDC applications.

3.3.1. Islanded operation

Description

The first case of the study aims to investigate the performance of MMC when it is working in an isolated grid. The load, represented by resistors, is directly powered by the MMC. This configuration tests its ability to provide power to grid loads without any other power source. The converter's behaviour regarding regulating the voltages at different system parts can also be analyzed before moving to more complex scenarios, such as when connected to an AC grid.

The MMC is powered by the DC bus, which is connected to an AC grid through an autotransformer and a rectifier. The AC side of the converter is connected to a three-phase passive load consisting of three 2500W resistors arranged in a star configuration, as shown in fig. 3.12. A three-phase contactor connects the loads, following the user command through an Imperix GPO, as shown in appendix B.

The autotransformer allows controlled power flow from the AC source to the MMC. However, it is only employed for the charging process and can be substituted by the pre-insertion resistor circuit described in 3.2.1. Both ways of starting up the converter are studied.

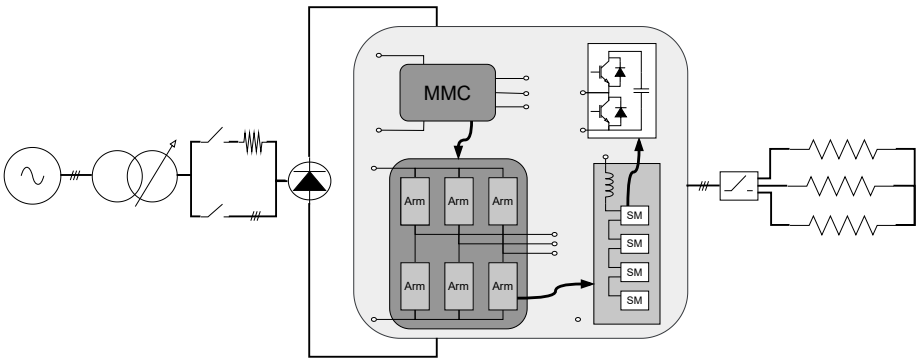

Figure 3.12: Electrical connection scheme employed.

Control scheme

Overview .

In the first case of study, the system is always isolated from the AC grid, so it can be simply divided into two phases: energization and operation, as in fig. 3.13.

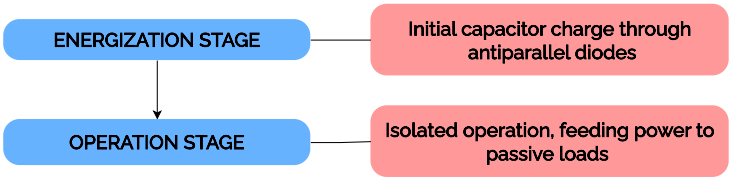

Figure 3.13: Islanded operation basic stages.

The energization is done from the DC bus, either with pre-insertion resistors or with the autotransformer. The capacitors' voltages naturally charge up to their operation voltage. Once the capacitors are naturally charged through the antiparallel diodes, the controllers and the PWM outputs are enabled, initiating the operation phase. During the operation phase, it is possible to directly move from the open-loop to the closed-loop approaches described later on.

Alternatively, it is also possible to have a single operation mode where the energization is done through the autotransformer with the open-loop voltage control approach. This single mode would be utilized throughout the energizing and operation phases without differentiation. Both strategies have been tested to see which is the optimal.

During the operation stage, the controllers involved can be divided into two blocks: the Higher-level control and the Voltage-Balancing control, constituting a cascaded structure, as in fig. 3.14.

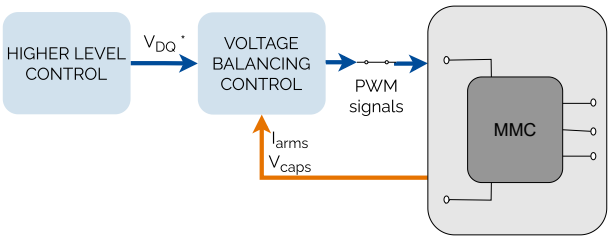

Figure 3.14: General structure of MMC control.

The first one provides the AC voltage reference the converter must generate at the AC bus. The second is the one that produces the PWM signals for the drivers to produce the desired output voltage, while keeping the system voltages balanced. For this thesis, the Voltage-Balancing control is fixed for all the studied cases. In contrast, the higher-level control is modified depending on the objectives of the particular case.

Voltage-Balancing control .

The voltage balancing control generates the references for the PWM drivers, the last stage of the implemented cascaded control (fig. 3.14). It is required to keep the capacitor and arm voltages balanced while producing the output voltage wave determined by the higher-level controls.

The bibliography already has studied different approaches for this control. A single strategy was implemented for all the cases under study since the primary objective of the thesis is more centred on studying power management, current control, synchronisation, and system stability rather than different balancing or modulation methods.

The control strategy is related to the modulation technique employed. In this case, the Phase-shifted PWM applies a phase displacement equal to $\frac{180}{N_c}$[2] to the carrier of each submodule of an arm, that compares to a common arm reference. Despite the evenly distributed load, it is necessary to ensure the balance of the capacitor voltages. An individual controller approach has been implemented, avoiding the need of a sorting algorithm. Notably, the independent control of each submodule implies considerable communication and computation effort, that may become too complex when the number of modules is large. However, this strategy has been maintained, since it is not the case for the laboratory prototype and the optimization of the modulation is not under the scope of this thesis.

The implemented control scheme comprises distinct stages in a cascaded approach, each serving a specific purpose in regulating the voltage levels within the MMC. The structure

[2]For Full-Bridge modules the displacement would be half that value.

shown in fig. 3.15 is similar to the one from [11]. Each phase has its controller to regulate the average capacitor voltage by controlling the circulating current through the leg. A previous controller provides an extra term to the circulating current to compensate for the upper and lower arms imbalance at each phase. Finally, each submodule has a dedicated controller that produces the reference for the corresponding PWM driver.

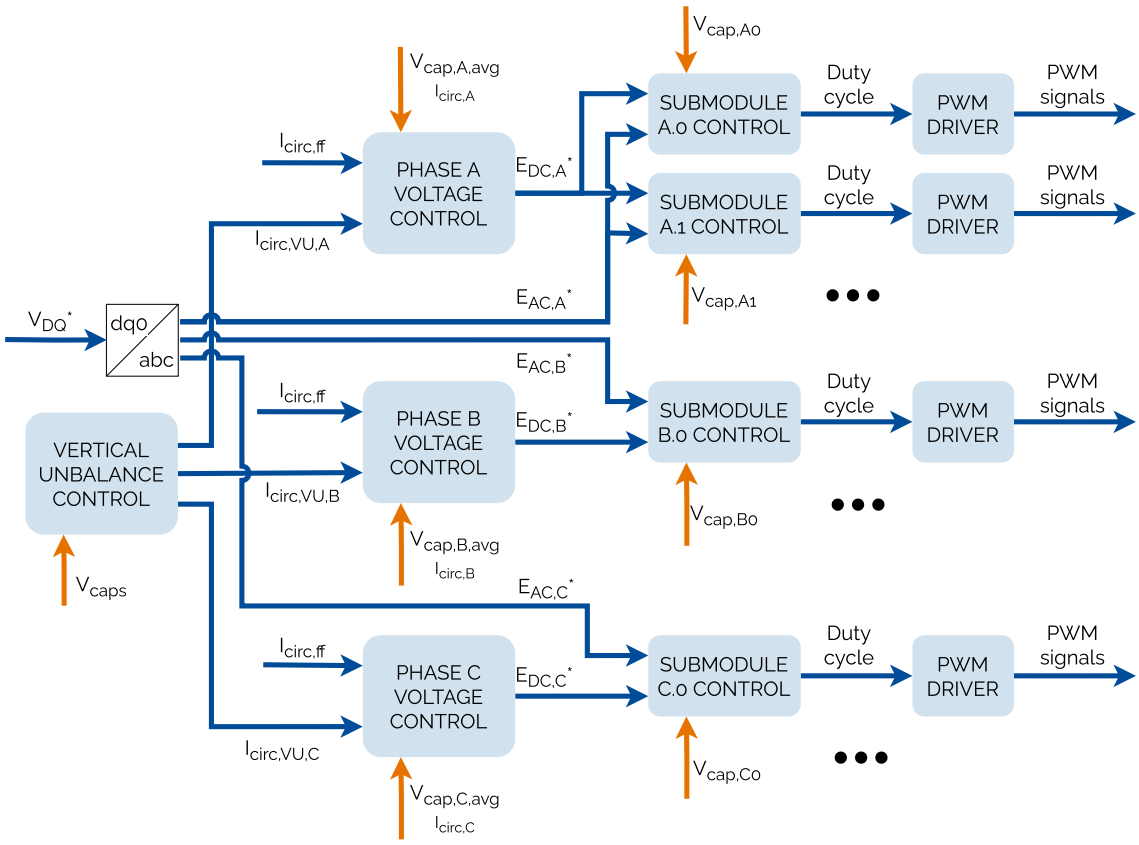

Figure 3.15: Voltage-Balancing control structure.

This structure is named in literature as closed-loop voltage control [10]. It differs from the other approaches to control the phases' circulating current and arms' energy (direct, closed-loop and hybrid voltage control) in the possibility of measuring the arms' energy and close their loop to control it. The vertical imbalance P controller mitigates the voltage imbalances among the MMC arms in each phase, by introducing an AC pulse at fundamental frequency on I^*_{circ}, as indicated in the eq. (3.1). A PI controller governs the average capacitor voltage for each leg, following a reference signal proportional to the voltage at the DC bus.

$$I^*_{circ,Vert.Imb.,i} = K_{circ,VI}(V_{caps,i,up,avg.} - V_{caps,i,low,avg.})cos(\omega t + \phi_i) \tag{3.1}$$

$$\frac{3}{2} \cdot (v_D \cdot i_D + v_Q \cdot i_Q) = P_{AC} = P_{DC} = V_{DC} \cdot I_{DC} \tag{3.2}$$

The output of this control is added to two feed-forward terms to form the input signal for the circulating current controller. One corresponds to the output of the vertical imbalance controller. The other term is the DC term corresponding to the active power exchange, which comes from the power calculation at the higher-level controller to fulfil eq. (3.2). The circulating current is responsible for charging or discharging the capacitors, according to the requirements of the previous controllers. It is regulated by a cascaded P controller that generates a DC voltage reference transmitted to the individual submodule controller (Fig. 3.16). Finally, the produced DC voltage reference also has a feed-forward term corresponding to the DC bus's measured voltage to enhance the controller's dynamics.

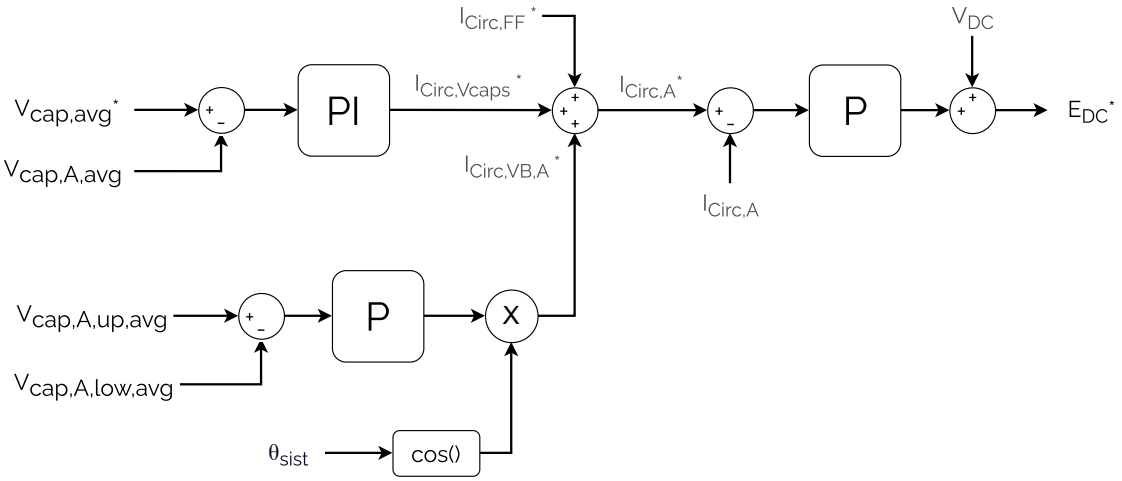

Figure 3.16: Phase voltage controller.

Following the phase voltage control stage, individual controllers are employed for each submodule within the MMC system. All submodules of a particular phase receive an AC voltage reference from the higher-level control and a DC voltage reference from the preceding phase voltage control stage (fig. 3.15).

In this way, all the submodules in a branch would receive the same voltage references, both AC and DC. From eqs. (2.1)-(2.2), the AC reference should be added (or subtracted) to the DC one to obtain the upper and lower arm voltages. The result, divided by the number of modules in the arms, gives the required voltage for each submodule. The duty cycle is calculated by normalising this value to the measured voltage at the capacitor.

This strategy would produce the desired voltage at the converter AC bus while controlling the arm energy but not the individual capacitor voltages, which could eventually diverge, leading to a failure. A P controller component regulates the individual capacitor voltage of the submodule with respect to the measured average capacitor voltage of the arm (Fig. 3.17). The controllers' output is added to the previous duty cycle calculation, promoting uniform voltage distribution across the capacitors in the arm.

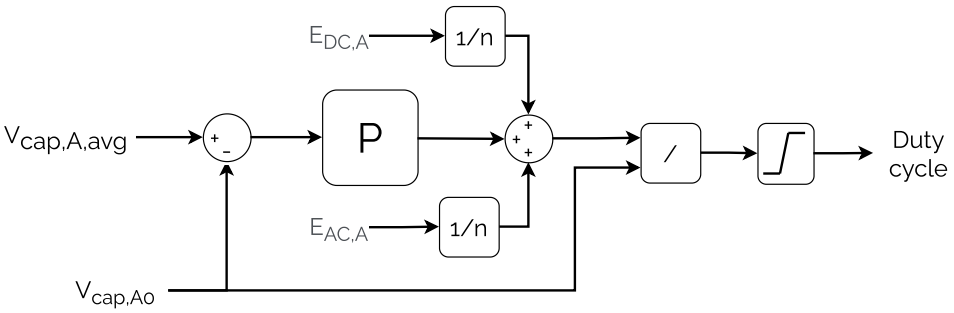

Figure 3.17: Individual submodule controller.

Furthermore, a recommended block from Imperix examples is incorporated into the control scheme to account for the effects of PWM dead time[3]. Detailed information of the tuning parameters of the controller can be found in the appendices of the thesis. They were obtained from the theory in [10] and later refined in simulation to avoid interference with higher level controllers and keep the system stability in all scenarios.

Higher-level control .

The MMC is the only power source for the grid's load. Therefore, the controller freely establishes the voltage magnitude and frequency. In the first stage, it can be controlled in an open-loop fashion, providing an arbitrary AC reference signal to the Voltage-Balancing control, as in fig. 3.18.

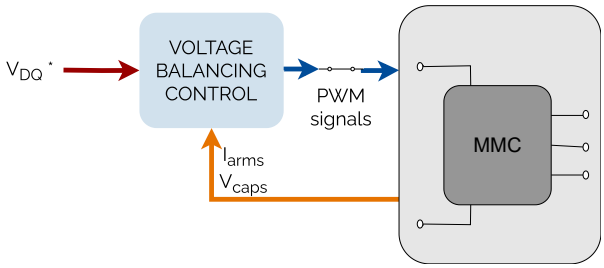

Figure 3.18: Open-loop voltage control.

[3]Intervals during which both the upper and lower power switches of a half-bridge are inactive to prevent simultaneous operation.

However, it is essential to note that the output voltage is not actively regulated in this scheme. Then, the attention focuses primarily on the voltage balancing among the arms and submodules of the MMC.

Alternatively, higher-level a current controller could be introduced to enhance the existing control scheme for efficient power management. It would produce the AC voltage reference for the voltage balancing controller so the current references defined by the user are accurately followed. Additionally, the system can also include a DQ voltage controller that provides the current references for the current controller in a cascaded structure that would controle the voltage at the load in a closed-loop approach (fig. 3.19).

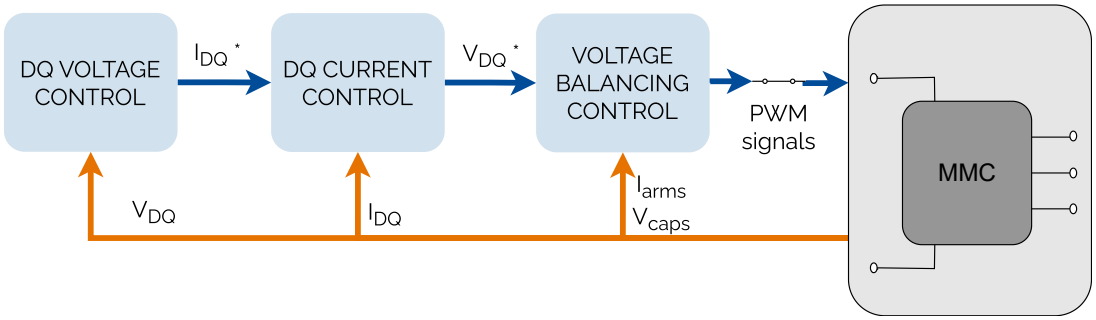

Figure 3.19: Closed-loop voltage control.

The main objective of this section was to focus on the voltage balancing controller and the energization steps of the system. However, this strategy was very straight-forward to test, as the DQ current controller was already developed and tuned for the case studied in section 3.3.2. The current controller is indeed detailed in that section.

The current control is implemented in the DQ (direct-quadrature) coordinate system. The DQ coordinate system, also known as the rotating reference frame, is handy for controlling power electronic converters. It simplifies the control algorithm by decoupling the current's active (D-axis) and reactive (Q-axis) components. This coordinate system choice allows for the employment of regular PID controllers to produce a sinusoidal signal.

The DQ transformation requires a reference angle representing the system's angular position. There is no grid to serve as a reference for synchronization, so an artificial angle is employed. A constant value $2\pi 50$ is integrated over time to generate this artificial angle, miming the angular position's rotation in a synchronized grid system oscillating at 50 Hz.

3.3.2. Grid Following operation

Description

In the second case of the study, the MMC is connected to an AC grid and operated in a grid-following mode. The system is powered from the DC side, which is connected to the AC grid through an autotransformer and a rectifier, as in section 4.1. However, the MMC's AC bus is connected to another AC grid instead of a resistive load. The pre-insertion resistor circuit described in section 3.2.1 is employed to facilitate the connection as depicted in Fig. 3.20.

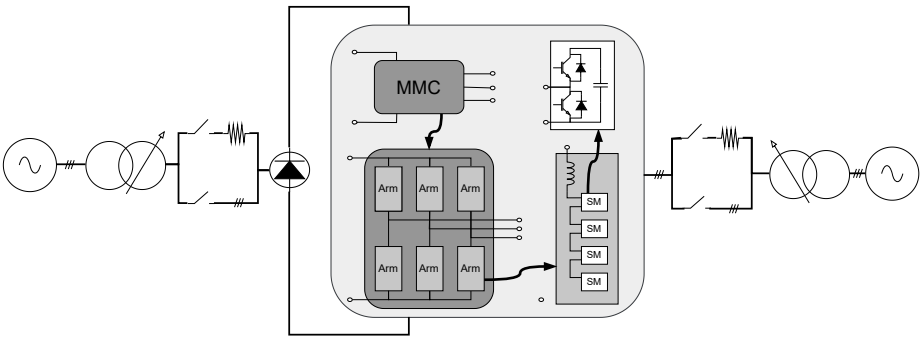

Figure 3.20: Electrical connection scheme employed.

The MMC's AC bus voltage must be synchronized to the AC grid before the connection to avoid disturbances or instability. This process requires the measurement of the 3-phase voltages at both sides of the AC side contactors, enabling the comparison and adjustment of the voltage waves prior to the connection.

However, measuring the phase voltages becomes challenging when the neutral point is not accessible. One solution to this problem is to obtain relative voltage measurements by referencing each phase voltage to the negative pole of the DC bus. This solution produces a DC component at the measurements, that must be eliminated, applying a transformation to the measured signals. It consists of adding the three measurements between themselves as if a phase-to-line transformation is applied and, afterwards, a line-to-phase one.

Control scheme

Overview .

The control scheme for the MMC's grid-following operation consists of four main stages: energization, synchronization, soft-connection, and final operation.

These stages fulfil the primary requirements for the grid-following operation mode, ensuring its effective integration into the AC grid. However, based on experience with the real-world test bench, two additional transitory steps have been introduced to ensure safety and mitigate potential issues. Additionally, the automated transition between the stages has also proved to be required, preventing unbalance problems when working in open circuit for long times.

The strategy is shown in Fig. 3.21, and starts with an energization phase with no active control on the MMC. The capacitors get naturally charged up through the antiparallel diodes, either using the pre-insertion resistors and/or acting on the autotransformer as explained in section 3.2.1. The capacitor voltages naturally reach half the operation voltage when charging through the diodes. The final capacitor voltage is achieved after the PWM outputs and the controllers are enabled.

Experience has shown that sudden activation of controllers in open-circuit produces transient charging currents that trip the protection mechanisms. That is why the soft-start stage was introduced, to gradually charge the capacitors up to the desired operational voltage level without excessive arm currents. During this stage, an AC voltage with a predefined low amplitude is outputted using the Open-Loop Voltage Control. The resulting currents are effectively kept below the tripping mechanism limit, ensuring a safe and controlled charging process for the capacitors.

The synchronization stage starts once the capacitors are fully charged, after a predefined time lapse for the soft-start. The aim is to ensure that the MMC's AC bus voltage is nearly equal to the grid's voltage. When the voltage difference is reduced to a sufficiently low level, the connection to the grid can be safely established.

It should be noted that no current flows through the converter during the synchronization process because the system is not connected to the grid yet. Thus, the switching harmonics are not filtered by the converter inductor, and the MMC AC bus voltage may have excessive harmonic distortion, which can lead to aliasing issues when the sampling frequency used is close to the switching frequency.

The sampling frequency is 20 kHz, which coincides with the effective $4 \cdot 5kHz$ switching frequency (both following the Imperix recommendations), making impossible the synchronization task. This issue motivated the use of the analog filter[4] available at the analog inputs, to measure all the three-phase voltages and currents (to keep the same delay).

[4]This filter corresponds to a 5th-order Bessel filter with selectable cutoff frequency, which was chosen to be 1.6kHz. To simulate the filter, the transfer function of such filter was discretized (with a sampling time 10 times higher than the execution time) and introduced before the ADC blocks corresponding to the mentioned measurements.

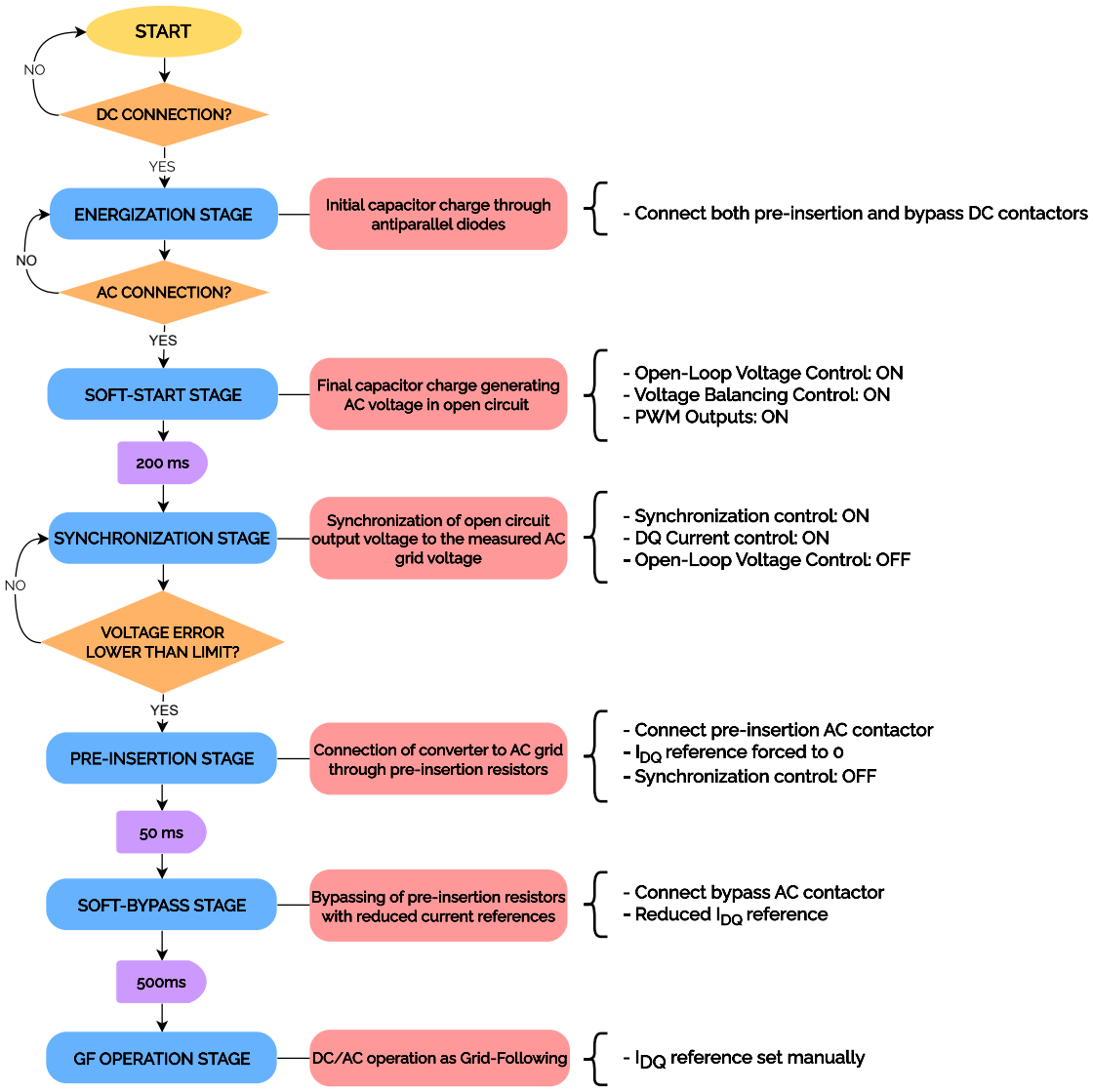

Figure 3.21: Stages towards grid-following operation.

Once the synchronization is achieved, the coupling is started with the pre-insertion phase. This phase establishes a controlled connection through the pre-insertion resistors to mitigate any potential current transients. The synchronization control is deactivated while the DQ current control remains activated. However, the current references are forced to zero to prevent any current flow through the pre-insertion resistors[5].

[5]It would cause a voltage drop occur between the grid and the MMC's AC bus. Consequently, voltages would diverge and the previous synchronization effort would have been useless, leading to dangerous transients at the subsequent bypassing of the resistors.

After the predefined pre-insertion time has elapsed, the resistors are bypassed and the system starts to operate as a grid-following converter directly connected to the grid. However, the current references are kept very low for a certain amount of time corresponding to the soft-bypass stage, to further enhance safety during the most critical transition.

Finally, at the operation stage the current references are no longer limited so the DQ current control follows the user-defined D and Q current references in a grid-following mode.

Grid-Following control .

The control scheme employed during the last three stages remains consistent: the grid-following control. The core of this control scheme is the DQ current controller introduced in section 3.3.1, that follows the commanded load current adjusting the AC voltage reference accordingly in a closed-loop manner. It is responsible for tracking the active and reactive power demands, using the manually settled D-Q current references.

The outputs are the D-Q voltage references which are subsequently forwarded to the voltage balancing controller (Fig. 3.22) to provide the PWM signals, as explained in 3.3.1.

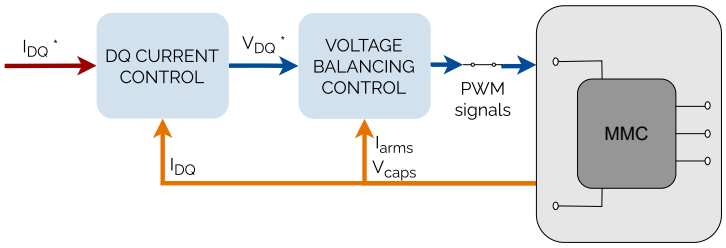

Figure 3.22: Grid-Following Control.

The angle for the DQ transformation is calculated from the real-time AC grid voltage measurements using a Phase-Locked Loop (PLL[6]). The PLL plays a fundamental role in grid-following operation of the converter, designed to keep synchronization with the grid while following the power requirements [7]. It allings the reference angle of the converter to the voltage phasor measured at the grid's connection point, so its Q component is always 0, as shown in Fig.3.23.

[6] A PLL is a control system that aligns the phase and frequency of an oscillating signal with a reference signal.

[7] This approach differs from a grid-forming strategy, where the converter actively participates in building and controlling the grid's voltage wave. This grid-forming strategy would be a separate topic that may be explored in future research or development beyond the scope of this thesis.

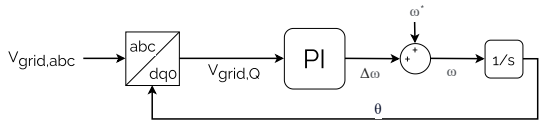

Figure 3.23: PLL used for Grid-Following synchronization.

In this way, the D and Q currents are directly proportional to the active and reactive power, respectively. Thus, the power can be tracked in open-loop [10] with accuracy (but with some static error) by using just the current controller, according to eqs: (3.4).

$$I_D^* = K\frac{P^*}{V_D} \tag{3.3}$$

$$I_Q^* = K\frac{Q^*}{V_D} \tag{3.4}$$

The current DQ control scheme in the system utilizes two PI controllers, for the D and Q components respectively. A feed-forward term of the grid's measured DQ voltage is introduced to enhance the performance, improving the system response and increasing the accuracy of the control. The D and Q components of the current are interrelated due to the derivative terms of the inductance equations. This cross-relation is compensated to avoid perturbations in one component when the other changes. The whole control structure is represented in Fig. 3.24.

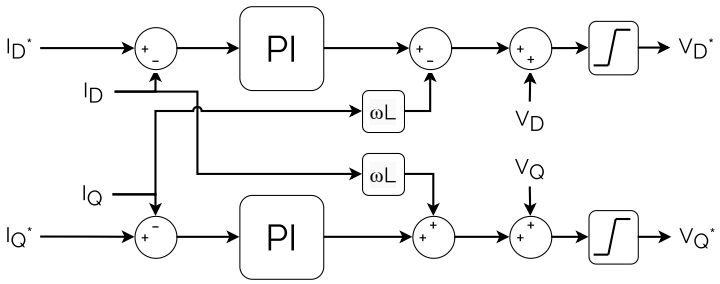

Figure 3.24: DQ current controller.

The output of the controllers is saturated at the nominal output voltage value to prevent exceeding the system's limits. The anti-windup is incorporated into the controllers to avoid integrator error accumulation, ensuring robust and stable control performance. The tuning parameters for the controllers are indicated in the appendix A. They were obtained by performing a state space analysis of the linear system composed by the arm impedances, the autotransformer and the AC grid, assuming that the voltage balancing controller is able to produce the desired AC voltage wave at the converter arms.

$$v_{ACbus,d} = v_{grid,d} + \frac{di_d}{dt}L_{tr} + i_d R_{tr} - i_q L_{tr}\omega \tag{3.5}$$

$$v_{ACbus,q} = v_{grid,q} + \frac{di_q}{dt}L_{tr} + i_q R_{tr} + i_d L_{tr}\omega \tag{3.6}$$

$$v_{cont,d} = v_{ACbus,d} + \frac{di_d}{dt}\frac{L_{arm}}{2} + i_d\frac{R_{arm}}{2} - i_q\frac{L_{arm}}{2}\omega \tag{3.7}$$

$$v_{cont,q} = v_{ACbus,q} + \frac{di_q}{dt}\frac{L_{arm}}{2} + i_q\frac{R_{arm}}{2} + i_d\frac{L_{arm}}{2}\omega \tag{3.8}$$

$$\frac{di_{d,error}}{dt} = i_d^* - i_d \tag{3.9}$$

$$\frac{di_{q,error}}{dt} = i_q^* - i_q \tag{3.10}$$

$$PI_{ContOut,d} = i_{d,error}KI_{DQc} + (i_d^* - i_d)KP_{DQc} \tag{3.11}$$

$$PI_{ContOut,q} = i_{q,error}KI_{DQc} + (i_q^* - i_d)KP_{DQc} \tag{3.12}$$

$$v_{cont,d} = PI_{ContOut,d} + v_{ACbus,d} - i_q(L_{tr} + \frac{L_{arm}}{2})\omega \tag{3.13}$$

$$v_{cont,q} = PI_{ContOut,q} + v_{ACbus,q} + i_d(L_{tr} + \frac{L_{arm}}{2})\omega \tag{3.14}$$

The equations of both the electrical system and the controller are eqs. (3.5)-(3.14). The differential terms were extracted to obtain the state space equations. Then, the controllers parameters were modified to locate the system poles within acceptable dynamic characteristics.

Synchronization control .

The synchronization stage has the objective of gradually reducing the voltage difference between the AC grid and the MMC's AC bus. A dedicated controller is implemented to achieve synchronization with the AC grid by adjusting D-Q current references. Fig. 3.25 shows the detail of the controller, composed of two equal PI controllers that compare the AC voltages at both sides of the AC grid contactor.

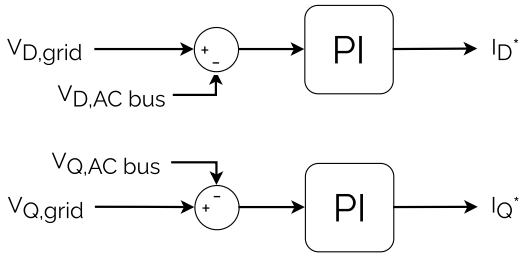

Figure 3.25: Synchronization Control Detail.

These references are followed by the cascaded DQ current and voltage balancing controllers, in place of the manually settled references of the operation stage (Fig. 3.26). The controller parameters were tuned iteratively in simulation to obtain acceptable synchronization time.

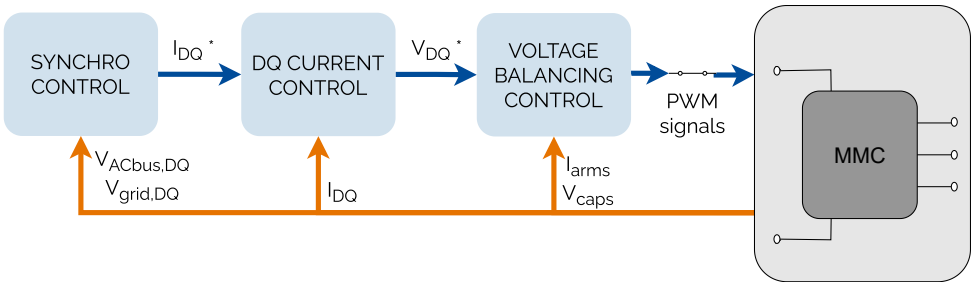

Figure 3.26: Synchronization Control.

With this approach not only the voltages match before the transition to the next stage, but also the subsequent current and voltage controllers are already active. Thus, when the connection starts and the synchronization control is substituted by the manually set current references, the initial controller output is precisely the one that drove the bus voltage to match the grid voltage. This procedure ensures a smooth transition helping to maintain stability during the following connection.

3.3.3. STATCOM operation

Description

In the study's third case, the MMC's DC bus is in open-circuit. At the AC side, it is connected to the AC grid through an autotransformer and the pre-insertion resistor circuit described in section 3.2.1, as shown in fig. 3.27. The MMC is designed to operate as a STATCOM, whose main objectives are to support the AC grid's voltage by actively modulating reactive power, as introduced in 2.2.4.

Regulating the DC voltage is crucial for maintaining the stable operation of the converter[8]. With an open circuit at the DC bus, the active power exchanged with the AC grid just affects system's stored energy (at the capacitors) and, proportionally, the DC bus voltage. Then, while the control of the reactive power serves the main objectives of STATCOM operation, control of active power is crucial to keep it stable.

[8]With Half-brige submodules, the MMC can only operate within a strict limit: $\frac{V_{DC}}{2} > V_{AC,peak}$; otherwise the submodules would reach overmodulation. If Full-Bridge submodules were employed, it would be possible to obtain lower voltages at the DC bus. In any case, the system voltages should be kept within acceptable limits.

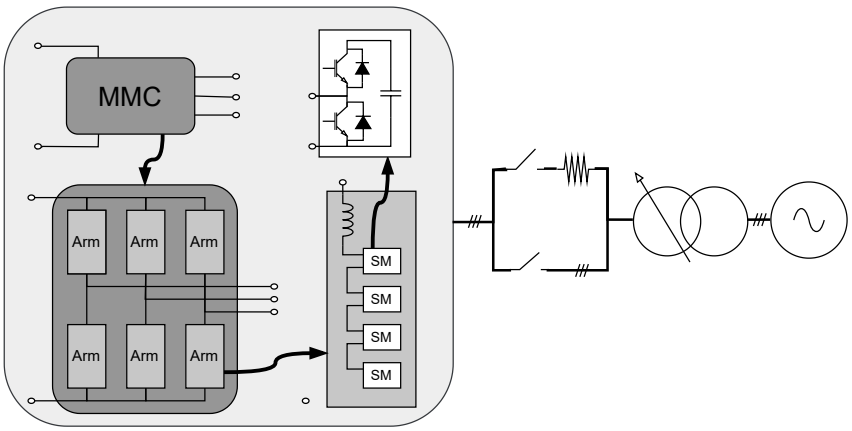

Figure 3.27: Electrical connection scheme employed.

Nevertheless, it is important to note that the operation of the developed system would remain consistent in the case that the MMC was connected to either another converter, an energy storage system or, in general, any kind of DC grid. The control objective would continue to be to maintain the DC voltage at the desired setpoint. Unfortunately, the DC side of the system studied is connected to a rectifier that can not absorb power towards the DC bus, so this functionality has not been tested within the scope of this thesis, as it would have imply using a DC source and DC contactors that were not available at the time.

This functionality where the MMC works towards a DC grid is extremely important for the HVDC application. A DC line must have one converter at each end and, while one is delivering power to the AC grid or the connected loads, the other end must be absorbing it from a source. If the incoming and outgoing power are not balanced, the DC bus voltage will vary, which could lead to instability. Thus, one of the converters must be in charge of absorbing the exact amount of power required: not only the amount of power exchanged at the delivering end, but also the necessary to keep the DC voltage at the setpoint value.

In this way, the controllers developed are essential for DC transmission applications where the MMC serves as the input port to an HVDC line or, more generally, an HVDC grid of some kind. Therefore, the study of MMC application to HVDC is completed, complementing the grid-following application developed in the second case of study, as each of the operation would apply to each one of the converters at the HVDC line.

Control scheme

Overview .

The control scheme implemented comprises five distinct stages designed to bring the MMC to operation, which are depicted in fig. 3.28. Contrary to sections 4.1 and 4.2, the converter is powered from the AC side, which also has two current limiting methods: the pre-insertion resistors and the manual action over the autotransformer. Based on the good results of the DC bus energization of previous sections, the preferred option was to fix the autotransformer voltage and rely on the resistors for the limiting action to avoid human errors.

During the energizing phase the PWM outputs are disabled, so the capacitors are charged through the antiparallel diodes until the equilibrium voltage. The PWM switches will be required to move their voltages towards the operation value, as happened when energizing from the DC bus.

After the initial energization stage, the challenge is to safely activate the controllers and PWM outputs, minimizing potential instabilities or transients. The primary objective of the synchronization stage is to ensure that the controllers generate an AC voltage reference that closely aligns with the actual grid voltage before enabling the PWM outputs.

The synchronisation phase starts after a fixed timelapse of 350 ms for the initial energisation. DC voltage and DQ current controllers work in a cascaded way during this phase, but the PWM outputs are still disabled. The synchronisation lasts until the voltage reference produced by the current controller equals the voltage measured at the AC bus terminals. This control scheme forces the operation controllers' output to match the grid voltage. Then, they will be already producing the grid voltage at the moment of activation of the PWM outputs, ensuring a smooth transition.

Following the successful synchronization, the control strategy shifts to managing the MMC as a STATCOM. However, experience has shown that the sudden activation of the PWM modules bypasses all the modules simultaneously during the activation instant. The soft-start stage is characterized by the activation of the PWM outputs while the pre-insertion resistors remain connected, serving as a temporal protective measure. Simultaneously, the synchronizing control is stopped, so the DC voltage and DQ current controllers begin to track the references of DC voltage and Q current. The capacitors are charged from the initial energization voltage to their operation voltage thanks to the action of the DC voltage control that regulates the D current reference. The Q current reference is forced to zero to minimize the current flow and the corresponding voltage drop at the resistors.

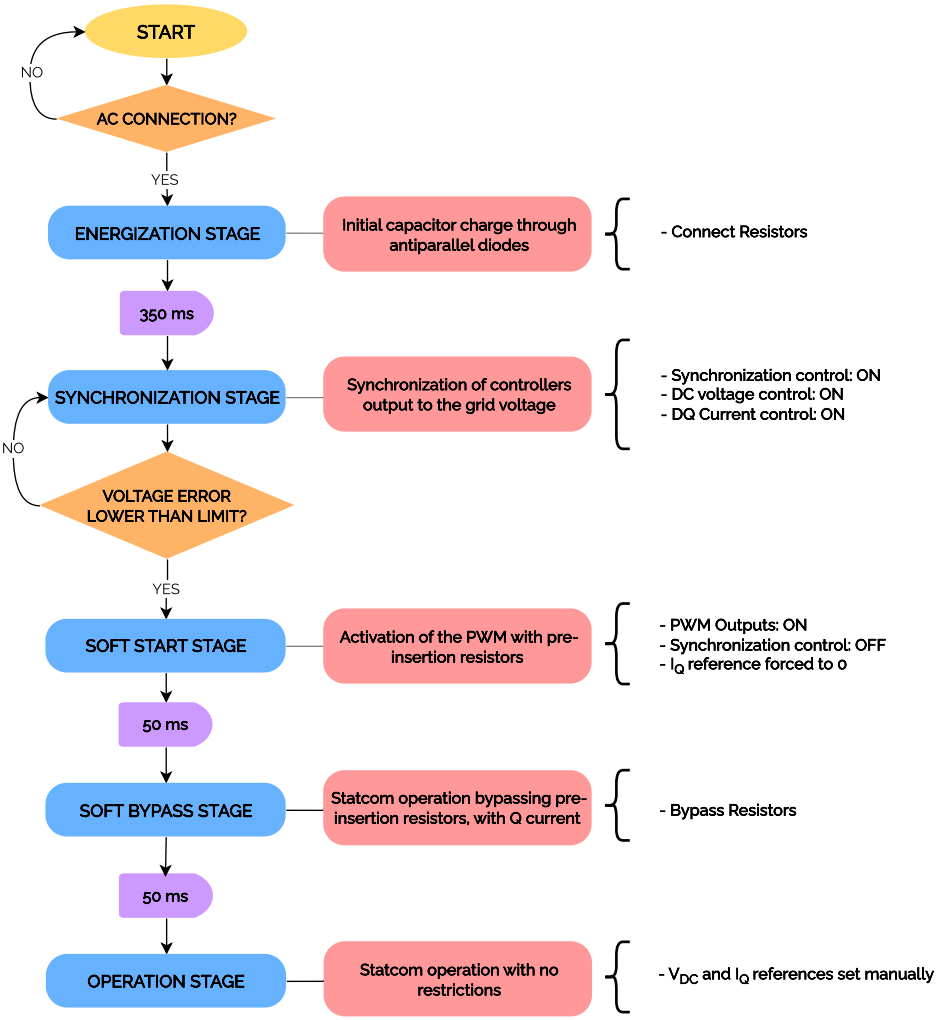

Figure 3.28: Stages towards STATCOM operation.

The soft-start stage is crucial during the first moments of PWM activation due to the simultaneous bypass of the switches. However, waiting until the operation voltages are fully reached to bypass the pre-insertion resistors is not essential. The DC voltage and current controllers have saturation and anti-windup effectively included in their loops, and this is enough to limit the currents if the resistors are bypassed after some milliseconds of the soft-start phase.

The necessity of accelerating the slow simulation times motivated the idea of bypassing the resistors after a few milliseconds and relying on the controllers to limit the currents. However, a soft-bypass stage of 200 ms has been included to always be on the safety side, where the Q current reference is still forced to zero. In this way, the only current that flows is the required to reach the reference DC voltage.

Finally, the MMC starts working as a "free" STATCOM. The references become the ones the user provides to fulfil its functionality as a voltage and reactive power compensator in the AC grid system.

DC voltage control .

During the STATCOM operation of the MMC, the MMC has to exchange reactive power with the AC grid. The current controller developed for grid-following operation in section 3.3.2 is employed acting on the Q component, which corresponds to the reactive power flow due to the PLL action, the Q component of the currentThe grid requirements would drive this reference in an actual STATCOM application, but in the experiments carried out, it is modified manually by the user as before.

On the other hand, it has been explained that active power affects the system's stored energy. I_D is directly proportional to the active power and, therefore, the variation of the stored energy (eq. 3.15). The stored energy at the submodule capacitors is related to the DC voltage as in eq. 3.16. Then, the relation of the D current and the DC voltage is employed to control this magnitude in a cascaded structure with the current control.

$$\frac{dE_{st}}{dt} = P = V_D I_D \tag{3.15}$$

$$E_{st} = 3\frac{C_{sm} V_{DC}^2}{N_{sm}} \tag{3.16}$$

A controller has been developed to keep the DC voltage at the desired level, which is required to operate the converter and its connected devices. The output of this controller is the D current reference that corresponds to the active power flow at the AC bus. The tuning was done by adding these energy equations along with the ones corresponding to the PI controller, eqs. (3.17)-(3.19), to the previously defined system (eqs. (3.5)-(3.14))[9].

$$\frac{dV_{DC,error}}{dt} = V_{DC}^* - V_{DC} \tag{3.17}$$

$$PI_{ContOut,Vdc} = V_{DC,error} Ki_{VDC} + (V_{DC}^* - V_{DC}) Kp_{VDC} \tag{3.18}$$

$$i_d^* = PI_{ContOut,Vdc} \tag{3.19}$$

The energy equations are non linear so the system was linearized around an equilibrium point with $V_{DC} = 450V$. Then, during simulations, the parameters were completely defined to account for the real system.

[9]Due to the cascaded structure, the systems can be also treated independently, as they are tuned to have very different velocity.

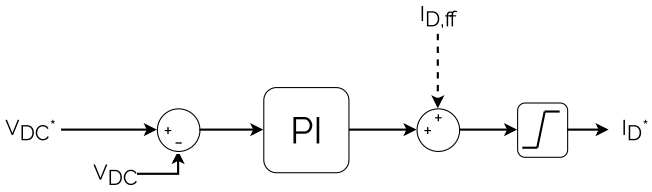

Figure 3.29: DC voltage controller.

The DC voltage control is formed by a PI structure that tracks the DC voltage reference, producing the D component of the current reference. It can be noted that, in the presence of a grid or element at the DC side of the converter, an additional active power exchange would occur between the MMC and the connected system. The D component of the current reference, which regulates the active power, would incorporate an extra term to account for this power exchange, as indicated by the dashed line in fig. 3.29. However, this case was not studied due to the structure of the DC bus connection, as already indicated.

The D and Q components of the current reference are derived from the voltage controller and the user-determined reactive power requirements, respectively, as shown in fig. 3.30. They are then fed as inputs to the DQ current control scheme explained in 3.3.2. As in the previous cases, the output of this controller is the voltage reference that is then provided to the output voltage controller, which is responsible for generating the PWM duty cycle for the submodules.

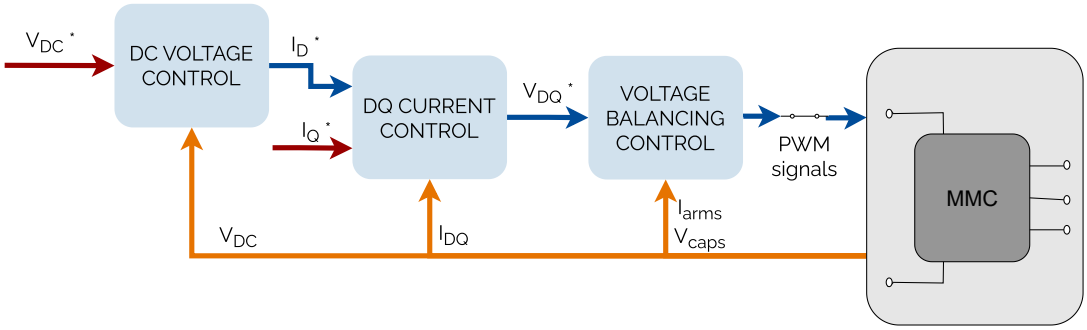

Figure 3.30: STATCOM operation.

Synchronization control .

A crucial step in initiating the operation is the synchronization process, which allows for the smooth activation of PWM signals through a dedicated controller.

The purpose of the synchronization controller is to ensure that the voltage reference generated from the DQ current control matches the AC grid voltage. Then, the PWM

outputs of the MMC can be enabled safely, minimizing any transient as the produced voltage at the beginning will be aligned with the measured voltage at the AC bus. This way, the AC bus voltage generated is close to the grid voltage when the PWMs are enabled. Moreover, the operation controllers already produce that exact voltage reference, ensuring a smooth transition towards the operation stage.

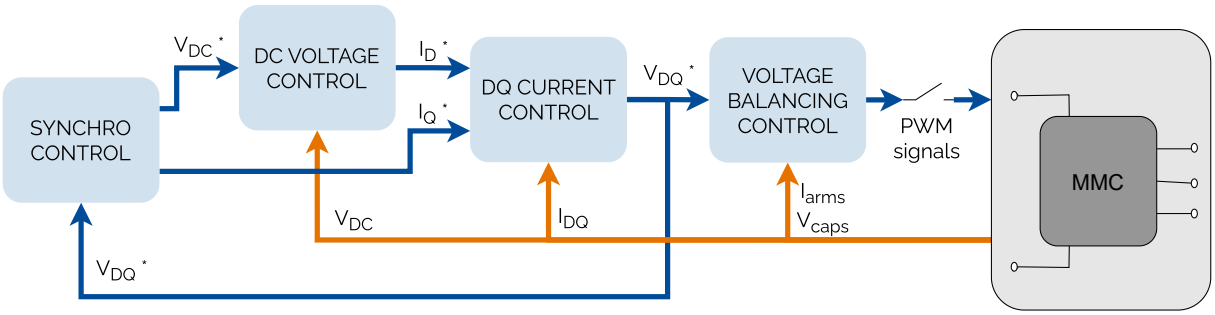

Figure 3.31: Synchronization to STATCOM operation.

As shown in fig. 3.31, this controller acts on the following controls (DC voltage and DQ current controls) in a cascaded way. It provides the reference values of Q current for the DQ current control and DC voltage for the DC voltage control, which produces the reference value of D current.

The control structure comprises two PI controllers that align the final voltage reference with the AC grid voltage up to a specific error threshold, the synchronization condition. Contrary to the synchronization control developed for the previous case, the PI must be differently tuned: the Q-axis one directly provides the Q current reference, while the D-axis one provides the DC voltage reference (fig. fig. 3.32).

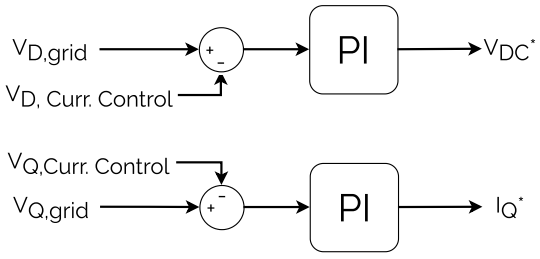

Figure 3.32: Synchronization controller.

When the synchronisation process finishes, the synchronisation controller no longer determines the references. Then, they are defined by the user's commands, as in fig.3.30.

4 | Analysis and results

This chapter of the thesis presents the different results obtained for each of the scenarios defined, including simulation and hardware experimentation.

The simulated results are a crucial component of this study, as they serve to check the effectiveness of the proposed control schemes before testing in the real system. During this stage, the controllers are tuned to produce the desired results, with particular attention given to ensuring that the electrical parameters do not exceed the operational limits. The tuned parameters are listed in appendix A.

After obtaining promising results from simulations, it is possible to test the software developed at the MMC test bench. The purpose is to validate the converter's design and control algorithms, closing the gap between theoretical analysis and real-world implementation. In this way, the control algorithms and connection processes can be employed as a base for future research with the laboratory prototype.

The graphs shown for each scenario are focused in certain parts of the operation that are significant for each case. By integrating all the results, the MMC will have been tested as a whole.

4.1. Islanded operation

4.1.1. Simulation

For the isolated operation scenario the test consisted in replicating the start up recommendations of the manufacturer: energize the converter with the autotransformer and the open-loop approach, then move to any desired control.

Figure 4.1 displays the system's development through different stages. The initial graph presents the activation of distinct control mechanisms at precise times. The second graph illustrates the state of the contactors that join or separate different system components at specific times. Together, these graphs visually demonstrate the system's progression and allow for the analysis of each separate stage.

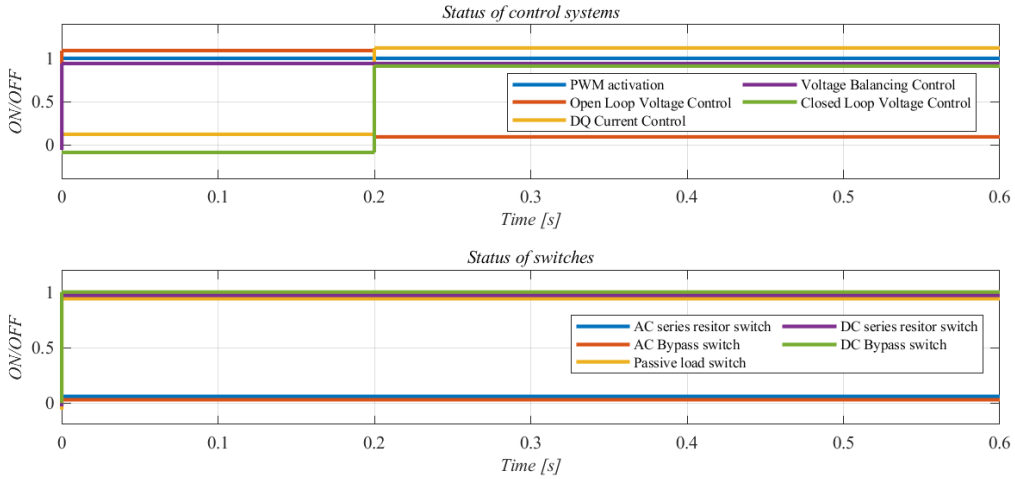

Figure 4.1: Controllers and switches status.

Both DC contactors are connected for the whole simulation, as well as the passive load one. Then, the pre-insertion resistor mechanism was not employed[1], and the capacitors' soft energization depended on the autotransformer's manual actuation. Logically, the AC contactors are not used in this scenario as the system is never connected to the AC grid. The PWM outputs, along with the open loop and voltage balancing controller, are enabled from the beginning.

This arrangement constitutes the suggested one to try out the MMC bench, so it was the first tested. This way, the voltage balancing controllers are tested while progressively increasing the autotransformer voltage. After 0.2 s, the open-loop voltage controller is substituted by the cascaded voltage and current controllers, which allow closed-loop control over the AC bus voltage.

Fig. 4.2 displays the evolution of arm currents and phase A submodules' capacitor voltages, showing the system's energy flow throughout the process. The capacitors are gradually charged during the first 0.1s due to the simulated actuation on the autotrafo. The arm currents remain under the nominal value of 10 A (RMS) during all stages. Since it is virtually impossible to manually move the autotrafo in less than 0.1s, it can be ensured that this process is safe and can be tried at the bench. The capacitor voltages are balanced thanks to the leg voltage controllers, independently of the higher level control approach of AC bus voltage.

[1]The pre-insertion resistor mechanism was tested aswell, but the results are included in section 4.2, so they are no presented here to avoid repetition.

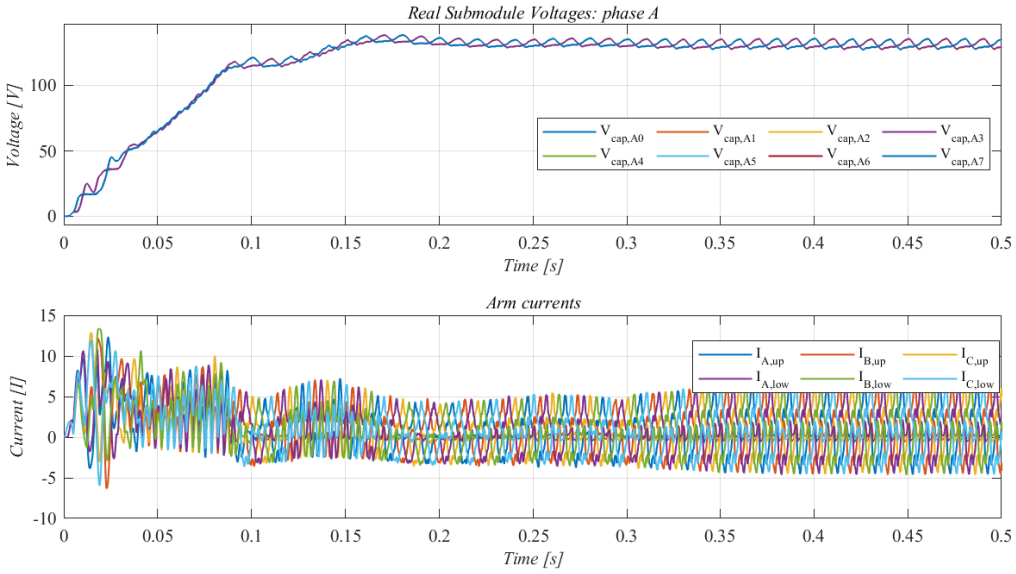

Figure 4.2: System's energy flow.

Close attention is given to the control mechanisms of the phase voltage controllers (fig. 3.16). The vertical imbalance controller corrects the deviation of the average capacitor voltage between the upper and lower arm in each leg, producing a sinusoidal component of the circulating current at the nominal frequency, as shown on the two left graphs of fig. 4.3.

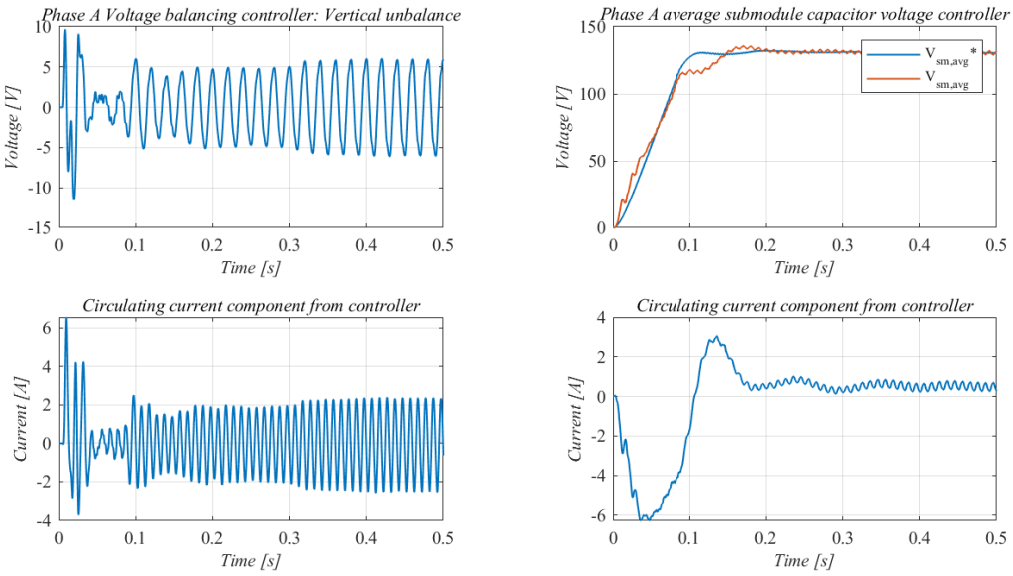

Figure 4.3: Branch voltage controllers.

On the right side, the phase voltage controller follows the average capacitor voltage reference by producing another component of the circulating current reference. These controllers are designed to keep the system balanced and stable. Both components are added to the feed-forward term (calculated to account for the real power exchanged) to form the total circulating current reference in the first graph of fig. 4.4.

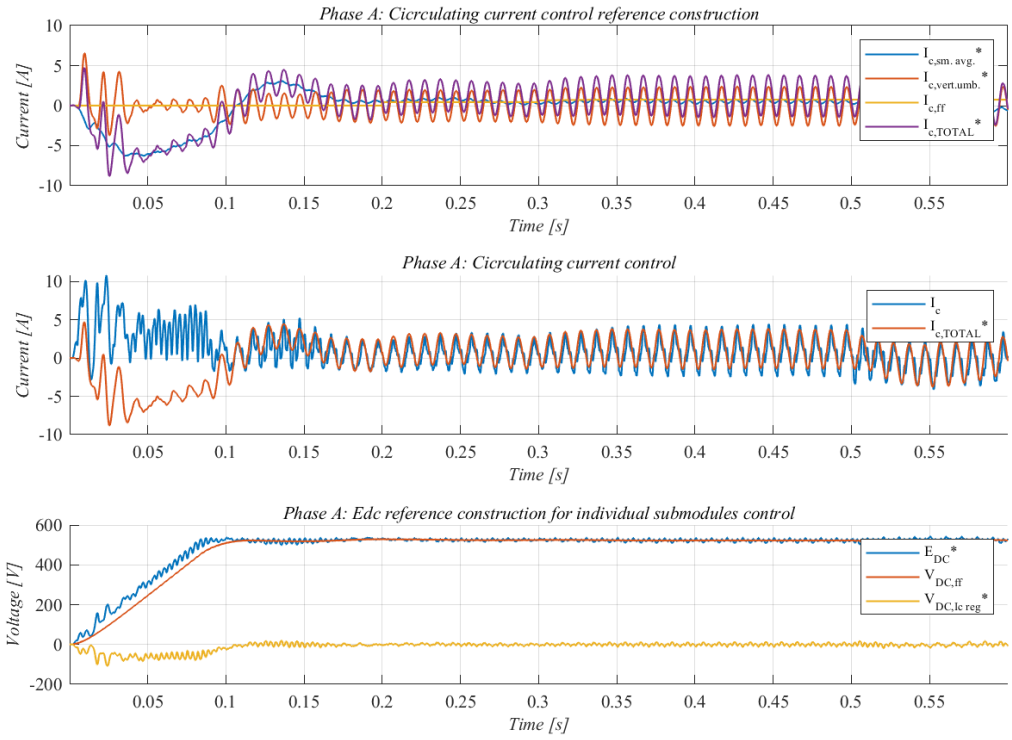

Figure 4.4: Circulating current control.

This reference is tracked by the cascaded circulating current controller (second graph) to produce a DC voltage signal. The signal is added to a feed-forward term with the measured DC voltage, making the DC voltage reference for all the individual submodule controllers of each phase, as shown in fig. 3.15.

On the other hand, the higher level control produces the AC reference for all the individual submodule controllers. This reference can be made in an open loop fashion or by controlling the AC voltage through cascaded voltage and current controllers.

Finally, the AC and DC voltage references are added up at each submodule controller, along with the control action to balance each capacitor voltage. Fig. 4.5 shows, in the first place, the individual capacitor voltage of one submodule with respect to the average value of the capacitors in the phase, showing that they are almost superimposed. The

regulator's output is the third term that forms the desired submodule voltage in the second graph. The ratio between the desired submodule voltage and the corresponding capacitor voltage provides the duty cycle signal for the PWM driver of each submodule. As expected, it comprises a sinusoidal signal with a DC offset.

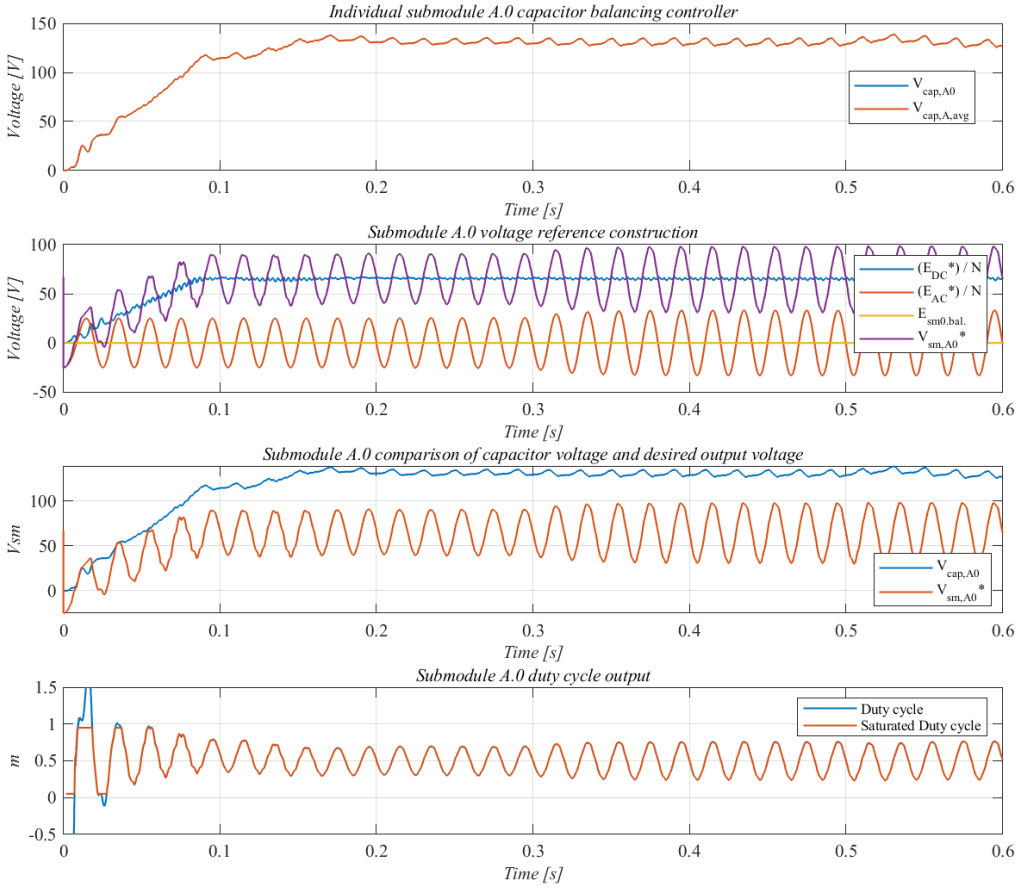

Figure 4.5: Individual duty cycle generation.

Fig. 4.6 shows the AC bus voltage control: before t=0.2s, the AC voltage reference is given in open-loop; the cascaded voltage and current controllers are enabled from this time until the end of the simulation controlling the AC bus voltage in closed-loop. From t=0.2s, both components of the AC voltage start to closely follow the reference, showing a settling time of 0.05 s with no overshoot. The load is purely resistive so the current is necessarily proportional to the voltage, even though the tunning of the current controller is kept exactly as in section 4.2 for grid-following operation.

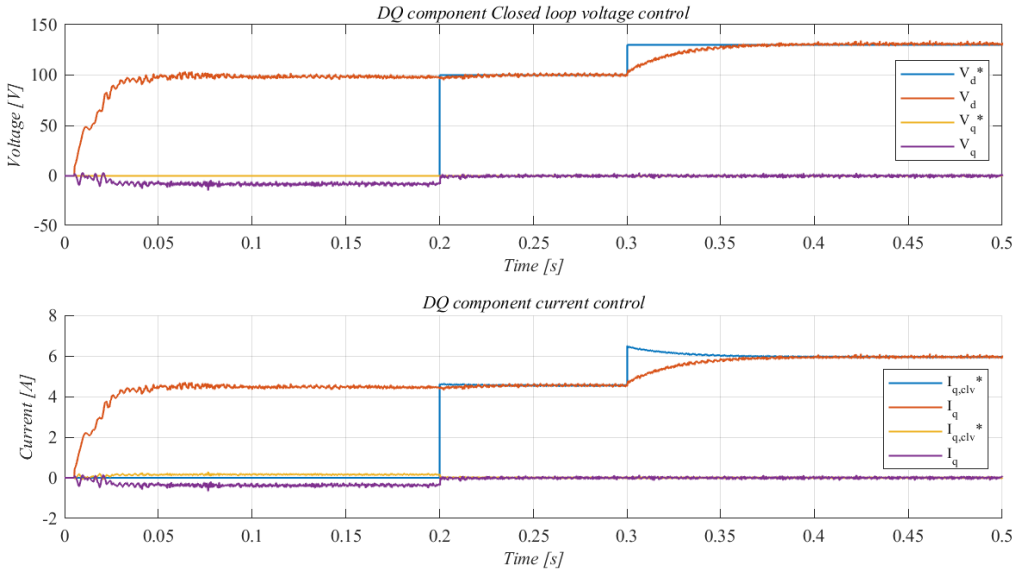

Figure 4.6: Closed-loop AC bus voltage control.

Finally, it is interesting to show a close view of the steady state, showing how the load currents follow a stable AC pattern of 50 Hz as intended and the capacitors of the different submodules are balanced. The submodules within an arm are almost superimposed, but oscillate with an amplitude of 4 V, with respect to the complementary arm of the same phase, as a consequence of the circulating current. This result is replicated at the steady state for all three cases, so it is not shown again.

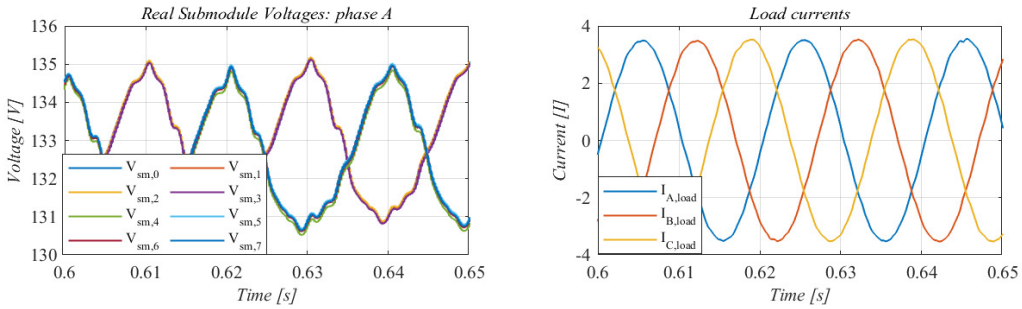

Figure 4.7: Steady-state operation of submodule capacitors and load currents.

4.1.2. Experimental results

After the promising simulation results, the work moved into practical implementation on the experimental test bench. Safety issues are crucial when testing the real MMC, especially when connecting and energizing different parts of the system.

The experiments were carried out progressively by increasing the DC bus voltage for the sake of safety, but only the final ones with the autotransformer at 100% are shown.

The firsts tests consisted in replicating the described simulation, following the recommendations of the manufacturer. A single operation mode with the open loop voltage control approach both for energization and operation, with no change in contactors or active controllers. The energization is included in the operation mode by manually acting on the autotransformer, as shown in fig. 4.8.

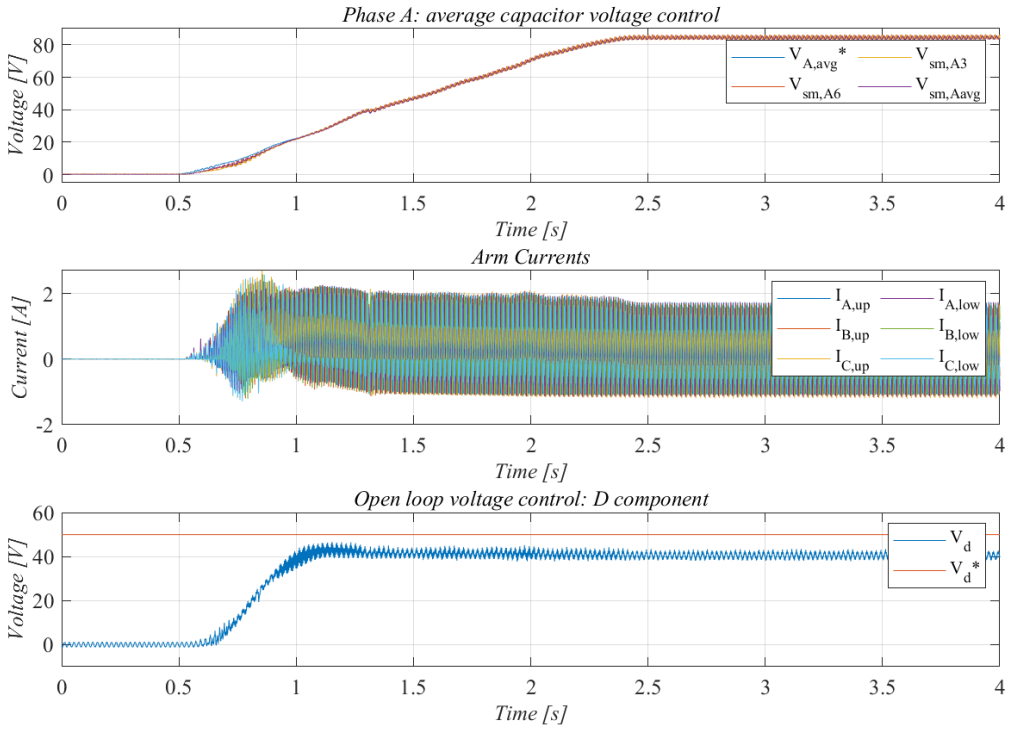

Figure 4.8: Energization with autotransformer during operation of islanded MMC.

The signals in the first graph are two randomly[2] selected capacitor measurements, the average capacitor voltage and the reference average voltage for the phase A controller (which is calculated from the DC bus voltage measurement and, therefore, only depends on the autotransformer). Then, the controllers increase the capacitor voltages proportionally to the manual variation of autotransformer voltage. As predicted, manual actuation is way slower than the simulated one, so the arm currents shown in the second graph are way lower than the nominal value.

[2]The Imperix interface during experimentation allows a maximum of 32 signals to be seen and exported simultaneously, so only some capacitor voltages have been registered.

The last graph shows the D component of the AC bus voltage, which increases until the capacitors have enough voltage to produce its steady state value. Due to the open-loop approach, it does not meet the reference. Fig. 4.9 complements the previous, showing the internal behaviour of the individual submodule controller (for submodule 0 of phase A as an example) during the manual energization while in operation mode. The controller receives the AC bus voltage signal from the open loop voltage control and the DC bus voltage from the phase voltage controller to produce the submodule's duty cycle signal.

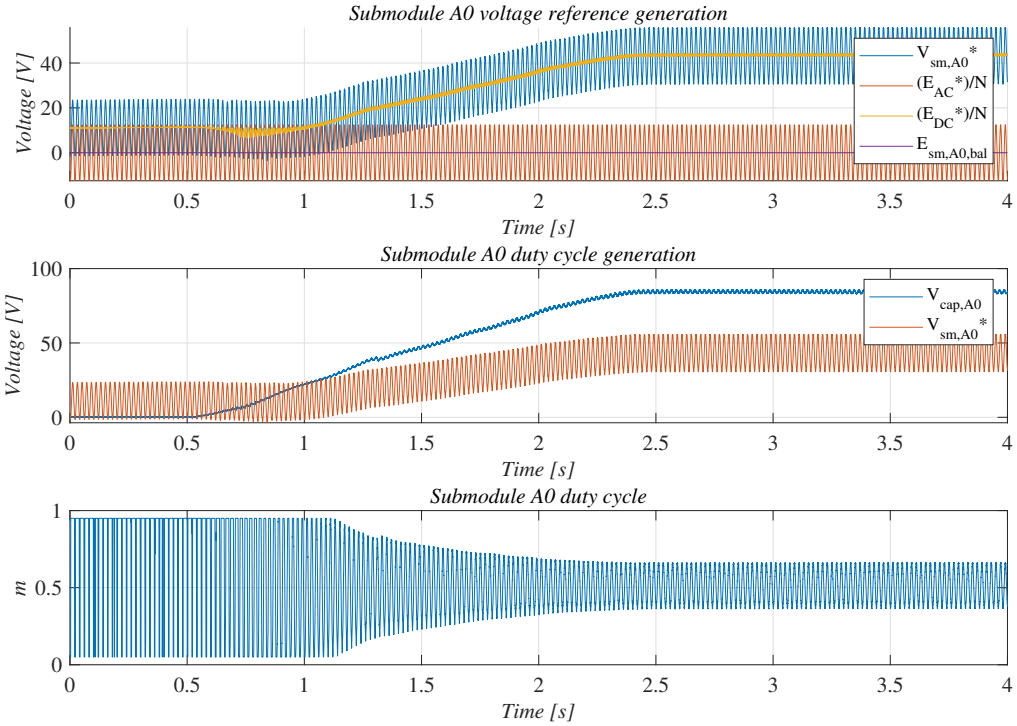

Figure 4.9: Energization with autotransformer during operation of islanded MMC. Individual SM controller.

The AC bus component remains constant, while the DC one increases proportionally when the DC bus voltage rises due to the autotransformer variation. As the capacitor voltage increases and overcomes the desired submodule voltage, the PWM modulation signal is no longer saturated and reaches the steady state along with the capacitor voltage.

However, acting manually on the autotransformer with the system in operation mode is effective but not very convenient and can lead to human errors. The following tests explored other energization methods. Fig. 4.10 shows the energization using the autotransformer at the DC bus but with no control enabled (before operation mode).

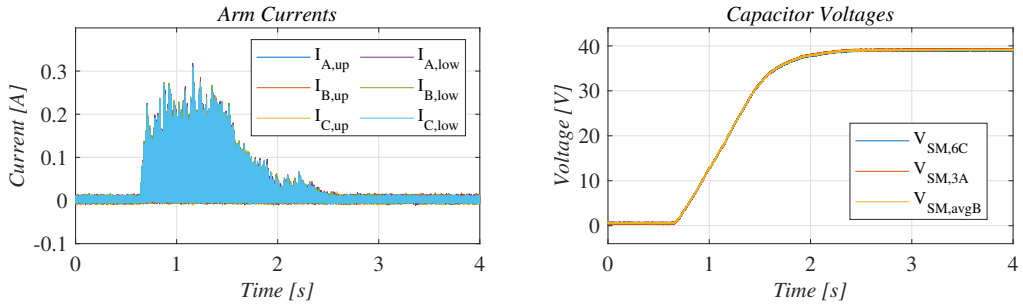

Figure 4.10: Initial energization from DC side with autotransformer.

Alternatively, fig. 4.11 shows how the pre-insertion resistors can restrict the energization currents without the autotransformer.

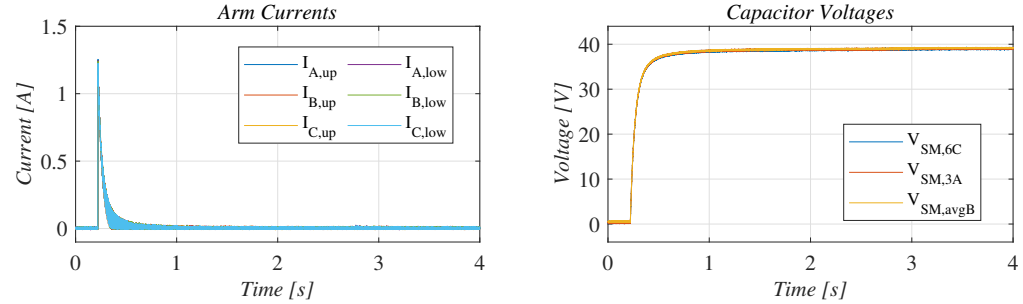

Figure 4.11: Initial energization from DC side with pre-insertion resistors.

In both cases, the capacitors are naturally loaded until the equilibrium value is reached, and the arm currents remain way lower than the nominal value of 10 A (RMS), proving that both are suitable energizing methods. It can be noted that the final capacitor voltage is half the value obtained in operation in fig. 4.8, the final energization must be produced when initiating the operation mode.

After the initial energization (either with the autotrafonsmer or the resistors), the PWM outputs and the required controllers should be enabled to produce the desired voltage at the resistors. Fig. 4.12 shows the moment in which the open loop voltage controller and the voltage balancing controller are simultaneously enabled and how the capacitor voltages are effectively balanced while tracking the average reference voltage, thanks to the action of the circulating current controller. Meanwhile, the arm currents are still below the nominal values, confirming the suitability of the whole process.

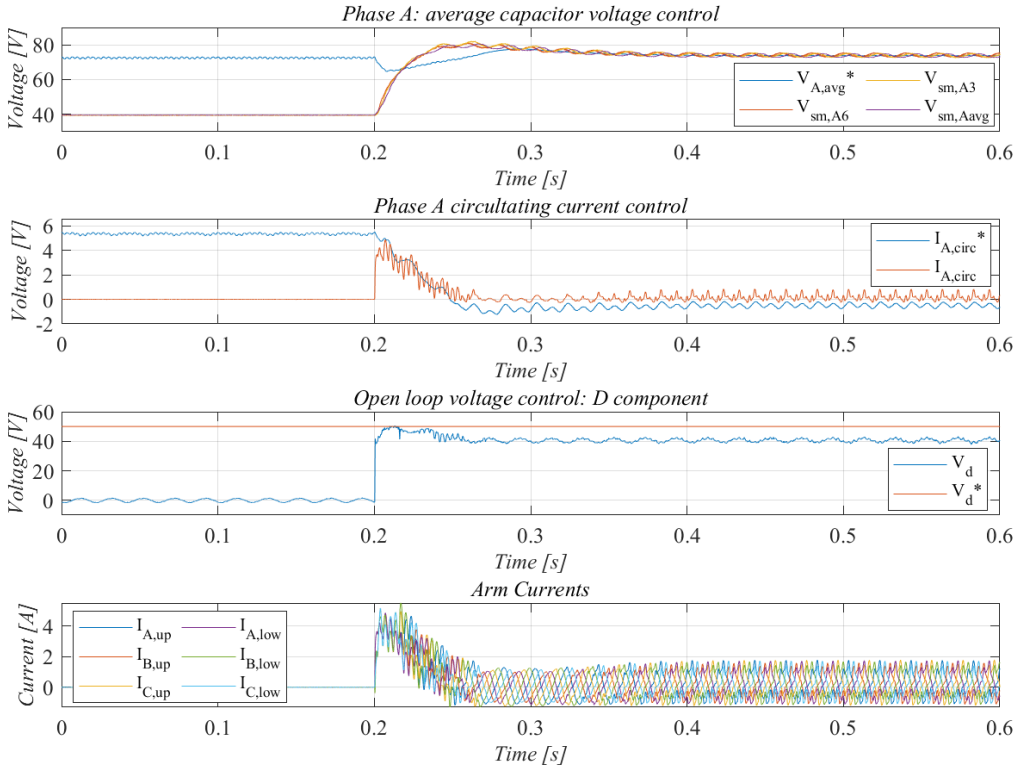

Figure 4.12: Final energization starting the operation mode.

Once in operation, it is possible to move from the simpler open-loop approach, designed for first energizations and focus on the voltage balancing controllers, to another higher-level approach in closed-loop. Fig. 4.13 shows the D component of voltage and current controllers for a reference change, showing close alignment to the results shown in the simulation.

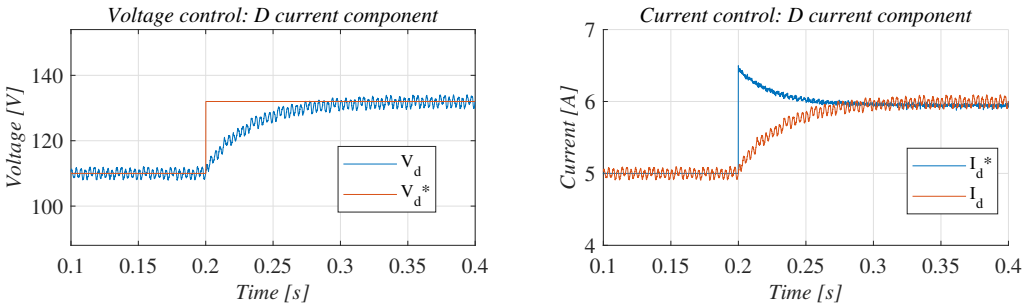

Figure 4.13: Higher-level voltage and current controls.

Finally, it is interesting to check the steady state operation of the load current and the capacitor voltages. Fig. 4.14 shows the three-phase currents and some randomly selected capacitor voltages (as the interface of Imperix only allows to see and export a maximum number of variables, and it was preferred to visualize one measure from each phase). It can be seen a similar behaviour than in simulation, a good quality 50Hz three-phase current and all the capacitor voltages oscillating around an stable equilibrium value at the fundamental frequency, corresponding to the periodic energy flow between arms.

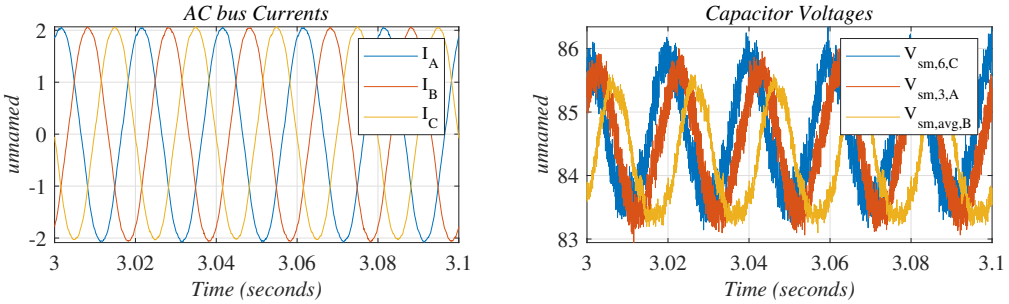

Figure 4.14: Steady-state operation of submodule capacitors and load currents.

4.2. Grid Following operation

4.2.1. Simulation results

The following simulated results illustrate the behaviour of the grid-following study case, to validate the effectiveness of proposed control schemes prior to testing the real system. In order to accelerate the simulation time, the time intervals between stages defined in section 3.3.2 have been reduced, compared to the ones used in section 4.2.2 during the real test-bench experiments to ensure the system's security.

Fig. 4.15 portrays the system's progression through various stages, as done in the first case, with the active controllers and the contactors' status. The passive load contactor is not utilized in this scenario. The DC pre-insertion contactor is enabled during the whole simulation while the DC bypass one is enabled after the first 100 ms, simulating the timer-relay actuation. Simultaneously, the PWM outputs are enabled, as well as the open loop voltage controller and the voltage balancing controllers, to reach the operational capacitor voltages for a fixed time-lapse of 50 ms.

Then, the open loop voltage controller is substituted by the synchronization and current controllers during the synchronization process. Once the synchronization phase is completed, the AC pre-insertion resistor contactor is activated. The synchronization control

is deactivated whereas the subsequent current and voltage controllers remain active.

The AC bypass contactor is activated after the 50 ms defined for the pre-insertion, leading to the soft-bypass stage and operation stage, where the MMC's AC bus is directly connected to the AC grid. The enabled controllers during these three last stages do not change, but the current reference is limited to ensure security during the transitions.

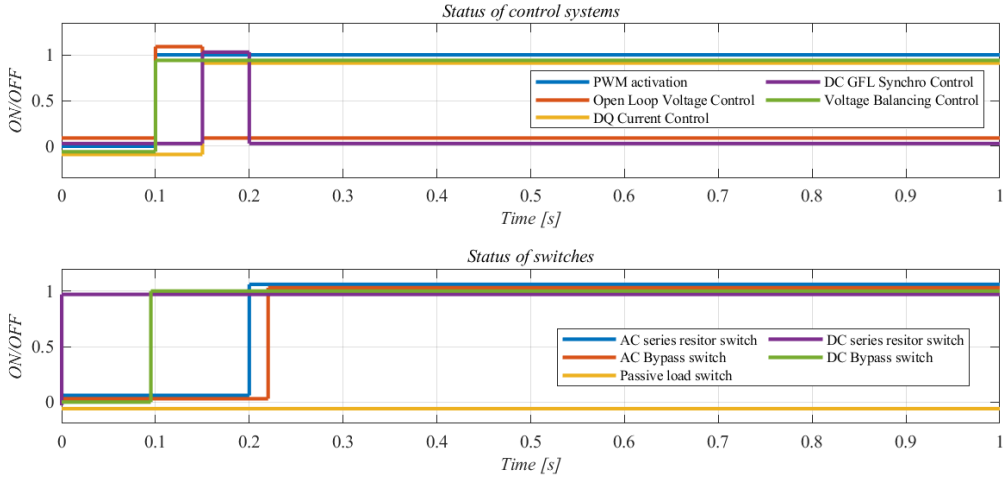

Figure 4.15: Controllers and switches status.

Fig. 4.16 provides a detailed analysis of the current control dynamics. The references are produced by the synchronization controller during the first 50 ms to match the voltages at both sides of the AC contactors. Then, they are forced to zero during the pre-insertion stage, and kept at very low values during the soft-bypass one. Afterwards, the references are manipulated to see how the control responds.

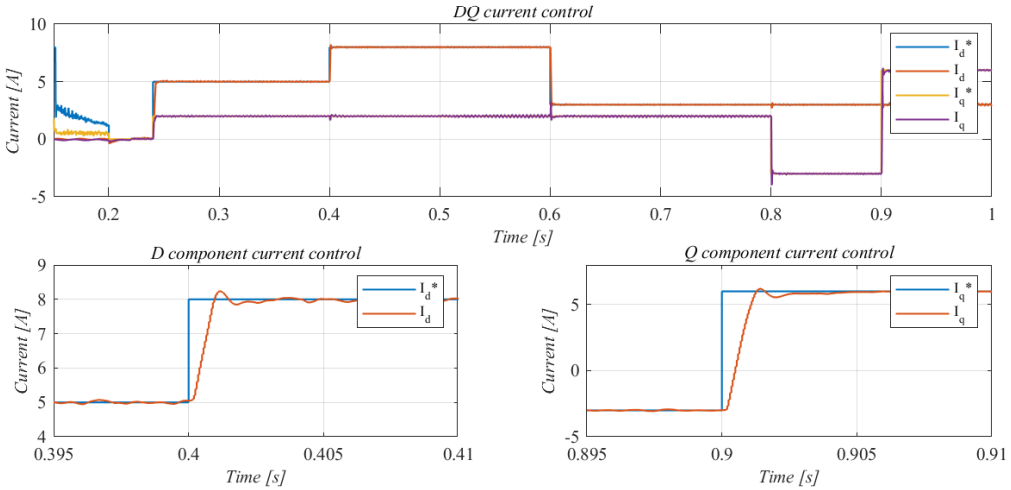

Figure 4.16: DQ current in simulation.

The control system exhibits less than 5% and a settling time of approximately 2 ms to reach and stabilize at its final value[3]. These features indicate that the developed DQ current control system effectively regulates the AC bus current within acceptable limits. The measured current contains a small ripple component, due to the switching, but it does not significantly impact the overall performance of the current control.

Fig. 4.17 details the synchronization process. The first graph depicts the progression of AC bus voltage and AC grid measurements (the voltages at each side of the contactor) during the synchronization phase in the DQ frame. Through the action of the synchronization controller, the D and Q current references are set so the voltage produced at the AC bus progressively converges towards the grid voltage value. This ensures a precise alignment between the MMC system and the grid, requirement for a smooth and successful connection.

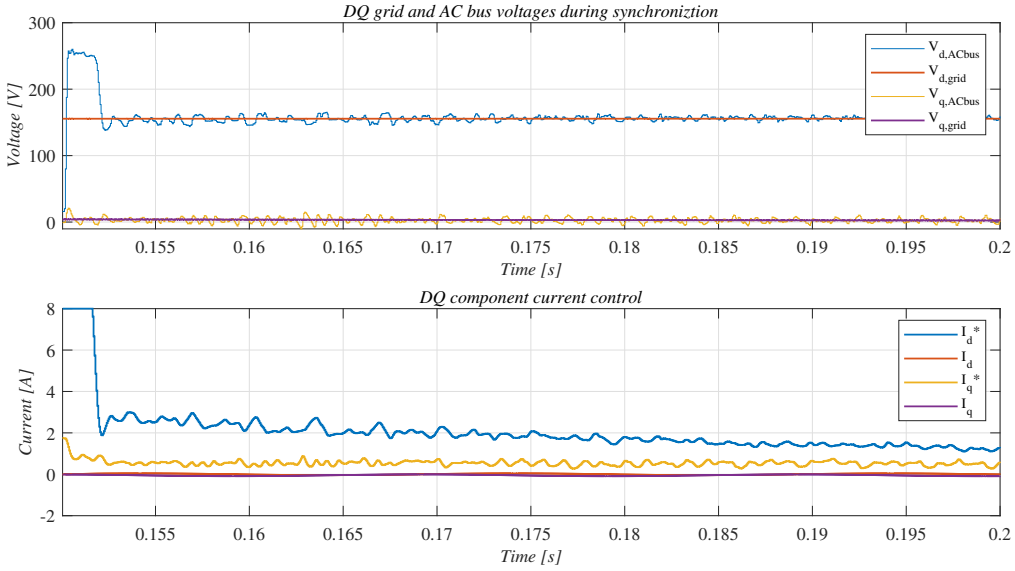

Figure 4.17: Synchronization process.

Fig. 4.18 shows the evolution of the arm currents during the whole process, along with the capacitor voltages of phase A submodules, representing the system's energy flow throughout the process. It can be observed that all the currents remain under the submodules' nominal value of 10 A RMS during all stages, proving that the process designed is successful and secure for the equipment. This confirmation allows for moving towards real bench experimentation and confronting the converter's performance with real-world challenges, considering factors such as noise and non-idealities that may affect its performance.

[3]It can be observed a slight difference between D and Q, due to the saturation of the controller's output, as the reference step was big

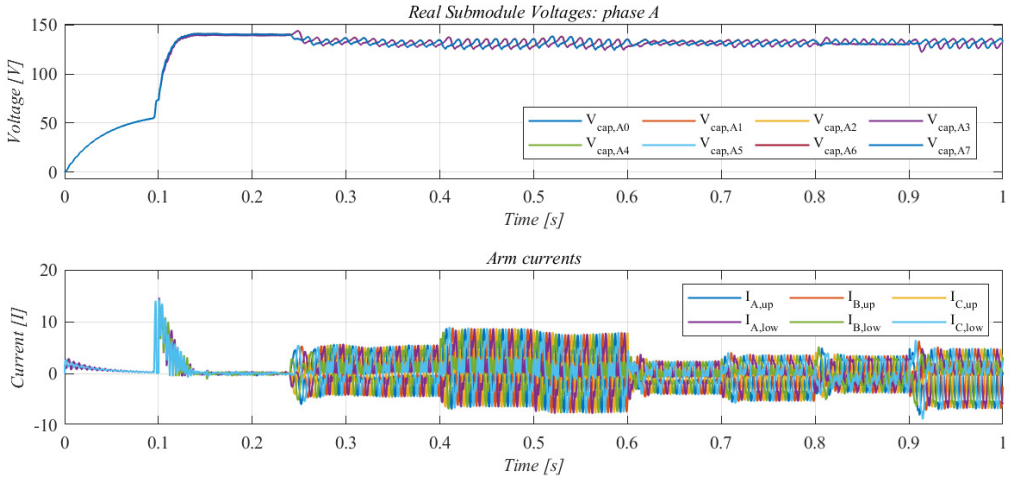

Figure 4.18: System's energy flow.

The steady state operation regarding the capacitors voltage balancing and AC bus current remains the same as in fig. 4.7, so the corresponding graph is not included in this and the following sections.

4.2.2. Experimental results

After obtaining promising simulation results, the focus shifted to the real-world challenges on the experimental test bench. When transitioning from simulation to the real test bench, the connection and energization processes are particularly significant regarding the system's safety. For this reason, the waiting times between stages have been enlarged to make real-time supervision and manual actuation possible.

The energization procedure is carried out as in section 4.1: the PWM outputs begin disabled, allowing the capacitors to be naturally charged through the antiparallel diodes from the DC side, either with the pre-insertion resistors or the autotransformer, as already displayed in figs. 4.10 and 4.11, so it is not repeated here.

After the initial energization, the user can manually activate the connection to the AC grid. The soft-start stage lasts a predefined timelapse of 200 ms, where a limited AC bus voltage is produced in open circuit by means of the open-loop voltage controller. Fig. 4.19 illustrates the result of this stage, achieving the final capacitor energization with safe charging currents, which never exceed the nominal 10 A(RMS).

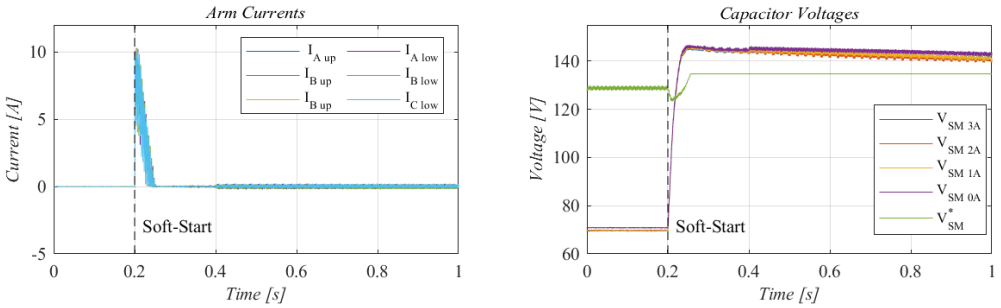

Figure 4.19: Final capacitor loading during soft-start stage.

Notably, the capacitors are slightly overcharged during this stage, exceeding the nominal operation value. This overload is corrected at the final operation stage because the diode bridge prevents the energy from flowing back to the DC bus, so the capacitors can only be discharged when the AC bus is no longer in open circuit.

Fig. 4.20 illustrates the AC output voltage behaviour during the synchronization stage, which automatically follows the soft-start after 200 ms. The AC output voltage is no longer limited but instead controlled to reach the grid voltage.

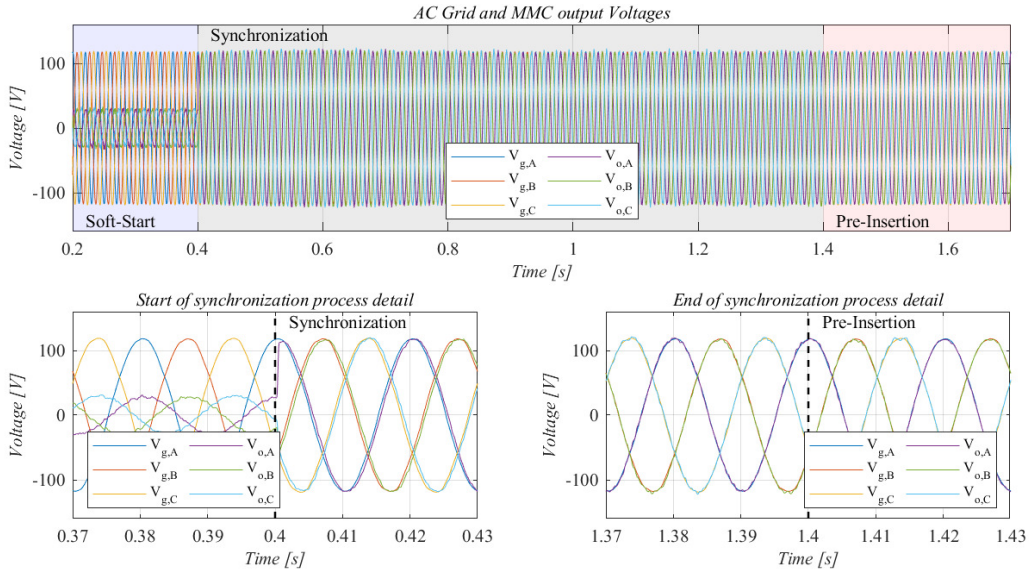

Figure 4.20: Synchronization of AC voltage to grid voltage.

The first graph depicts the evolution of the grid voltage and the output voltage throughout the entire process of 1 s. The second and third graphs provide a closer look at the transitions into and out of the synchronization stage, respectively. As the synchronization stage progresses, the voltage waves steadily converge, ultimately resulting in a near-match.

After the energization and synchronization stages have been completed, the connection of both grids can be safely carried out, transitioning towards the operation state. As already introduced, two intermediate stages (pre-insertion and soft-bypass) enhance safety and stability as the system transitions from synchronization to operation. Subsequently, the system enters the final operation stage, where the AC bus is directly connected to the AC bus and the current references are released and allowed to be modified by the user, reaching Grid-Following operation. Fig. 4.21 illustrates the whole process.

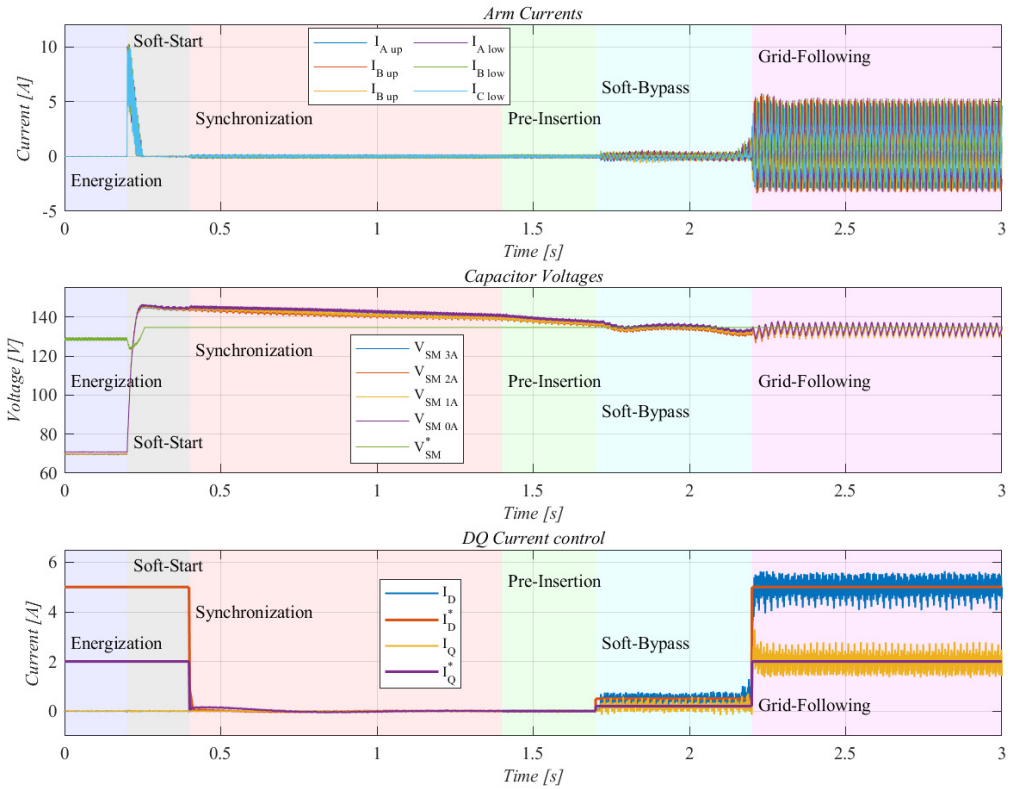

Figure 4.21: Grid-following connection full connection process.

The first graph shows the arm currents throughout these stages, demonstrating that the transitions occur without any dangerous current peaks flowing through the submodules. The additional "security" stages play a pivotal role in ensuring the smooth and safe progression through each transition.

The second graph shows the evolution of some capacitor voltages. During the initial stages, the capacitor voltages are allowed to acquire an overcharged state. As the system connects to the AC grid, the balancing control ensures that the capacitor voltages are kept well-balanced and track the desired operation value.

The third illustrates the evolution of the D and Q components of the current during the whole process. The DQ current control is enabled at the synchronization stage, following the references defined by the synchronization control, alligning to the measured values along the process. The current references are deliberately forced to zero in the pre-insertion stage and kept limited to low values during the soft-bypass stage. Finally, the current references are set free, allowing the user to manipulate and adjust them as needed.

Fig. 4.22 depicts the details of the DQ current controller. The Q-axis components have been skipped to avoid unnecessary repetition. The first graph shows the succession of reference changes used to test the system's response. The second provides a zoom of one of the transients to check the dynamics, which show pretty similar to the simulation one.

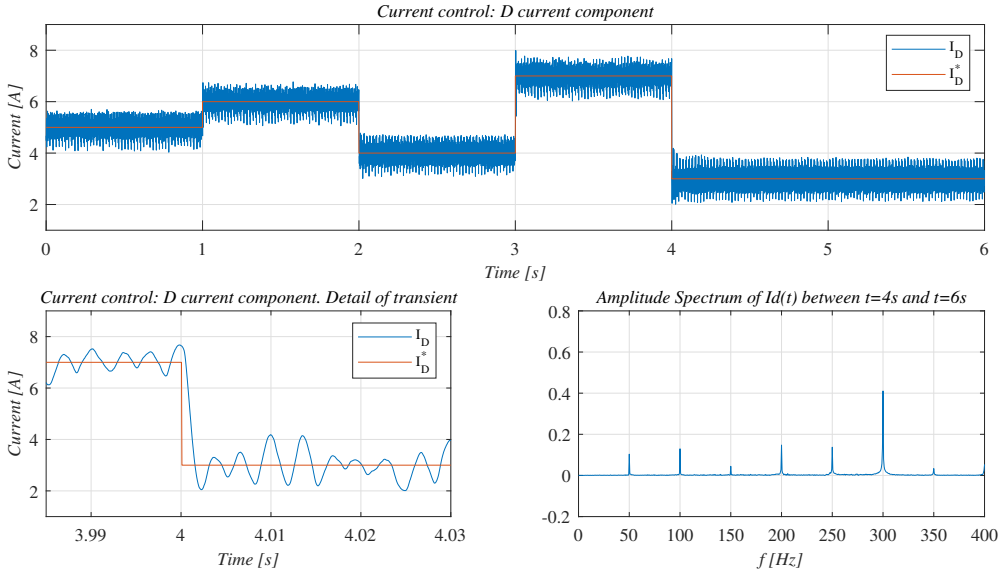

Figure 4.22: Current controller behavior: D component.

The signal has an evident harmonic content that did not show up in the simulation. Frequency analysis allows the identification of the source of the distortion. The oscillation is mainly due to a harmonic component at 300 Hz, as shown in the third graph that zooms at the most significant harmonic components. After studying the situation, it was concluded that the reason is that the grid that feeds the laboratory is also feeding the whole building, which has a lot of electronic devices (mainly computers and other converters) that introduce harmonic content due to voltage rectification.

In fact, both DC and AC transformers had to be plugged to the same point of the grid's laboratory. If they were connected to different plugs, the differential switches of the laboratory tripped, due to the structure of the electricity protections at the lab.

Then, the diode rectifier at the DC bus, which is a great source of harmonics, is directly connected to the AC bus circuit (only separated by the autotransformers). The THD was not so evident at the initial stages, as the power through the rectifier was almost null, unlike the one after the connection is stablished.

This result not only validates the work done, but it also proves that it is robust even in low-quality grid conditions. However, it leads to some enhancements to the system. One possibility is to act on the DC bus, either introducing a filter or substituting the rectifier by a DC source with DC pre-charge circuit (however, the quality of the grid due to the rest of devices can be still low). It is also possible to connect the AC bus to another devices such as analog amplifiers that simulate in real time a more complex system such as the PCC of a WPP or whichever system desired. Exploring these alternatives is in the roadmap of the research project, but it is beyond the scope of the thesis.

4.3. STATCOM operation

4.3.1. Simulation results

The following simulated results demonstrate how the system behaves for the third case of study, validating the proposed control schemes before testing in the real system, as done with the previous cases.

Fig. 4.23 provides a detailed visualization of the system's evolution throughout the stages, considering the electrical configuration and the control schemes acting on it.

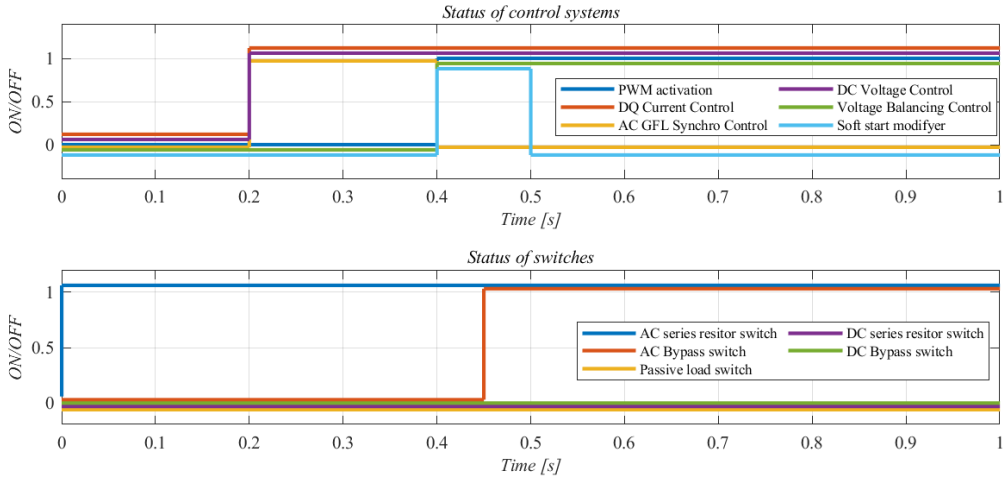

Figure 4.23: Evolution of controls and switches.

The DC bus and passive load contactors are not utilized. Conversely, the AC pre-insertion resistor contactor remains activated throughout the entire simulation. Initially, PWM outputs are turned off, and no active control is present, corresponding with the capacitors' natural charging process through the antiparallel diodes and the pre-insertion resistors.

The necessary controls for synchronization between the AC bus and the grid voltages are activated after the energization, as explained in 3.3.3. The PWM is enabled once the synchronization condition is successfully met. Then, the synchronizing control is no longer needed, but the cascaded controls remain enabled. The control signals include the soft start modifier that forces the Q current reference to zero to minimize the current flow while the capacitors reach their final voltage.

Once the predefined time has elapsed, the bypass contactor is enabled, initiating the transition to the soft bypass stage. The soft-start modifier signal still restricts the Q current reference in this stage. Finally, the reference is set free, marking the transition to the operation phase.

Figs. 4.24 and 4.25 depict the synchronization process in which the synchronization control is cascaded to the DC voltage controller and the DQ current control (fig. 3.31) to produce a final voltage reference that matches the measured grid voltage.

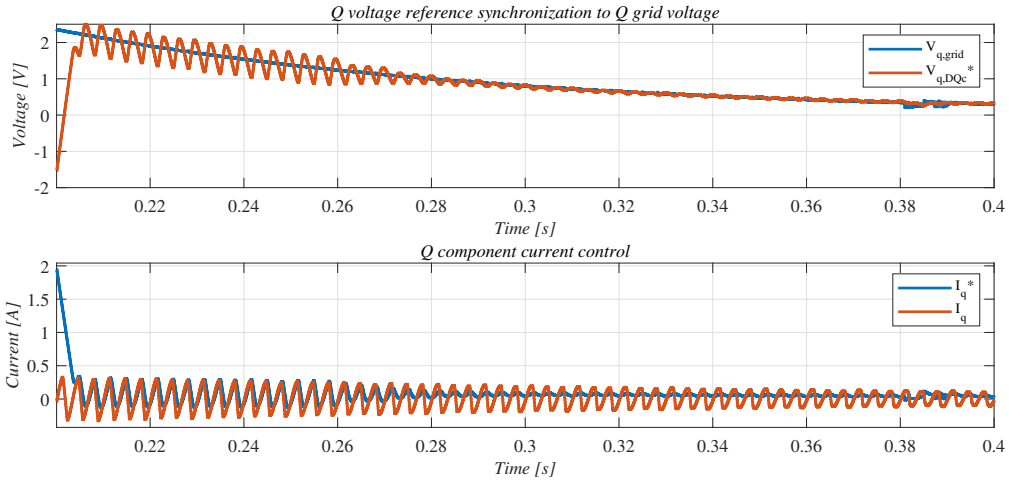

Figure 4.24: Controllers synchronization to the grid (Q component).

Fig.4.24 focuses on the Q axis, showing how the difference between the Q components of the measured grid's voltage and the voltage reference given by the DQ current control moves the Q current reference until the error disappears. The current measurement is oscillating due to the natural load of capacitors through the diodes, as the process starts before reaching the equilibrium value. Even the PLL still has not stabilized the Q

component at 0 V. This case is due to the low waiting times employed to accelerate the simulation, which is not expected for real experimentation.

Fig. 4.25 shows how the D axis follows the same idea but with the intermediate DC voltage controller. In this case, the velocity is limited due to the saturation of the current control output. Again, the measured DC voltage during synchronization is still increasing, as the process starts before equilibrium.

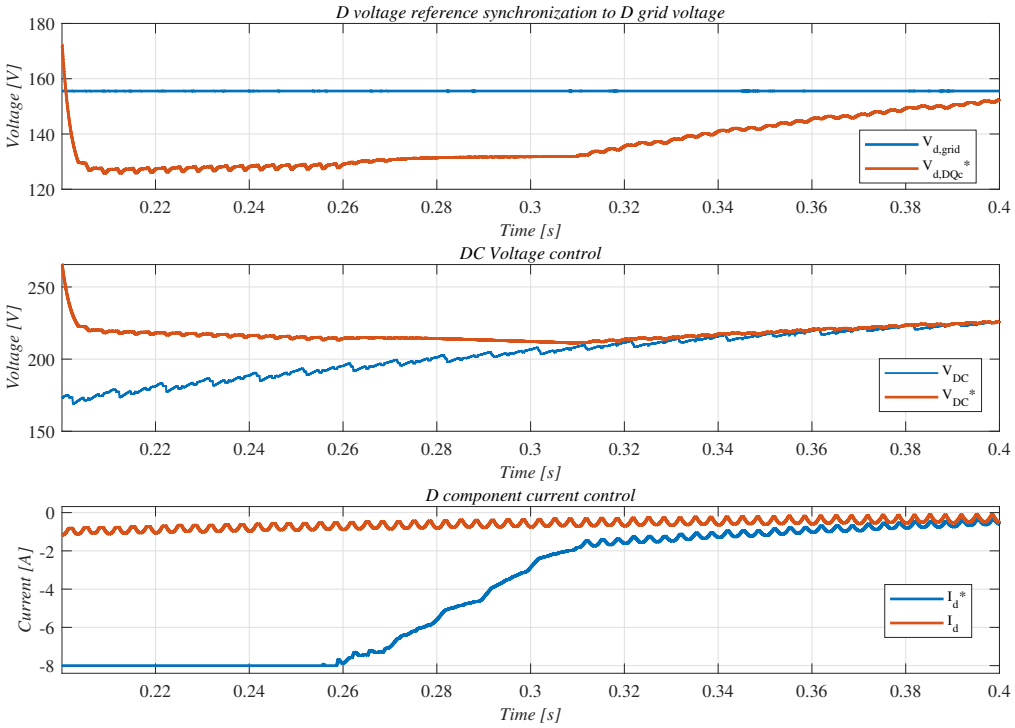

Figure 4.25: Controllers synchronization to the grid (D component).

Fig. 4.26 presents the system's performance during the transition to operation stage. From t=0.2s to t=0.4s, the graphs replicate the synchronization process in 4.25. Once the PWM is enabled, the DC voltage controller tracks the reference operation value through a cascaded action with the D current controller. This process charges the capacitors until the operation voltage is reached. From t=0.4 s to 0.45 s, the increase rate is limited by the pre-insertion resistors. The resistors are bypassed way before reaching the final operation value to further reduce the simulation times. The bypassing generates a transient that, however, is kept below the nominal value of the currents thanks to the DQ control action. However, this must be ensured with the real prototype.

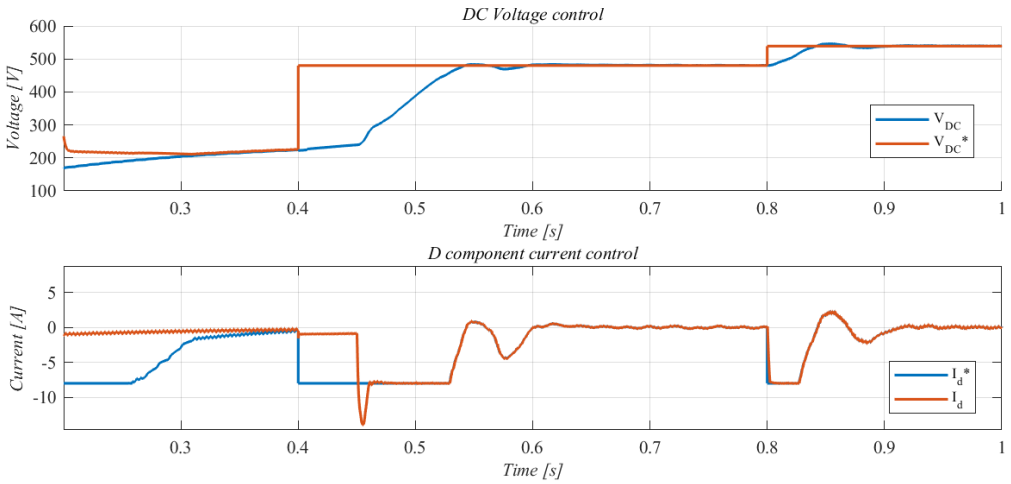

Figure 4.26: Operation controllers.

During these transitions, the Q-current reference was kept at 0 to minimize extra current flow. Afterwards, the system is in STATCOM operation, and some transients are carried out to test the dynamics. The Q current component tracks its reference (which would be set by the user to fulfil the reactive power requirements of the AC system and adjust the voltage at the connection point). The dynamics correspond to the DQ current presented in section 4.2.1, so it is not shown here to avoid repetitions.

The DC voltage control dynamics exhibit an overshoot below 5% and a settling time of 0.05 seconds, a relatively slow response compared to the current control. This difference corresponds to the cascaded nature of the control system The D component of the current accurately tracks the reference signal provided by the DC voltage control to maintain the DC voltage at the desired operational point. The saturation of the current reference prevents over-currents when there are significant DC voltage errors, as when the resistors are bypassed before reaching the operation voltage.

Fig. 4.27 illustrates the evolution of the system variables related to its energy: the capacitor voltages and the arm currents. Initially, the capacitor's voltage increases smoothly through the pre-insertion resistors. When the PWM outputs are enabled, the system continues to charge slowly through the resistors. The voltage-balancing controller operates from this point, keeping the voltage balance as in the previous scenarios. Following the bypassing of the pre-insertion resistors, the rise in voltage is more pronounced until the operation value is reached. The average capacitor voltages reflect the DC voltage transients seen in the previous figure during the operation stage.

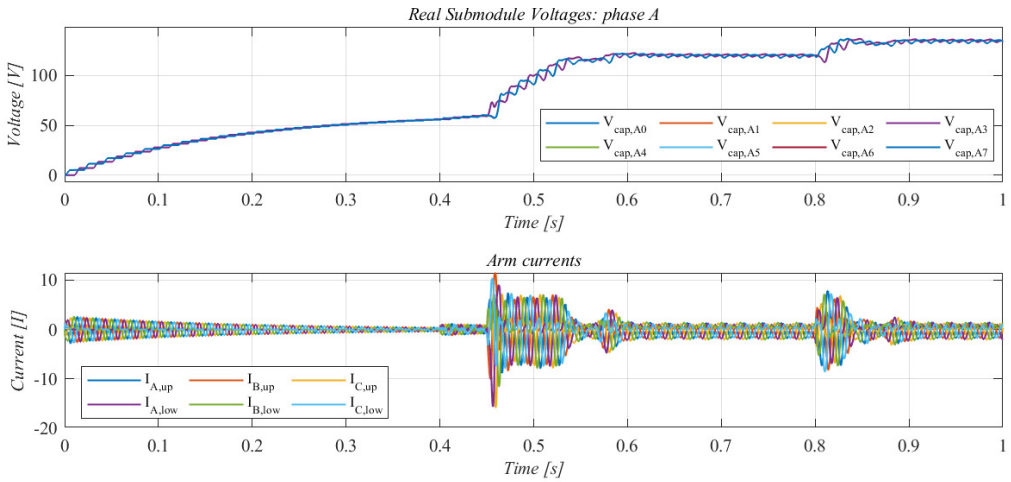

Figure 4.27: System energy.

There are not any over-nominal arm current peaks throughout the process, which proves the starting strategy's efficacy in maintaining system stability and safety. However, these conclusions must be confirmed with the experimental bench, where the real-world behaviour will determine whether or not the starting strategy is valid.

Again, there is no need to show a detailed graph of the steady state operation regarding the key variables of submodule capacitors and AC bus currents, as they are the same shown in fig. 4.7.

4.3.2. Experimental results

The favourable simulation results led to physical experimentation on the test bench. The energization and connection processes involve risks that motivated the enlargement of the waiting times between stages, compared to the ones in simulation.

Fig. 4.28 depicts the key system variables during the energization phase through the antiparallel diodes with the PWM outputs disabled. The resistors effectively restrict the arm currents to a maximum value of 2.2A, significantly lower than the nominal value of 10A (RMS), ensuring system safety. All the capacitors are simultaneously charged up to the same equilibrium value, as when energizing from the DC bus.

Contrary to the simulation, there is no need to reduce time between stages in the test bench, so the synchronization can begin already in the equilibrium point. The synchronization process does not involve any physical process, as the objective is to match the current controller's output to the measured grid's voltage (fig. 3.31).

The PWMs are still blocked so the behaviour does not differ from the simulated one, it is just a bit faster since it begins at the equilibrium value. Therefore, it is unnecessary to show repeated graphs.

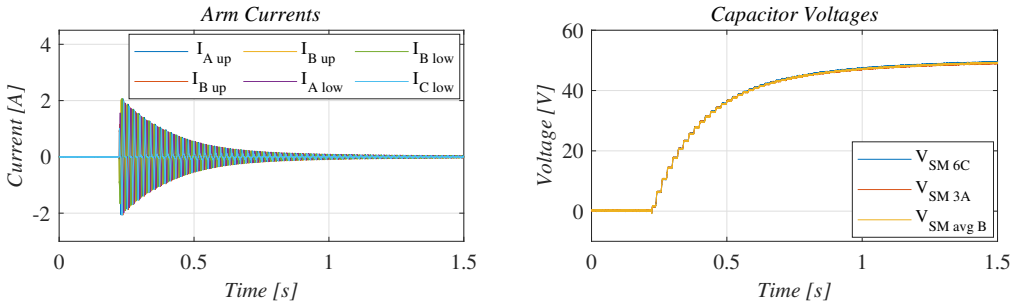

Figure 4.28: AC side initial energization

The soft-start stage can begin when the synchronization condition is met. In the first test (fig. 4.29), it is not interrupted by the next stage as in 4.3.1 (where the simulation times where critical), to see how the DC bus and capacitors reach their final voltages with the pre-insertion resistors. The first graph shows the gradual increase in the DC bus voltage due to the DC voltage controller's action over approximately 2 seconds. It is proportional to the increase in the capacitor voltages at the second graph. An oscillation in the voltages is observed once they reach their final value, but it only happens while the resistors are connected, so it can be disregarded.

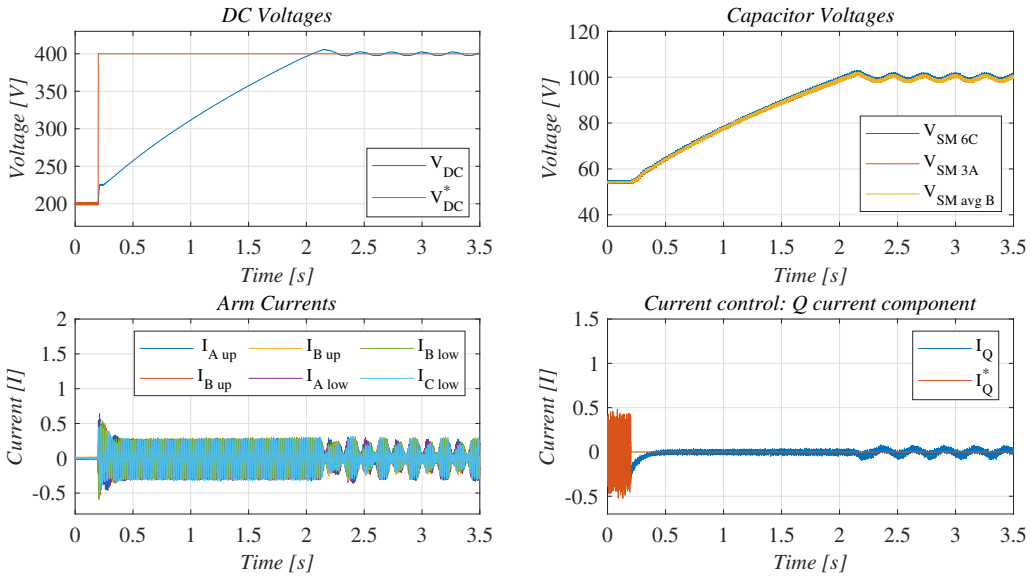

Figure 4.29: Extended Soft-start until operation voltage.

The third graph shows the arm currents throughout the entire soft-start process. The resistors effectively prevent any current peak during the PWM activation instants. After that, the currents remain consistently limited to levels below 0.5A throughout the process. Finally the fourth graph shows the evolution of the Q component of the AC current, , which is forced to zero in order to minimize the current flow through the resistors.

However, the resistors are only mandatory during the initial PWM activation instant. That is why the process is accelerated with the soft-bypass stage to reduce simulation times. Fig. 4.30 demonstrates the whole transition to the operational stage after a shorter soft-start period of 200 ms and a soft-bypass period of 200 ms. The first graph illustrates the arm currents and the capacitor voltages. A transient occurs as the resistors are bypassed, resulting in a peak current of nearly 6 A, still considerably far from the nominal 10 A (RMS).

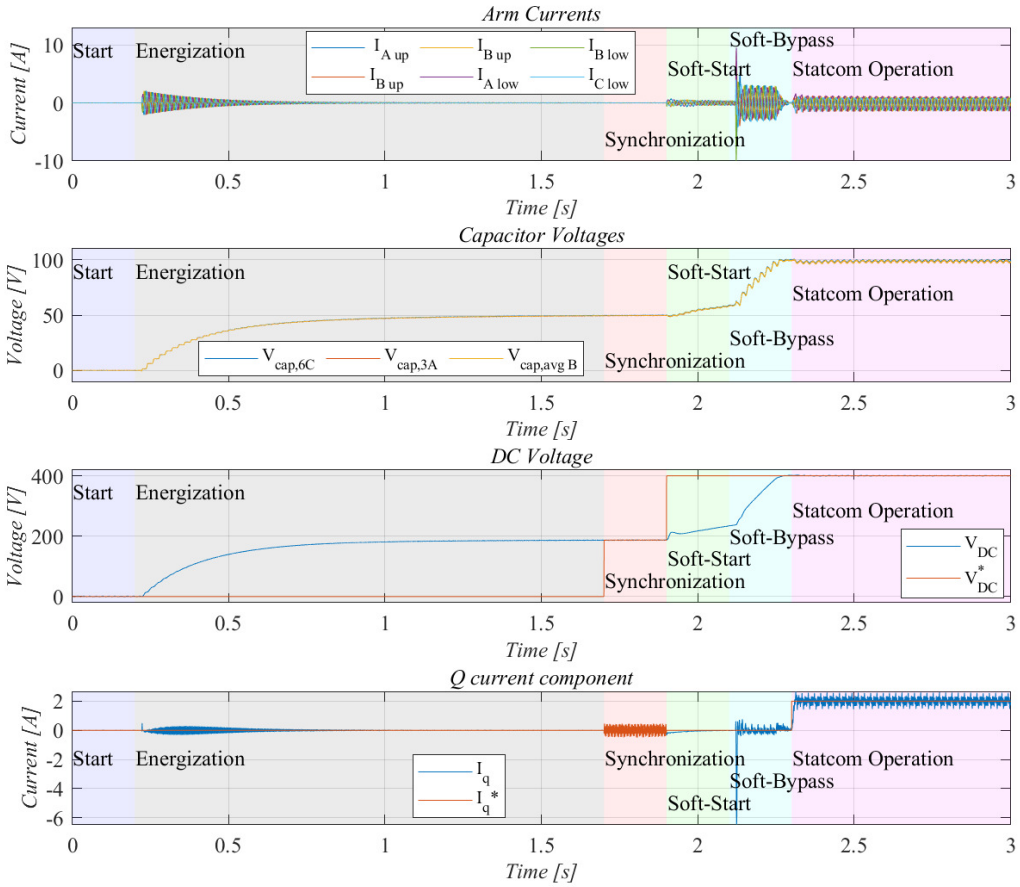

Figure 4.30: Transition to STATCOM operation.

A shorter soft-start stage does not compromise the system's safety and still effectively limits the magnitude of the transient current during the PWM activation. Thus, waiting until the operation values are fully reached is unnecessary, confirming the suitability of the strategy developed for faster simulations.

The second graph corresponds to capacitor voltages, directly proportional to the DC voltage in the third graph. The voltages reach their operational value in approximately less than 200 ms[4]. The last graph shows the Q component of the DQ current control that follows an independent reference signal. During the soft-start and soft-bypass stages, the Q component reference is intentionally forced to zero. Subsequently, the user can set the Q component reference freely; in this case, it is adjusted to a chosen value of 2A, enabling the system to exchange the desired reactive power.

Once the operation stage has been safely established, it is possible to analyse the behaviour of the developed control in detail. Fig. 4.31 shows how the MMC fulfils the STATCOM objective of regulating the local AC voltage by extracting or injecting a specific amount of reactive energy into the power system.

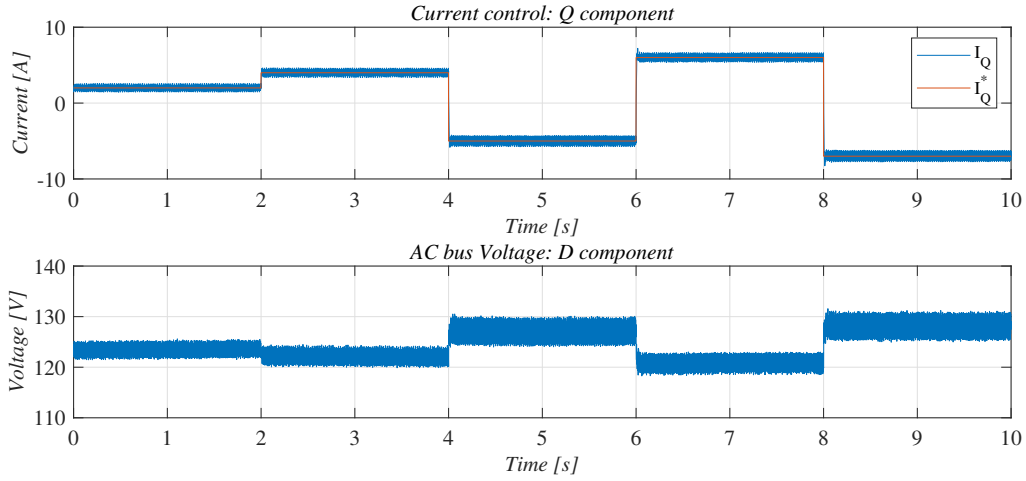

Figure 4.31: Reactive power control in STATCOM operation.

The first graph illustrates how the DQ current controller tracks the manually-set Q reference, as in 4.2.2, achieving the desired reactive power exchange with the grid. The dynamic response and THD characteristics correspond to the ones commented in 4.2.2 for grid-following operation. The second graph shows the impact of the reactive power flow on the AC voltage amplitude, represented by its D component.

[4]However, it is worth noting that the settling time of the DC voltage is constrained by the saturation of the current reference, which ensures the safe and controlled operation of the system.

The observed direct effect proves the control system's effectiveness in regulating grid voltage by manipulating reactive power[5].

The second objective of the system is the regulation of the DC voltage. Keeping the DC voltage at the reference value ensures the MMC converter's stable and reliable operation when working as a pure STATCOM or as the input port to an HVDC line or grid, as explained in 3.3.3. This regulation process involves active power exchange between the converter and the AC grid, corresponding to the AC current's D component.

Fig. 4.32 depicts the DC voltage regulation. The first graph shows the dynamics of the DC voltage tracking the defined reference. The second graph details the transient response of the DC voltage, showcasing a slight overshoot of approximately 5% but reaching a stable operating point within a settling time of roughly 0.1 seconds.

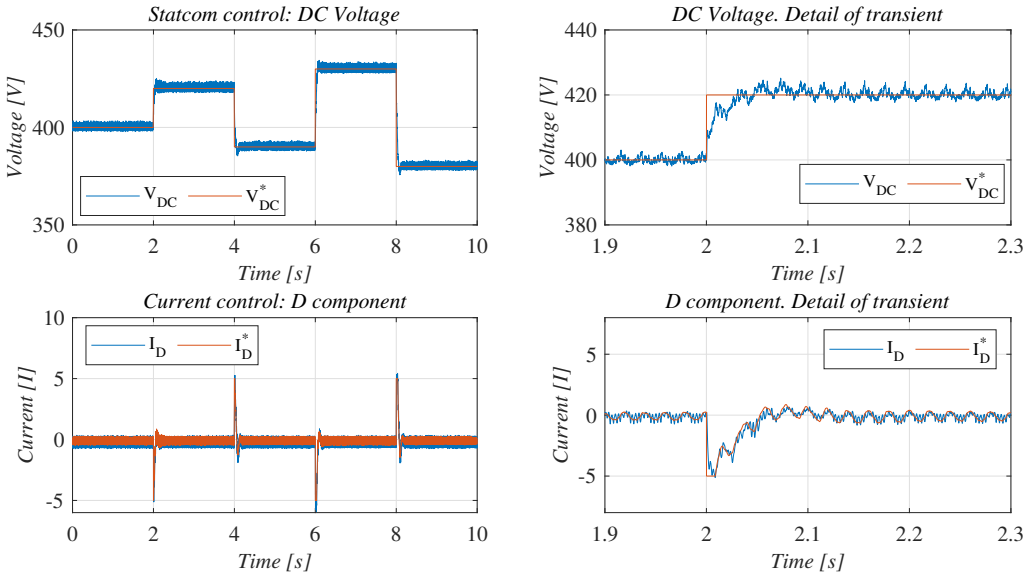

Figure 4.32: DC voltage control in STATCOM operation.

The third and fourth graphs detail the D component of the DQ current control cascaded to the previous. The D current reference closely follows the output of the DC voltage control, ensuring proper DC voltage regulation. The dynamics of the current control correspond to the observed in section 4.2.2, more than 20 times faster than the voltage regulator ones, resulting in proper cascaded operation.

[5]Notably, the voltage is measured at the MMC side of the autotransformer. The system is a laboratory-sized converter whose power is low compared to the grid's, so the effect on the actual grid voltage is minimal, unlike the one that could have a real-sized MMC.

5 | Conclusion

An investigation on modular multilevel converters has been conducted along the thesis. Initially, the context of application for these converters has been introduced to understand why the current electrical framework necessities require them. Then, an overview of the structure, operation and applications is presented. A Simulink model representing a laboratory prototype has been employed to simulate different scenarios. The results are verified by conducting the same experiments in the physical prototype.

Three different operation modes have been studied: islanded mode, grid-following mode and STATCOM mode. Not only the modes themselves have been considered, but also the energizing, synchronization, and connection methods that are required to conduct the system towards the operation. The three modes are complementary, covering a wide range of MMC applications.

The islanded operation studies how the converter can feed a passive electrical grid without the support of other generators. This scenario can be applied to an isolated high-voltage grid powered by an MMC or to different situations that may require a solo operation from the MMC, such as energize areas from the main grid after blackouts or other events.

The grid-connected operation constitutes one of the main applications of the converter, in which it works in synchronization with the main grid (grid-following) and transmits the active and reactive power commands. In this way, a renewable energy source, energy storage system, or any other element connected through an HVDC system can deliver the power demanded at each instant. In addition to the grid-following operation, the synchronization process has been studied as well, which is crucial for establishing the connection of the elements mentioned above to an active grid.

Finally, the STATCOM mode allows the study of how the converter can be employed in high-voltage AC systems to increase their transport capacity by acting on the AC voltage magnitude through the control of the reactive power flow. However, this specific application can be extrapolated to other systems with active power flow towards the DC bus, such as energy storage or HVDC industrial systems requiring DC voltage control. Furthermore, this concept is also employed at the input converter of an HVDC line (or

grid), which is in charge of keeping the DC link voltage so that the other(s) converter(s) can deliver the demanded power working for example, in grid-following as in the previous case.

In conclusion, a wide range of MMC applications has been tested, employing three different operation modes. Additionally, reliable synchronization and connection methods have been developed to take a real-world converter to those operation modes. These developments constitute a solid base for future investigation and experimentation with the laboratory prototype.

5.1. Future work

This project is conducted within the scope of a research project at UPV. The aim of the project is grid-forming control for advanced integration of renewable energy in HVDC-based systems with MMCs. This study of advanced grid-forming controls is beyond the scope of an MSc thesis. That is why the task of commissioning the recently purchased laboratory prototype and developing the initial control methods has been dedicated to this issue. Once the system is fully operative, the work will turn towards the study of grid-forming control strategies that are currently required by the electrical system.

Grid-forming control techniques are required to achieve a high penetration of power electronics-based renewable energy sources for decarbonised electric systems. The aim of the project, which is to continue the work done in this thesis, is to provide significant progress in this field. The operative prototype will be the means of experimentally validating the developments achieved.

Bibliography

[1] H. Akagi. Classification, terminology, and application of the modular multilevel cascade converter (mmcc). *IEEE Transactions on Power Electronics*, 26(11):3119–3130, 2011. doi: 10.1109/TPEL.2011.2143431.

[2] H. Akagi. New trends in medium-voltage power converters and motor drives. In *2011 IEEE International Symposium on Industrial Electronics*, pages 5–14, 2011. doi: 10.1109/ISIE.2011.5984128.

[3] S. Allebrod, R. Hamerski, and R. Marquardt. New transformerless, scalable modular multilevel converters for hvdc-transmission. In *2008 IEEE Power Electronics Specialists Conference*, pages 174–179, 2008. doi: 10.1109/PESC.2008.4591920.

[4] Z. Guying, J. Daozhuo, and L. Xiaorang. Modular multilevel converter for unified power flow controller application. In *2012 Third International Conference on Digital Manufacturing and Automation*, pages 545–549, 2012. doi: 10.1109/ICDMA.2012.129.

[5] S. Kenzelmann, A. Rufer, M. Vasiladiotis, D. Dujic, F. Canales, and Y. R. de Novaes. A versatile dc-dc converter for energy collection and distribution using the modular multilevel converter. In *Proceedings of the 2011 14th European Conference on Power Electronics and Applications*, pages 1–10, 2011.

[6] S. Kenzelmann, D. Dujic, F. Canales, Y. de Novaes, and A. Rufer. Modular dc/dc converter: Comparison of modulation methods. In *2012 15th International Power Electronics and Motion Control Conference (EPE/PEMC)*, pages LS2a.1–1–LS2a.1–7, 2012. doi: 10.1109/EPEPEMC.2012.6397405.

[7] A. Lesnicar and R. Marquardt. An innovative modular multilevel converter topology suitable for a wide power range. In *2003 IEEE Bologna Power Tech Conference Proceedings,*, volume 3, pages 6 pp. Vol.3–, 2003. doi: 10.1109/PTC.2003.1304403.

[8] R. Marquardt. Modular multilevel converter: An universal concept for hvdc-networks and extended dc-bus-applications. In *The 2010 International Power Electronics Conference - ECCE ASIA -*, pages 502–507, 2010. doi: 10.1109/IPEC.2010.5544594.

[9] R. Marquardt. Modular multilevel converter: An universal concept for hvdc-networks and extended dc-bus-applications. In *The 2010 International Power Electronics Conference - ECCE ASIA -*, pages 502–507, 2010. doi: 10.1109/IPEC.2010.5544594.

[10] K. Sharifabadi, L. Harnefors, H. P. Nee, S. Norrga, and R. Teodorescu. *Design, control, and application of modular multilevel converters for HVDC transmission systems*. Chichester, West Sussex, United Kingdom, 1st ed. edition, 2016. ISBN 9781118851555.

[11] D. Siemaszko, A. Antonopoulos, K. Ilves, M. Vasiladiotis, L. Ängquist, and H.-P. Nee. Evaluation of control and modulation methods for modular multilevel converters. In *The 2010 International Power Electronics Conference - ECCE ASIA -*, pages 746–753, 2010. doi: 10.1109/IPEC.2010.5544609.

[12] D. Siemaszko, A. Antonopoulos, K. Ilves, M. Vasiladiotis, L. Ängquist, and H.-P. Nee. Evaluation of control and modulation methods for modular multilevel converters. In *The 2010 International Power Electronics Conference - ECCE ASIA -*, pages 746–753, 2010. doi: 10.1109/IPEC.2010.5544609.

[13] N. Thitichaiworakorn, M. Hagiwara, and H. Akagi. Experimental verification of a modular multilevel cascade inverter based on double-star bridge cells. *IEEE Transactions on Industry Applications*, 50(1):509–519, 2014. doi: 10.1109/TIA.2013.2269896.

[14] F. Zhang, G. Joós, and W. Li. A transformer-less modular multilevel dc-dc converter with dc fault blocking capability. In *2017 IEEE Southern Power Electronics Conference (SPEC)*, pages 1–6, 2017. doi: 10.1109/SPEC.2017.8333576.

[15] S. Zhang, B. Li, Y. Zhang, D. Cheng, X. Zhao, W. Wang, and D. Xu. A novel modular multilevel transformerless step-down dc/dc converter. In *2019 IEEE 4th International Future Energy Electronics Conference (IFEEC)*, pages 1–6, 2019. doi: 10.1109/IFEEC47410.2019.9014655.

A | Appendix A

System ratings	
Submodule's nominal voltage	$V_{SM,nom} = 400V$
IGBT maximum peak voltage	$V_{IGBT,max} = 600V$
Submodule's nominal current	$I_{SM,nom} = 10A(rms)$
IGBT maximum peak current	$I_{IGBT,max} = 50A$
Diode rectifier maximum current	$I_{DR,max} = 100A$
System's nominal power	$P_{MMC,nom} = 15kW$

Table A.1: System ratings of Imperix MMC.

MMC Control parameters		
Individual SM control	$KP_{sm} = 0.013$	$KI_{sm} = 0$
Circulating current control	$KP_{cc} = 6.66$	$KI_{cc} = 22$
Phase voltage control	$KP_{pv} = 6.66$	$KI_{pv} = 22$
Vertical unbalance control	$Kp_{pv} = 0.4$	$KI_{pv} = 5.5$
DQ Current control	$KP_{DQc} = 1.6$	$KI_{DQc} = 686$
DC voltage control control	$KP_{VDC} = 10$	$KI_{VDC} = 20$
Synchronization (DC) control	$KP_{SyncDC} = 35$	$KI_{SyncDC} = 1200$
Synchronization (AC,D) control	$KP_{SyncAC,D} = 0.2$	$KI_{SyncAC,D} = 20$
Synchronization (AC,Q) control	$KP_{SyncAC,Q} = 0.5$	$KI_{SyncAC,Q} = 5$

Table A.2: Parameters and settings of implemented controllers.

MMC Electrical parameters			
$L_{arm} = 2.3mH$	$R_{arm} = 0.05\Omega$	$C_{SM} = 1.35mF$	$R_{SM} = 0.005\Omega$
$L_{tr} = 2mH$	$R_{pre} = 47\Omega$	$R_{load} = 22\Omega$	$P_{max,load} = 7.5kW$

Table A.3: Parameters and settings of the system's plant.

PWM blocks		
Type	Carrier-based-PWM	
Carrier-shape	Triangle	
Phase[1]	$0.25 \cdot i (0 \leq i \leq 4)$	
PWM parameters update rate	Double-rate	
Dead-Time	$t_{dt} = 400ns$	
Switching Frequency	$f_{sq} = 5kHz$	
ADC blocks		
Sensitivity	$S_{voltagesensors} = 2.46mV/V$	$S_{currentsensors} = 99mV/A$
Gain	$G_{voltagesensors} = x4$	$G_{currentsensors} = x2$
Analog filter cut off frequency	$f_{co,voltage} = 6.4kHz$	
Sampling Frequency	$f_s = 20kHz$	

Table A.4: Signal interfacing configuration parameters

B | Appendix B

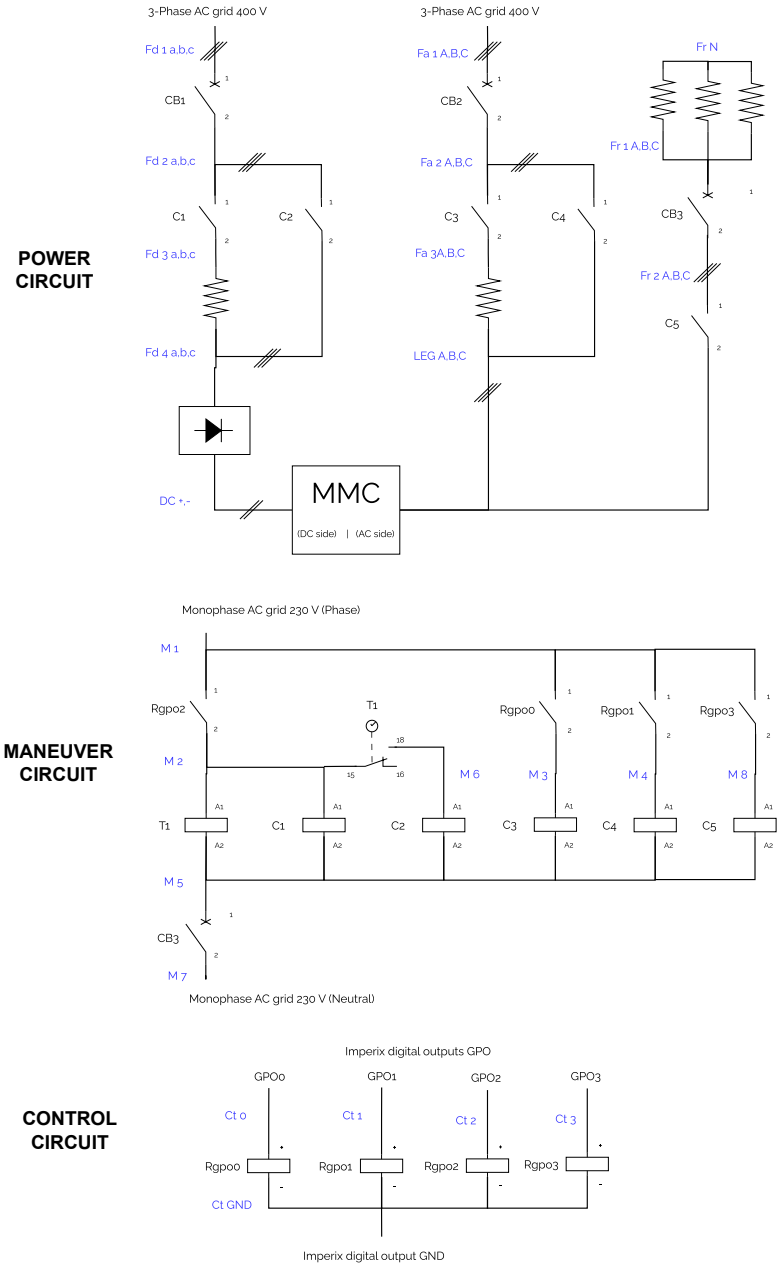

Figure B.1: System connection electrical diagram.

List of Figures

List of Tables

Acknowledgements

I take the chance to acknoledge and thank and acknowledge the people that has accompanied me along this journey:

To morris, for being present for me all this time despite the difficulties.

A Ramón, Jaime, Gala, Patri, Álex y todos los compañeros del laboratorio del AI2, con los que he compartido mis aventuras con el Imperix.

A mi familia y en especial a mi madre por su insistencia en no empezar a trabajar antes de acabar el master ... cuánta razón tenías.

A mi Ale, mi mayor apoyo, me haces fácil lo que parece imposible. Gracias por estar siempre.